DOCTOR OF PHILOSOPHY

A study of carbon based materials for energy applications

Goher, Qammar Sultan

Award date:
2012

DOCTOR OF PHILOSOPHY

A study of carbon based materials for energy applications

Qammar Sultan Goher

2012

University of Dundee

A Study of Carbon Based Materials for Energy Applications

Qammar Sultan Goher

Submitted for the Degree of

Doctor of Philosophy

from the University of Dundee

Division of Electronic Engineering and Physics

School of Engineering, Physics and Mathematics

University of Dundee

Nethergate, Dundee DD1 4HN, U.K

2012

Dedication

To my Parents and Wife

Acknowledgements

First of all the author is so grateful to ***Almighty Allah*** how provide resources and enabled author to work on this research project. Grateful acknowledge goes to ***Federal Urdu University of Arts, Sciences and Technology Pakistan*** which trusted on me and gave me scholarship for my PhD.

The author is most grateful to ***Prof. Mervyn John Rose*** for his invaluable supervision in this research work throughout a busy and troubled time. He was so kind and helpful in all the research work and thesis proof reading I never felt difficulty.

The author would like to appreciate ***Dr. Yong Fan*** contribution for his wonderful support in characterization of CNTs and graphene. He guided me how to use TEM, SEM, AFM and STM and always ready for spectroscopic analysis. Much gratitude goes to ***Dr. Saydullah Persheyev*** for his guidance in sample preparation and characterization of samples and invaluable advices in this research. Many thanks go to ***Dr. Andrew Hourd*** for his guidance in Ink-Jet printing technique for the preparation of graphene planes.

Special acknowledgement goes to ***Stuart Anthony*** for his kind help in sample preparation and the use of PECVD system for the growth of CNTS and graphene. Actually he did a lot in this research. I am thankful to ***Dr. Gary Callon, Callum Moore*** and ***all the staff members of Electronic Engineering & Physics*** for their help and encouragement. Thankful to my colleagues ***Jin Yao*** and ***Mahadi Halim*** for the nice time we spent during this research.

Acknowledge goes to ***Prof. Andre Geim research group*** (condensed matter research group) ***Manchester University***, which guide me how to prepare graphene.

Finally I would thankful to my parents, wife and all family members who always prayed for my success.

Qammar Sultan Goher

Declaration

This is a declaration that the candidate is the author of this thesis, that all references cited have been consulted by the candidate, that the work in this thesis was done by the author and that this work has not been previously accepted for a higher degree.

Qammar Sultan Goher

Summary

Carbon based materials such as CNTs and graphene have been widely studied over the last few years. The outstanding electrical and mechanical properties of these materials attracted researchers to find ways to grow and use them in nano-devices. Among the different techniques, PECVD is a relatively simple and low temperature process. It facilitates the growth of CNTs and graphene on particular sites of the substrate. The objective of this research project was to study the growth of CNTs and graphene using PECVD system and to employ them in renewable energy devices. Excimer laser processed materials were also the focus for flexible material for fuel cells and other applications to show the way to a one step manufacturing process that lends itself to large area and low cost processing using standard tools.

In the growth of CNTs, the roll of a buffer layer and catalyst materials were studied in depth. Different metals were tested for best results in optimising nanotube growth for the selected applications. The role of the buffer layer in the formation of nanoparticles and their surface adhesion was studied. Different materials were used as a catalyst and analysed for best performance in the PECVD system. Growth parameters such as temperature, pressure, gas flow rate and plasma power were studied during the growth of CNTs in the PECVD system. The growth of graphene has been conducted in two ways: firstly, by the traditional mechanical exfoliation technique (with the help of Manchester University) and second by PECVD techniques.

Polymer materials are promising flexible substrates for electronic and energy devices. An excimer laser was used to transform thin metallic films into nanoparticles which could play the role of the catalyst in proton exchange membrane fuel cells. In this study experiments have been conducted into a single step process to convert the poly ethylene naphthalate (PEN) surface to a robust mesoporous carbon material that conducts electrons, whilst depositing the catalyst. Such a technique has been developed for the first time in this work. Laser modification here produced a conical carbon structure and dense arrays of well defined catalysts.

A prototype fuel cell was designed and crafted to employ the laser processed PEN as a proton exchange membrane. Some experiments were conducted regarding the transport of protons through laser processed PEN and the conventionally used fuel cell electrolyte, Nafion. It has been observed that the hydrophilic property of Nafion allowed proton transport across this material. It was also observed that PEN is not a good membrane for protonic transport. This material does not have free sites for vehicle transport. The catalytic activity of laser ablated Ni nanoparticles on PEN substrate was studied in temperature programme reaction (TPR) and it was observed that the metallic nanoparticles had some activity at higher temperature. Both Ni and Pt nanoparticles were tested as catalysts on the standard Nafion electrolyte. It was observed that Pt is active for the hydrogen combustion reaction and Ni has less activity for this purpose. It was not expected in this work that efficient hydrogen transport through the polymer would occur, but that future modification of the internal chemistry of PEN can be developed.

Acronyms Used

BEI : Back scattered electron image

BNTs : Boron nitride nanotubes

CNF : Carbon nano fibre

CNTs : Carbon nanotubes

CVD : Chemical vapour deposition

DVM : Digital Multimeter

EDX : Energy dispersive X-ray

ELC : Excimer laser crystallized

FED : Field emission display

FLG : Few layer graphene

HRSEM : High resolution scanning electron microscope

HRTEM : High resolution transmission electron microscope

MEMS : Micro-Electro-Mechanical system

MWNTs : Multi-walled carbon nanotubes

PECVD : Plasma enhanced chemical vapour deposition

PEMFC : Proton exchange membrane fuel cell

PEN : Poly ethylene naphthalate

RF : Radio frequency

SEI : Secondary electron image

SWNTs : Single walled carbon nanotubes

TFT : Thin film transistor

TPD : Temperature programmed deposition

TPR : Temperature programmed reaction

Table of Contents

List of Figures

List of Tables

Structure of the Thesis

The thesis is structured in seven chapters:

Chapter 1 presents an introduction to CNTs, market of CNTs, energy challenges and environment.

Chapter 2 is a comprehensive literature review of carbon based materials such as CNTs and graphene. It describes a critical analysis on the growth of CNTs and graphene, their properties and applications.

Chapter 3 consists of a review of nano-composite materials on flexible devices. The applications of nano composites is also analysed regarding energy and environment.

Chapter 4 explains the experimental techniques used in this research. The techniques for the deposition of thin films for catalyst are described. The experimental set up developed for the growth of CNTs and graphene is also explained here. An overview of characterisation techniques used to analyse CNTs and graphene is also given.

Chapter 5 is totally dedicated to the growth and characterisation of CNTs and graphene. All the growth parameters are explained. The role of the buffer layer and the catalyst is also discussed.

Chapter 6 of this thesis explains the excimer laser technique for the large scale production of nanoparticles on polymer substrates and conducting a-Si for a number of applications.

Chapter 7 covers the catalytic activity of laser processed metallic nanoparticles in the proton exchange membrane fuel cell.

Chapter 8 summaries all the results which were achieved in this research and suggests future work.

CHAPTER 1 INTRODUCTION

In the middle of the twentieth century, an extraordinary increase in the research of carbon based material especially carbon fibre was observed. In the mid 1980`s the discovery of fullerene opened doors for researchers to work in this area. The discovery of carbon nanotubes (CNTs) by Ijima [1] in 1991 enhanced research in this area. After twenty years a big breakthrough in carbon research was observed with the discovery of single layer graphene.

Researchers are now trying to grow and manipulate CNTs and graphene in nano-devices for electronic applications. There are some challenges related to the growth of CNTs, such as growth at low temperature, large scale production and the growth on particular sites of the substrate. Research is also underway to find some techniques by which they can be grown on polymers for new plastic electronics devices.

1.1-Current Status of CNTs in Market

From the first recorded discovery of nanotubes, it was predicted that CNTs could be produced in bulk but initially the growth rate was very low. The quality of tubes was a major issue because in initial growth techniques, the tubes produced were a mixture of nanotubes, nanofibres, and amorphous carbon. There were no special techniques to separate tubes at that time. Also, the tubes were formed in metallic and semiconducting forms. The separation process of as-grown CNTs was difficult. Now there are many companies which are producing CNTs in bulk, but not yet in kilograms. As the production of CNTs by chemical vapour deposition (CVD) and plasma enhanced chemical vapour deposition (PECVD) started, the quality was much improved. According to the report published by GIA [2], the global CNTs

industry is surging after the economic recession in 2008-09 and this boost will increase the global market of CNTs up to US$7.72 billion by the year 2015. The role of research institutions in the development of the CNT industry is crucial; they are trying to find potential applications of CNTs. Military, aerospace industry and renewable energy applications are expected areas which will increase the uses of CNTs and graphene in coming years.

1.2-Energy Challenges

If we think back to about two centuries ago, there were no motorcars, computers, aeroplanes or electricity generators.. Now we have modern travel facilities and a luxurious life at home with proper heating, cooling, cooking, and entertainment systems. All these facilities have been provided through energy. As the population of the world is increasing and new inventions are involved in our life, the demand for energy is increasing.

Sources of energy include crude oil, natural gas, coal, the sun, wind and water. But today, the main sources of energy are crude oil, natural gas and coal. Because of the increase in energy demand, fossil fuel resources are not fulfilling the demands and will start declining as shown in graph in Figure 1.1. We need new sources of energy because no one wants to live as we did two centuries ago. Also, we need a new clean source of energy which meets the demands of future.

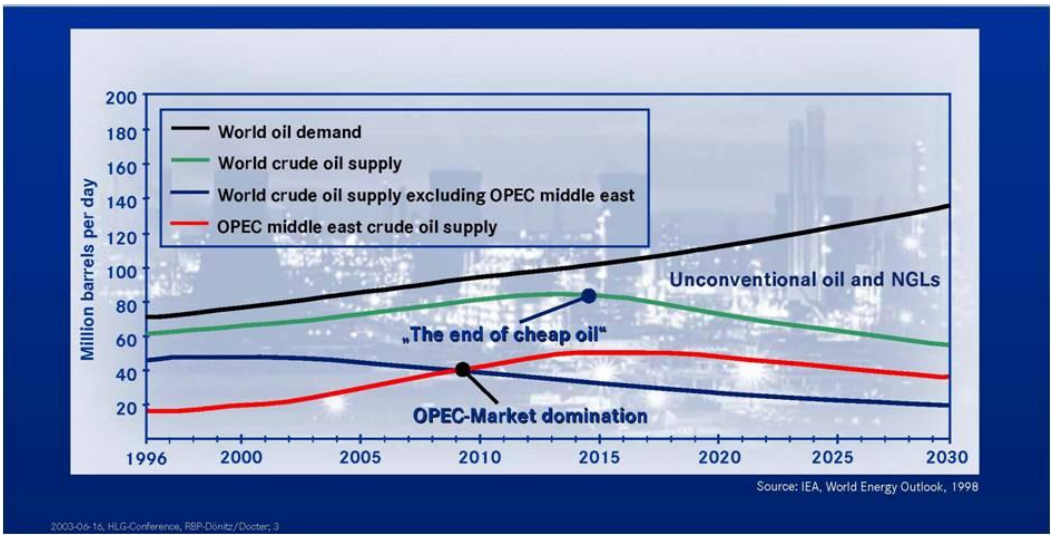

Figure 1.1 Crude oil supply and world oil demand

We need new sources of energy to overcome the energy demands of the future and for a clean atmosphere for the next generation.

Research is being carried out in different themes in energy such as solar energy, wind energy, hydropower, bio energy and fuel cells. These sources of energy are relatively environmental friendly. Still the efficiency of all these systems is very low and research is ongoing to improve it. Also, because of new products the market is very active. Hopefully in the future the manufacturing cost will decrease, and cheaper materials will be in the range of the common man.

1.3-Environmental Pollution

Added to the energy supply and security question is an environmental issue. The exhaust of all engines (machines) goes to the environment, which is now badly affected through the use of fossil fuel resources. The data over the century is showing that environmental and water pollution is increasing rapidly.

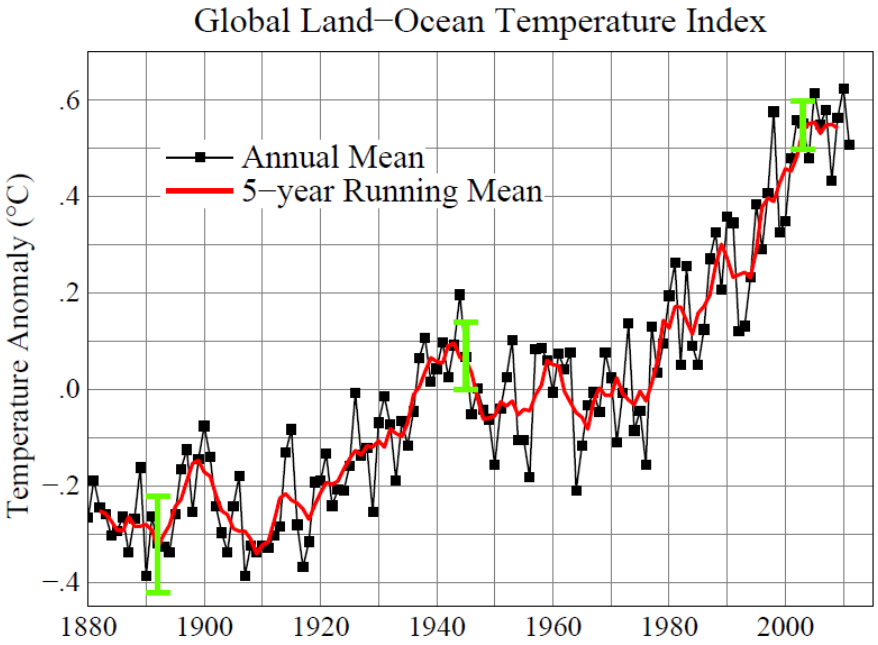

Figure 1.2 Global mean surface temperature change from 1880-2009 [3]

This environmental pollution is increasing the carbon dioxide (CO_2) level in the atmosphere causing the green house effect with the result of global warming as shown in Figure 1.2. The fourth assessment report by the IPCC (Intergovernmental Panel on Climate Change) argues that the rise in average global temperature was 0.74°C during the 20^{th} century [4].

This increase in temperature will cause sea levels to rise and many islands will be submerged under the sea in future. The poisonous gas carbon monoxide (CO) emitted from chemical industries is also damaging the ozone layer which is impeding its effect in working as a UV filter between the sun and earth [5].

1.4-Renewable Energy and Fuel Cells

To fulfil the energy requirements of the world, research is ongoing to find new sources of energy. In place of big energy generation systems, small systems are suitable for some applications, especially in remote areas. Mostly the renewable energy plants are environmentally friendly. The new available renewable energy

resources are predominantly solar energy, wind energy, wave energy and fuel cell technology. A fuel cell works like a mechanical system which takes hydrogen fuel from a fuel tank in place of oil or gas and generates electricity. Fuel cells working on H_2 produce only water as a product, which is helpful for a clean environment.

1.5-Scope and Objectives of this Research

A main objective of this thesis is the improvement of the growth conditions of CNTs by using PECVD and to use these tubes in energy applications. Particular attention will be devoted to overcoming current problems related to chamber in the PECVD system and to improving the growth conditions with this system. In addition, the use of CNTs in the improvement of catalytic efficiency of nanoparticles in fuel cells for energy and its water splitting activities will be investigated.

In this research we will try to prepare polymer membrane for the PEMFC with a single step process which will make polymer conducting by carbonizing the surface of polymer substrate by excimer laser irradiation and creation of metallic nanoparticles in the thin film of metal. This technique will be cheaper, easy and fast for the preparation of PEMFC. The efficiency could be less than Pt particles but by using CNT-nanoparticles composites this could be boosted. The details how to prepare nanoparticles with laser irradiation will be discussed in Chapter 6. The performance of nanoparticles on PEN and Nafion will be described in Chapter 7.

A main problem with the growth of CNTs in PECVD is the creation of catalyst nanoparticles by heating and plasma treatment. On the application side of CNTs, separation of tubes is a big problem as is the solubility of tubes in liquids such as a water base biological and medical application. A number of tools were used in this research including SEM, AFM, and TEM etc. for the analysis of carbon structures. A further objective of this research is to integrate CNTs and graphene with laser processed novel a-Si:H material.

Another theme to this research work was the processing of carbon based polymeric materials using laser techniques with the aim of transforming surfaces to mesoporous

high surface area conducting carbon, with the simultaneous deposition of metallic or semiconducting nanoparticles. This forms the basis of a potential large area process with applications in fuel cells, water splitting and photocatalysis (artificial photosynthesis).

The main objectives of the research described in this thesis are to

1. Design and build a system for the growth of CNTs
2. Control the growth process parameters
3. Creation of nanoparticles for CNTs
4. Growth of CNTs
5. Growth of graphene
6. Laser processing of polymer substrates and nano-dots
7. Nano-composites for energy

References

1) S. Iijima, *Nature* **354,** 56(1991)
2) Carbon Nanotubes- *A Global Strategic Business Report* by Global Industry Analysts, Inc. Sep 2010
3) J. Hansen, M. Sato, R. Ruedy, K. Lo, D.W. Lea and M. Medina-Elizade, *PNAS* **103**(39), 14288(2006)
4) IPCC, 2007: Summary for Policymakers. In: *Climate Change 2007: The Physical Science Basis. Contribution of Working Group I to the Fourth Assessment Report of the Intergovernmental Panel on Climate Change* [S. Solomon, D. Qin, M. Manning, Z. Chen, M. Marquis, K.B. Averyt, M. Tignor and H.L. Miller (eds.)]. Cambridge University Press, Cambridge, United Kingdom and New York, NY, USA.
5) IPCC/TEAP Special Report: Safeguarding the Ozone Layer and the Global Climate System 2003

CHAPTER 2 BASES AND REVIEW OF CARBON ELECTRONICS

Carbon has long been an interesting topic in the engineering and scientific community but over the last four decades it is quite a lot researched in the world. Research is ongoing on all the allotropes of carbon, their physical properties, bonding and applications. New allotropes were researched for strong light weight nano-devices. Carbon is the material which enabled researchers to study it up to the atomic level physically.

This chapter aims to briefly explain the basics of carbon electronic carbon bonding structure, its allotropes and historical developments in the field of carbon. A major focus is CNTs; their discovery, physical properties, growth models and synthesis. Research and development in the field of CNTs and their applications will be discussed in this chapter in depth. Research on single layer graphene is also discussed here.

2.1-Carbon

Carbon has been known since earliest human civilization in the form of charcoal and soot. The word carbon came from the Latin word ***Carbo*** meaning charcoal. The earliest discovered allotropes of carbon were graphite and diamond. According to the available data, Egyptians and Samaritans used carbon (charcoal) in 3750 BC for the reduction of copper, zinc and tin ores in the manufacture of bronze. The Chinese used diamond for the first time for the purpose of polishing [1].

Carbon is a member of Group I4 of the periodic table. It has four electrons in the valence shell with electronic structure:

$$1s^2\ 2s^2\ 2p^2$$

Since carbon needs eight electrons in its outermost shell to complete its orbitals, so each electron of carbon in its outer most shell forms a covalent bond by sharing electrons with neighbouring atoms. These electrons may be from carbon or other compounds such as hydrogen. This unique bonding property of carbon gives rise to millions of organic compounds.

2.1.1-Hybridisation

Combination of atomic orbitals to create new orbitals is known as hybridisation, which mostly occurs in partially filled orbitals. Hybridisation explains the bonding structure and electrical conductivity of compounds. Carbon has two types of hybridisation, sp^2 and sp^3. In sp^3 hybridisation, one s orbital mixes with three p orbitals and make four sp^3 orbitals. In the sp^3 bonding structure, each atom of carbon makes strong covalent bonds with four neighbouring atoms giving a tetragonal structure. The best example of such a bonding structure is diamond. In sp^2 hybridisation, one s orbital mixes with two p orbitals and make three sp^2 orbitals. One p orbital remains unchanged and electrons in that orbital behave like free electrons as shown in Figure 2.1. Graphite is an example of sp^2 hybridisation and is a semi-metal.

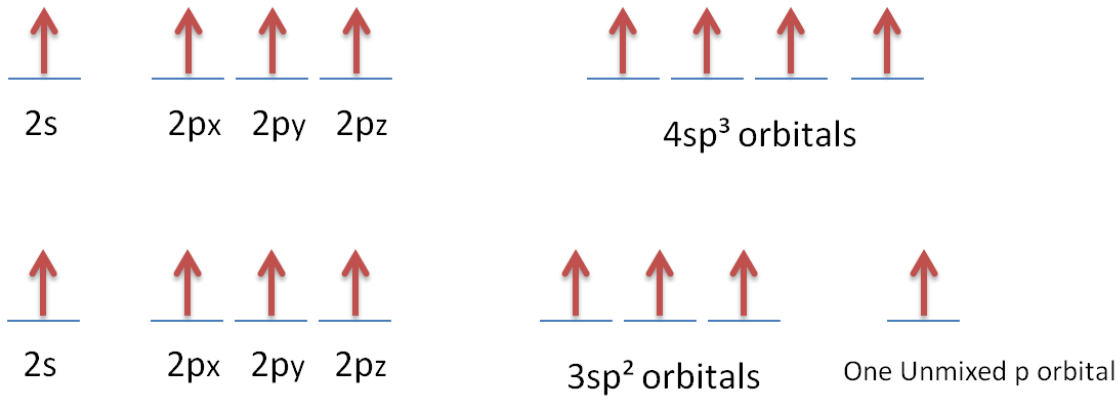

Figure 2.1 sp^3 and sp^2 hybridisation in carbon

2.2-Allotropes of Carbon

Different structural arrangements of carbon atoms cause a big variation in physical properties; from the hardest material to the softest, conducting to semiconducting and bulky material to shortest diameter nanotubes. The most common allotropes of carbon are diamond, graphite, fullerenes, amorphous carbon, CNTs and graphene.

2.2.1-Graphite

Graphite is the second natural form of carbon that occurs in the earth's crust. It is soft and gray/black in colour with a high melting point. It is a good conductor of heat and electricity.

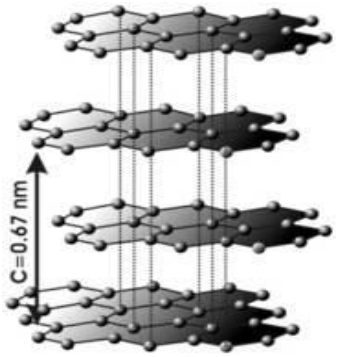

Figure 2.2 Atomic layered structure of graphite [2]

In the graphite crystal, the s orbital mixes with two p orbitals only, and each of the carbon three new sp^2 orbitals points to one of the three vertices of a triangle which

lies in the *x-y* plane (for instance). Three electrons occupy these orbitals and one electron stays in the p_z orbital which is directed perpendicular to the *x-y* plane. Hence, the carbon atoms are bonded by three σ bonds (the charge density lies between two atoms) and one π bond (the charge density is concentrated above and under the *x-y* plane, perpendicular to the atomic bond). Since there is no preference as to which atom the p_z-electron should bond to, the bond formed (π bond) with all three neighbours is weaker than the σ bonds. This electron is free to move and contributes to conduction. Furthermore, the π bond stabilizes the structure and "locks" it in the plane. The whole crystal is made of sheets held together by weak Van der Waals forces, separated by a distance of 3.40 Å as shown in Figure 2.2. This gives softness to the structure [2-3].

2.2.2-Diamond

Diamond is the hardest known natural material. It has different colours depending upon impurities, but pure diamond is colourless. Because of its hardness, diamond is used in glass and silicon wafer cutting. Diamond is a good thermal conductor its thermal conductivity is four times greater than copper and a bad conductor of electricity.

Figure 2.3 Atomic arrangements in diamond [5]

The electronic configuration of diamond is $1s^2 2s^2 2p^2$. In order to create covalent bonds in diamond, the s orbital mixes with the three p orbital to form sp^3 hybridisation. The four valence electrons are thus equally distributed among the sp^3orbitals, while each orbital points to one of the four corners of a tetrahedron. The

tetrahedral structure, together with the highly directed charge density, gives strength and stability to the bonds. All the bonds in diamond are of the same length (1.54 Å), with the same bond angle (109.47°). Each carbon atom in diamond is surrounded by four atoms by covalent bonds and hybridization is sp^3 as shown in Figure 2.3. Diamond is a nearly non-conducting semiconductor with a large band gap of 5.5 eV.

2.2.3-Fullerenes

A collection of hollow carbon molecules made of a cage of interlocking pentagons and hexagons is known as fullerenes. The first fullerene C_{60} was discovered in 1985 by Harold W. Kroto et al. [6] by laser evaporation of graphite in a high density helium flow. They suggested the structure of this super-stable species a truncated icosahedrons, a polygon with 60 vertices and 32 faces, 12 of which were pentagonal and 20 hexagonal. Donald Huffman and Wolfgrang Krätschmer [7] used arc discharge methods to produce C_{60} on a large scale. In 1996 the Chemistry Nobel Prize was awarded to Robert F. Curl Jr, Sir Harold W. Kroto and Richard E. Smalley for their discovery of fullerene.

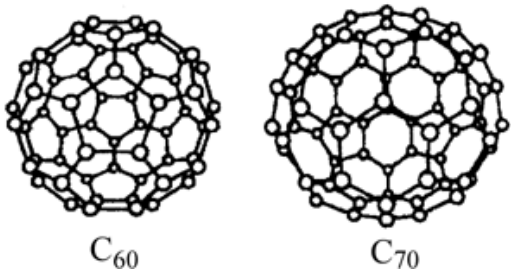

Figure 2.4 family of fullerenes [8]

There are other members of the fullerene family, which have also been synthesized (as shown in Figure 2.4).

2.2.4-Amorphous carbon

During the irradiation of diamond by atoms, many bonds are broken, leading to point defects and eventually to clusters of defects as shown in Figure 2.5. At a high enough irradiation dose, amorphisation of the crystal structure may occur and two specific amorphous forms of carbon may appear: the tetrahedrally bonded diamond-like amorphous carbon which will be denoted by *ta-C* and the sp^2 bonded graphite-like amorphous carbon named a-*C*.

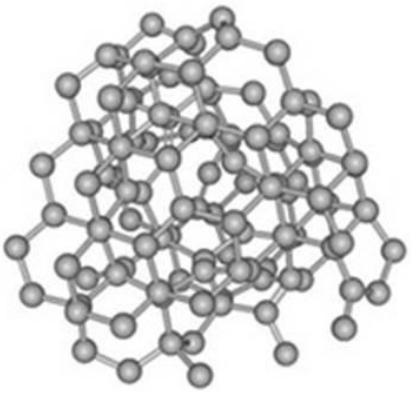

Figure 2.5 Molecular structure of amorphous carbon [9]

These two structures can be distinguished clearly by their macroscopic and microscopic properties. The former material has higher density, is transparent, electrically insulating and much harder than the latter. From the microscopic point of view, the ratio of fourfold, diamond-like bonds to three-fold, graphite-like bonds (sp^3/sp^2) determines the kind of structure obtained.

2.2.5-Graphene

Graphene is a single atom thick layer 2-dimensional sheet having sp^2 bonded carbon atoms, and has potential to be used in next generation electronic devices. It is the thinnest, strongest and most conducting material known to man having excellent ballistic electron transport, high thermal conductivity and super hydrophobicity [10-12] as shown in Figure 2. The first reported few-layer graphene (FLG) was prepared by mechanical exfoliation of graphite in 2004 by Novoselov et al. [13]. In 2010, A. K. Geim and K. S. Novoselov were awarded the Nobel Prize in Physics for their ground-breaking experiments on the preparation of single atom layer thick graphene.

The exceptional electrical and mechanical properties of graphene suggest its use in ballistic transistors, field effect transistors, sensors, transparent conducting electrodes in touch screens and other display devices. In the last two years, research in the growth of graphene and its applications in the nano-devices industry have increased enormously. New techniques have been introduced to synthesise single layers of graphene on a suitable substrate for some applications. The most recently used technique to grow free standing few layer graphene (FLG) on a substrate is CVD [14]. This technique was used for the first time in 2006 to grow FLG on a Ni foil at 850°C from pyrolysis of camphor [15]. After a few years Yu et al. reported the growth of 3 to 4 layer graphene on Ni foil by thermal CVD at 1000°C with a precursor gas mixture of CH_4, H_2 and Ar on a moderate cooling rate (10 °C/s [16]. Li et al. [17] recently reported the growth of excellent quality mono-layer graphene on Cu foils at low temperature by using solid (PMMA) and liquid (benzene) carbon sources in CVD.

There are some publications about the growth of graphene by PECVD [18-20]. Obraztsov et al. for the first time in 2003 reported the growth of nano-structured graphite-like carbon (NG) on Si wafer by using a d.c discharge plasma [21]. The NG films prepared were thicker at most of the places. Wang et al. [22] prepared sub-nanometre thickness graphene films on a variety of substrates (Si, SiO_2, Ti, Cr, Ta, Mo etc.) by using radio frequency plasma with CH_4 and H_2 precursor gases at a temperature of 680°C. PECVD is the technique which is also selected for the growth of graphene in this research work. There are many other routes to prepare graphene such as chemical methods, thermal decomposition of SiC and Ru [23-24].

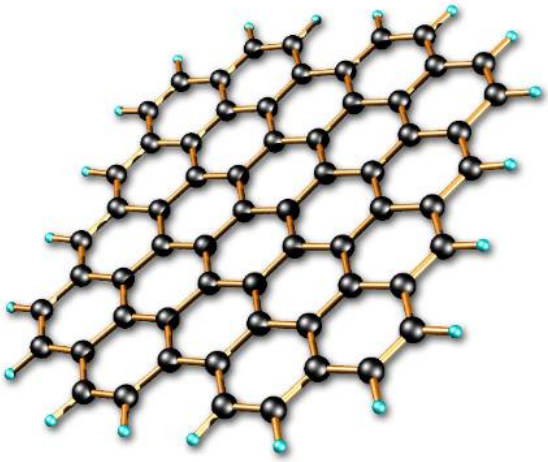

Figure 2.6 Single sheet of graphene [25]

The extraordinary properties of this two-dimensional material have many potential applications such as large current fast switching electronics, transparent conductors, sensors and many more.

A study of the mechanical strength of graphene-composite was conducted at Rensselaer Polytechnic Institute and illustrated that graphene could prevent fracture and fatigue failure. It was predicted that graphene could be helpful in improving the mechanical properties of wind turbines and aircraft wings [26]. The high carrier mobility in graphene made it possible to fabricate high speed transistors [27]. The strong bonding between graphene and DNA made it possible to make graphene-DNA biosensors. Research conducted by Tang et al. [28] found that graphene-DNA biosensors are highly durable because graphene protects DNA from being broken down by enzymes.

2.3-Carbon Nanotubes (CNTs)

. Currently, two CNTs are rolled up graphene sheets which are of two types:

1. Single walled carbon nanotubes (SWNTs)
2. Multi-walled carbon nanotubes (MWNTs)

SWNTs can be described as a sheet of graphite hexagonal ring of atoms, rolled in a cylinder closed at both ends by fullerene-like end caps. The diameter of SWNTs is ~1nm and their length is from a few nm to microns (large aspect ratio ~1000) so they can be considered as nearly one-dimensional structures. MWNTs consist of several concentric nanotubes. The diameter of these tubes ranges from 2 nm to 100 nm depending upon the growth conditions.

The history of carbon fibres is not new; scientists have been researching this area for over 100 years. The first carbon filament produced from thermal decomposition of gaseous hydrocarbon was explained by Hughes and Chamber [29] in 1889. In 1976 Oberlin et al. [30] published a paper in which they discussed a carbon fibre which resembled SWNTs. They produced carbon fibre by pyrolysis of benzene and ferrocene at higher temperature. The authors did not claim CNTs because at that time, although electron microscopes were powerful tools to study the structure of carbon filaments, the images did not explain the number of walls clearly.

Table 2.1:* *Historical development in carbon based material [31]

Serial No.	**Year**	**Discovery**	**Authors**
1	1889	Carbon filament production by thermal decomposition of hydrocarbon gases	T.V. Hughes and C.R. Chambers
2	1976	Hollow carbon fibre	A. Oberlin, M. Endo, T. Koyama and M. Endo
3	1985	Fullerenes	H.W. Kroto, R.F. Curl and R.E. Smalley
4	1991	Multiwall carbon nanotubes(Arc discharge)	S. Iijima
5	1993	Single wall carbon nanotubes	S. Iijima and T. Ichihashi

The Figure which was published by Oberlin et al. in 1976 shows the size of the tube which is approximately 5 nm as shown in Figure 2.7 (left). Now, it is possible from calculations that SWNTs may have 5nm diameter, but it is rare (in some techniques).

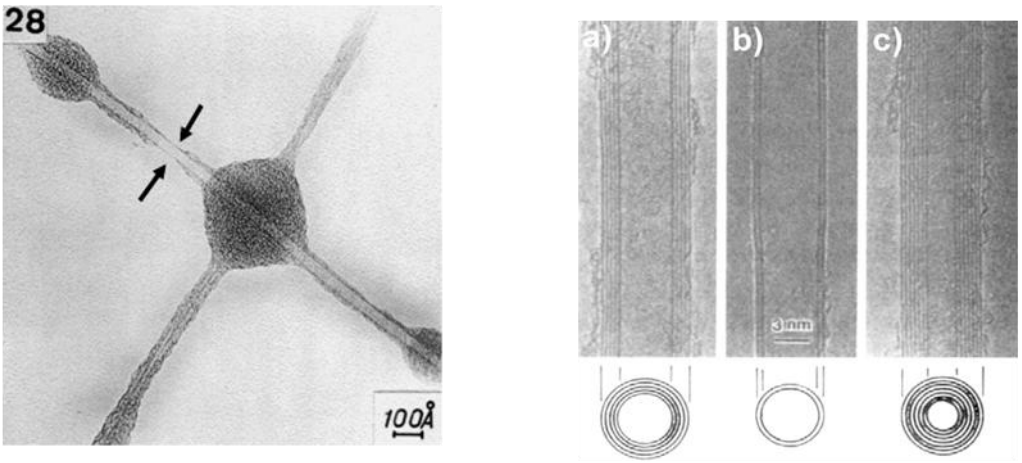

Figure 2.7 TEM image of nanotubes grown by A. Oberlin et al. [30] (left) and S.Iijima micrographs of CNTs [32] (right)

In 1991 during the studies of C_{60} by arc evaporation S. Iijima [32] found a new type of carbon (carbon nanotubes) by changing the helium pressure in the chamber, these tubes were MWNTs. By using HRTEM and electron diffraction Iijima counted the number of walls of the nanotubes as shown in Figure 2.7 (right). This was the biggest breakthrough in carbon research at that time. In 1992 the bulk production of CNTs by using arc discharge was started [33]. After the discovery of MWNTs, in 1993 S. Iijima and T. Ichihashi [34] observed SWNTs which had diameters from 1.1 to 1.3 nm.

In the early 1990s, research was started to calculate the electronic properties of CNTs. Two research groups, Hamada et al. [35] and Saito et al. [36] for the first time theoretically calculated the electronic properties of individual SWNT. They also predicted the existence of CNTs in metallic and semiconducting forms by explaining the chirality vector and diameter of nanotube. By the end of the 1990s the electronic properties of nanotubes had been confirmed experimentally [37-38]. The transport properties of CNTs were measured by De Heer et al. in 1995 [39]. The mechanical strength and elasticity of CNTs made it a very attractive material in nano-materials engineering [40-42].

CNTs have exceptional physical properties. These tubes are stronger than steel, a better conductor than copper and their size is so small that we need special microscopes to study them. We know the motion of electrons in the nanotube remains along the circumference which reduces carrier scattering processes and the electrical resistance. The confined motions of electrons in circumference allow MWNTs to carry current densities up to 10^7 A/cm^2 without being destroyed [43]. McEuen et al. [44] observed ballistic transport in SWNTs by using a gold-coated AFM tip as a movable metallic contact. Their results showed resistance per unit length of ~4 kΩ/μm, a mean free path of ≈ 2 μm and a room temperature resistivity of ≈10^{-6} Ωcm. Thus the conductivity in metallic SWNTs is equal or better than the conductivity of metals like copper at room temperature. Kim et al. [45] demonstrated that MWNT has a thermal conductivity of more than 3000 $Wm^{-1}K^{-1}$ at room temperature.

A carbon nanotube is very stiff due to the strong carbon-carbon chemical covalent bonding between the individual carbon atoms. There are many theoretical models explaining the mechanical properties of CNTs. J.P. Lu [46] investigated the elastic properties of nanotubes by using an empirical force-constant model. By his calculations, he found that the Young's modulus of nanotubes is 1 TPa and shear modulus ~0.5 TPa. He also demonstrated that the elastic properties in nanotubes are insensitive to the radius, helicity and number of walls. Wong et al. measured the bending stress of MWNTs with the help of an AFM tip [47]. They fixed one end of the nanotube on the substrate and moved the other end using the tip of AFM. The Young's modulus measured by that technique was ~1.28 TPa.

2.3.1-Structure of CNTs

A single-walled CNT is a seamless cylinder which can be thought of as being made from a rolled up two-dimensional single sheet of graphene having a hexagonal network of carbon atoms. The peculiar electronic properties of CNTs depend upon the rolling angle which directly affects the crystal geometry and chirality of nanotubes. There are three types of nanotubes depending upon the rolling angle.

1- Armchair
2- Zig Zag
3- Chiral

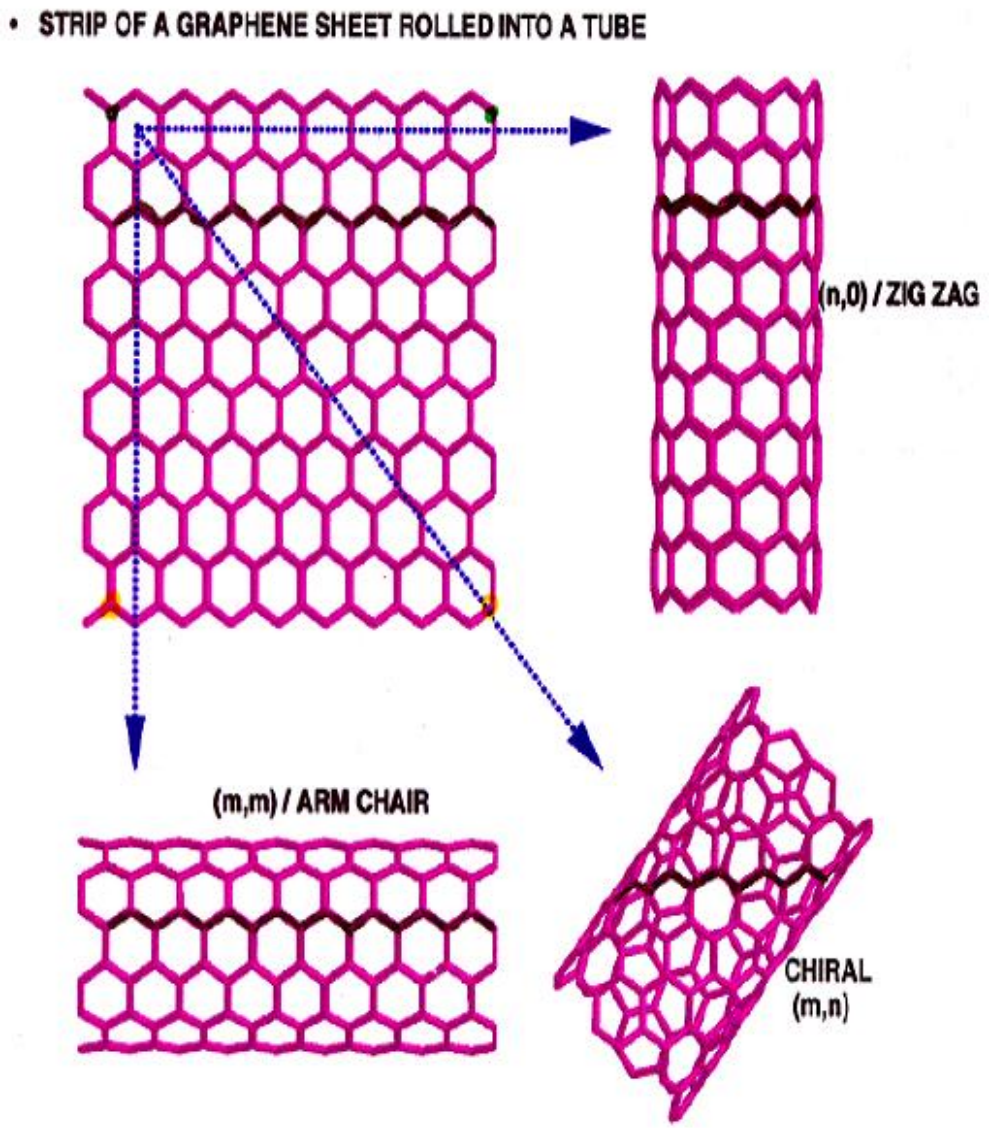

Figure 2.8 Different types of SWNTs

If the graphene sheet is "rolled up" from top to bottom, armchair SWNT will be formed as shown in Figure 2.8.. These tubes are metallic in nature. If the rolling direction is from left to right or from right to left, the tube will be Zig Zag as shown. These tubes are semiconducting in nature. If rolling direction is from one edge to the

other diagonally, the tube will be Chiral as shown Figure 2.8. These tubes are metallic in nature.

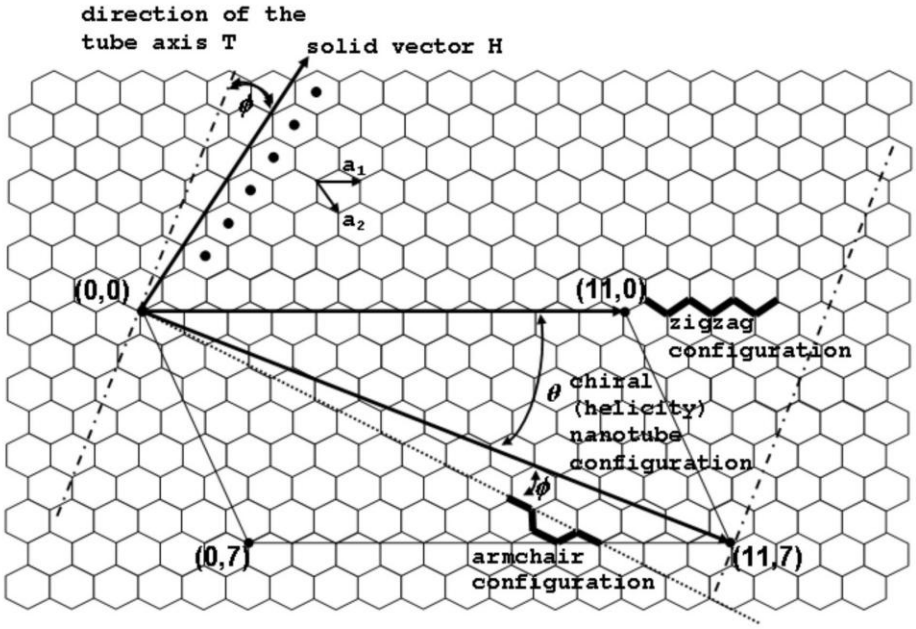

Figure 2.9 Division of the graphene layer for nanotubes such as: zig zag, armchair, and chiral [48]

The circumference of SWNTs can be explained by a Chiral vector $\mathbf{C_h}$ which is defined by two unit vectors $\mathbf{a_1}$ and $\mathbf{a_2}$ in the hexagonal lattice of graphene as shown in Figure 2.9.

$$\mathbf{C_h} = n\mathbf{a_1} + m\mathbf{a_2} \qquad (2.1$$

where n and m are integers

The diameter of a nanotube can be found by the following formula

$$d_{CN} = [3a_{c\text{-}c}(m^2+m*n+n^2)]^{1/2} \qquad (2.2$$

Where d_{CN} is diameter of nanotube, $a_{c\text{-}c}$ is the carbon carbon bond length= 1.44 Å, and the Chiral angle 'θ' is the angle between Chiral vector $\mathbf{C_h}$ and a1 where

$$\theta = \tan^{-1}[\sqrt{3}*m/(2n+m)] \qquad (2.3$$

and $0 \leq \theta \leq 30°$

The electrical conductivity in a SWNT can be found by a simple formula.

$$(2n+m)/3 = q \qquad (2.4$$

If q in equation 2.4 is an integer, the tube will be metallic such as in the armchair case, otherwise it will be semiconducting. By using this formula it is observed that a third of tubes are metallic and two thirds are semiconducting. The role of chirality in the conductivity of SWNTs has been explained with the help of the tight binding model [49].

2.4-Band Structure and Physical Properties of CNTs and Graphene

The band structure of SWNTs is most similar to the structure of graphene which is a two-dimensional sheet of carbon atoms arranged in a honeycomb lattice. The band structure of graphene has been calculated [50] for both σ and π bonds and it is observed that the directional in-plane σ bonds do not contribute to electrical conduction because of their distance from the Fermi level. The σ bonds are energetically stable and localized; they do not contribute to electrical conduction. The dispersion relation for π and π* can be expressed as

$$\qquad (2.5$$

where γ = 2.75 eV is the nearest neighbour overlap integral and k_x, k_y are the components of vector k in (k_x, k_y) plane. The sign refers to the upper (π) and lower (π*) energy bands [36]. The electronic energy dispersion as a function of two dimensional wave vector k in the hexagonal Brillion Zone (BZ) is shown in Figure 2.6. In the first BZ there are two points **K**= [(2π/3a), (2π/3√3)] and =[(2π/3a), -(2π/3√3)], where the lattices decouple and form Dirac point.

(Note: In graphene we consider an infinite boundary along x or y-axis but in case of CNTs, a periodic boundary condition along the circumference has to be considered).

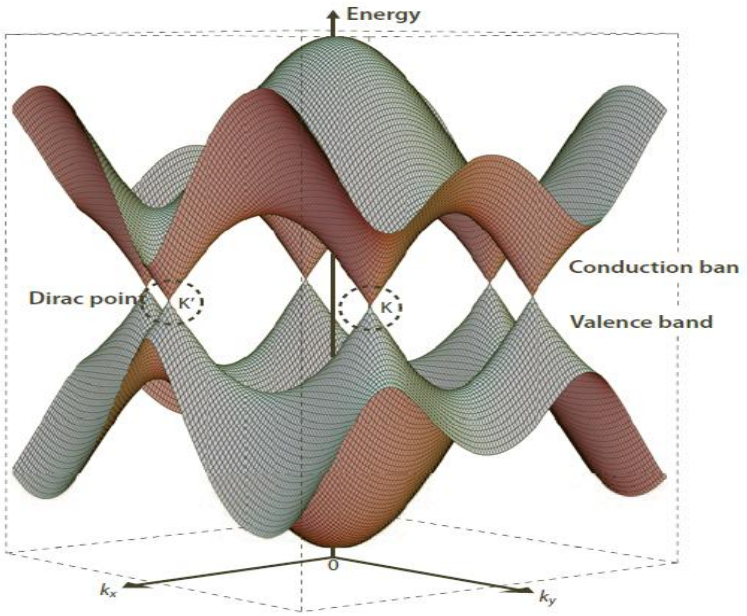

Figure 2.10 Band structure of Graphene near the Fermi level in K space [51]

At the points K and , the energy bands are degenerate as shown in Figure 2.10. If a cutting line passes through a K-point, the energy bands have a zero energy gap and the density of states at Fermi level has a finite value. This corresponds to a metal CNT. On the other hand, if a cutting line does not pass through a K-point, the CNT has a finite energy gap between valence and conduction band and the tube will be semiconducting.

2.5-Synthesising Techniques of Carbon Nanotubes

There are numerous techniques for the growth of CNTs from bulk material to a single aligned tube. Now kilograms of CNTs are grown on a daily basis. The most popular techniques for the large scale production of high quality CNTs are:

1. Arc Discharge
2. Laser Ablation
3. Chemical Vapour Deposition
4. Plasma Enhanced CVD

2.5.1-Arc discharge synthesis

The simplest and most commonly used evaporation technique for the growth of CNTs is arc discharge. In this method, a high current arc evaporates carbon electrodes and produces MWNTs. For the growth of SWNTs using this technique, a thin layer of metallic catalyst is mandatory [52]. The arc discharge system consist of a vacuum chamber with two carbon (graphite) rods working as electrodes with, a gap of ~ 1mm as shown in Figure 2.11. Helium or argon gas flows in the chamber for the purpose of cooling. When a d.c voltage of 20 to 25 V is applied across the carbon electrodes, to pass high current in the range of 70 to 100 A in the presence of 100 to 500 Torr gas pressure, it creates a high temperature (~3000 °C) discharge between the electrodes. This high temperature discharge evaporates the anode rod and makes carbon soot. The carbon soot can be collected from the cathode as well as from the chamber walls. In the growth of MWNTs using arc discharge there is no need of a catalyst, but for SWNTs a thin layer of transition metal catalyst is needed on the tip of the anode. The tubes grown by arc discharge are mostly aligned in the direction of the current flow [53].

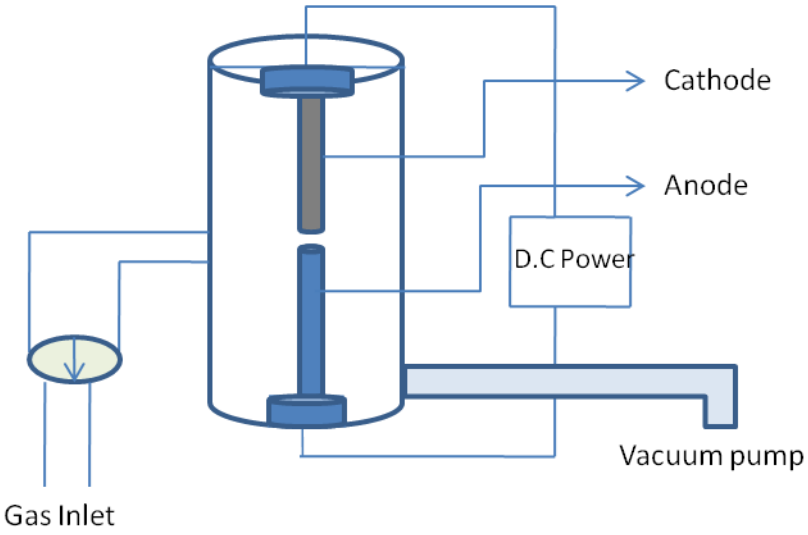

Figure 2.11 Schematic diagram of arc discharge system

Arc discharge is good for the bulk production of MWNTs, but SWNTs could be produced with the addition of some transition metal catalyst on the tip of graphite cathode.

2.5.2-Laser ablation

Laser ablation is an efficient technique to grow MWNTs and SWNTs by vaporisation of a graphite target. In this technique bulk production of SWNTs is possible with the help of a transition metal catalyst deposited on a graphite target. Laser ablation techniques for the growth of CNTs were first introduced in 1995 by Smalley's group at Rice University [54] as shown in Figure 2.12. This technique is very similar to the arc discharge method, but nanotubes grown by it are pure and the production rate is high.

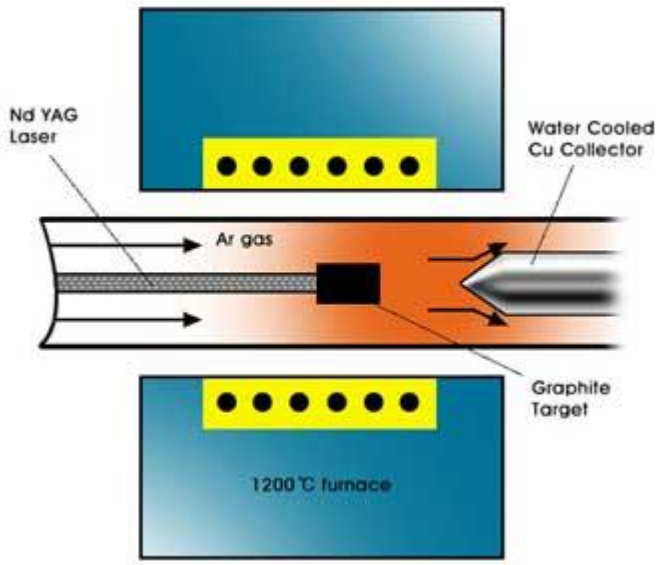

Figure 2.12 Schematic drawings of a Laser ablation appratus, adopted from "The Wondrous World of Carbon Nanotubes" [55]

The laser ablation system consists of a quartz tube with a graphite target. The laser beam enters through a window and strikes the target giving temperatures in excess of 1200 °C. The gas used in the laser ablation process is usually either argon or helium. If the target (graphite) has some conformly mixed catalyst layer on it, then SWNTs are produced [56]. Different types of lasers are available for laser ablation such as single pulsed, double pulsed and continues lasers.

2.5.3-Chemical vapour deposition (CVD)

CVD is the most popular and economical technique for the growth of SWNTs and MWNTs with the help of metal catalysts. This method has been used for the patterned growth of nanotubes on particular sites. It has been used for the deposition of high quality thin films for nanometre size from the gaseous phase on solid substrates such as Si wafers [57]. Crystal growth of electronic materials is also possible with this technique. In the CVD growth system the substrate should be covered with catalyst nanoparticles, which work as a seed for the growth of CNTs. In CVD growth, the carbon feedstock gas molecules react with solid nanoparticles on the substrate and start crystal growth [58]. In this technique, substrates are placed with quartz boat holder in the quartz tube at a high temperature furnace where feedstock gases are allowed to pass over the substrate as shown in Figure 2.13. With

solid-gas interaction CNTs start to grow. The main components of a CVD system are a temperature control unit, vacuum control unit, gas control unit and exhaust control unit. Teo et al. [59] have discussed the detailed procedure for the growth of CNTs in a CVD system.

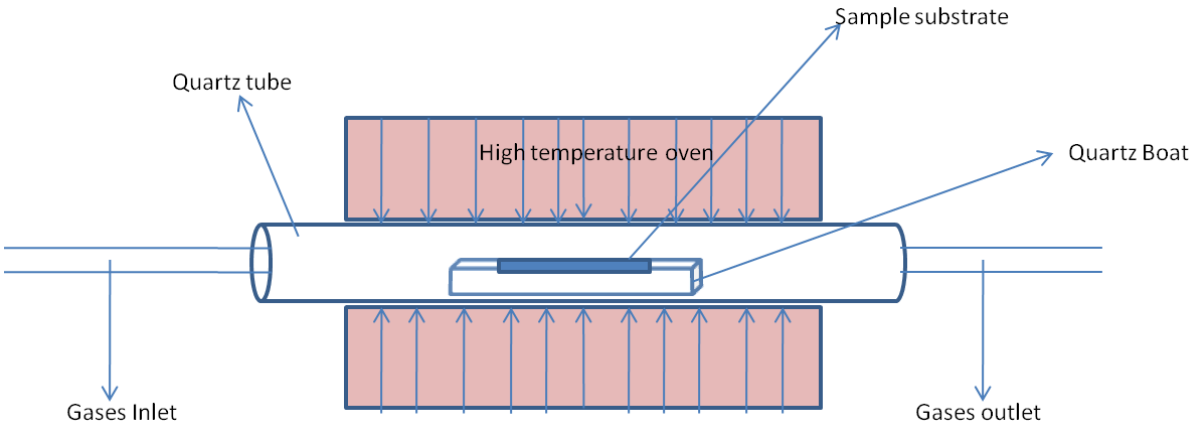

Figure 2.13 Schematic drawings of a CVD system

2.5.4-Plasma enhanced CVD (PECVD)

PECVD is the method selected for the growth of CNTs in this research study. It is a modified form of CVD by which high quality nanotubes could be grown at relatively low temperature [60-62]. In a PECVD system, electrical energy creates plasma to initiate a homogeneous gas phase chemical reaction. By this technique, surface growth of CNTs is possible on patterned catalyst layers for nano-electronic devices such as electron field emission displays, transistors, bio sensors and hydrogen energy storage devices [63-66].

Production of both SWNTs and MWNTs are possible by this technique. In the growth of nanotubes the catalyst nano-seed is very important and the size of the nanoparticles determines the diameter of the CNT.

There are different techniques to create the plasma in PECVD such as d.c, R.F, inductively coupled and microwave plasma. Plasma decreases the activation energy of the nanoparticles to initiate growth.

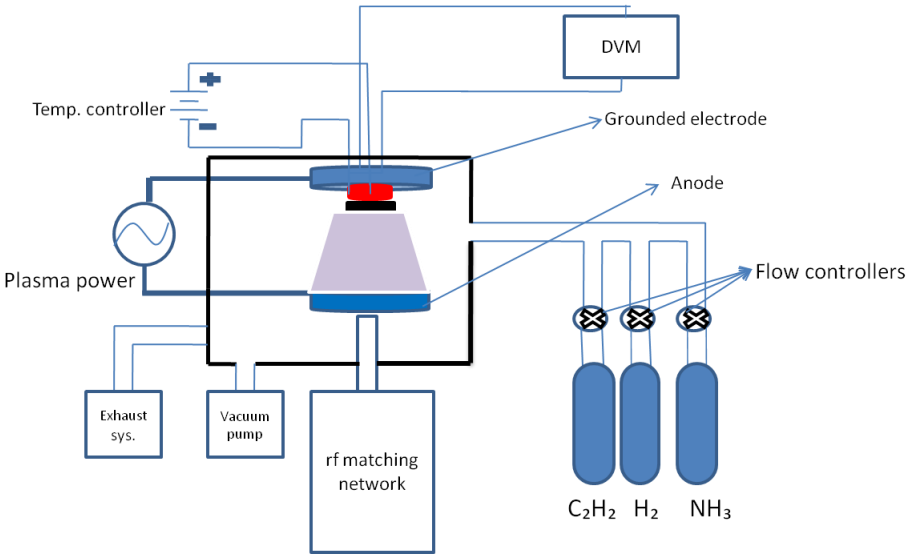

Figure 2.14 Schematic diagram of PECVD system

Nanotubes can be obtained with the help of radio frequency PECVD at low temperature, but there are some limitations with the use of R.F plasma. Firstly CNTs are not well aligned; secondly defective growths [67]; and thirdly MWNTs are produced. These issues could be reduced with the help of the catalyst and buffer layer.

2.5.4.1-Role of the catalyst in the growth of CNTs

A catalyst is very important in any chemical reaction, because it increases reaction rate by decreasing activation energy of the desired reaction. The role of the catalyst in the growth of CNTs is always crucial in the sense of growth and quality. The catalyst nanoparticles are the active nucleation sites for the growth of CNTs, also determining the properties of a tube (diameter, size and distribution). This strongly depends on the properties of the catalyst particle such as size, shape, angle of contact and particle distribution. Transition metals such as nickel (Ni), cobalt (Co) and iron (Fe) are favourable catalysts for the growth of CNTs because they form metastable carbides during reaction [68]. Some alloys of these transition metals such as Ni-Fe, nichrome and Co-Mo are also good catalysts [69-70]. During growth, the catalyst interacts with the surface of the substrate under Van der Waals forces and tubes start to grow on those particular sites where the interaction between nanoparticle and substrate is weakest [71].

2.5.4.2-Role of buffer layer

The role of the buffer layer in the growth of CNTs with PECVD is not so clear, but through the use of a buffer layer the growth density of CNTs was increased [72]. Another benefit of the buffer layer is in field emission applications where this layer plays the role of the cathode electrode underneath the CNTs [73].

The selection of suitable metal material as the support layer is always a challenge because of the conflict and ambiguity reported in literature. Some researchers support aluminium (Al) as the buffer layer because of its low evaporation temperature and higher catalytic efficiency [74-76]. Others have a different opinion and they think that CNT growth is not possible with an Al support layer since its melting temperature (650°C) is very close to the growth temperature of the CNTs. At normal CNT growth temperature, Al will melt and trap catalyst particles, and this prevents the CNT from growing [77]. There are some other publications which support other transition metals such as Cr, Cu, Ti and Ta for the growth of CNTs [78-82] because of their higher melting point. This thesis aims to resolve this problem regarding the buffer layer.

2.5.4.3-Role of plasma power

The collection of free ions and electrons in gas discharges is known as plasma [83]. Plasma plays a very important role in the formation of nanoparticles and decomposition of carbon feedstock gas. In CNT production it also decreases the activation energy of carbon atoms to precipitate and grow hexagonal structured CNTs. One more important role of plasma is the generation of an electric field between the electrodes which is helpful in aligned growth of nanotubes.

2.6-The Growth Mechanism of CNTs

The growth of CNTs by catalytic techniques follows two types of model. If the interaction energy between the substrate and catalyst is weak, then the as-grown CNTs will follow a tip growth model and the nano metal particle will be on the tip of the nanotube. On the other hand, if the interaction energy is greater, then the CNTs

will follow a base growth model and the metal nanoparticles remain on the bottom of the tubes. The schematic draw of growth models in shown in Figure 2.15.

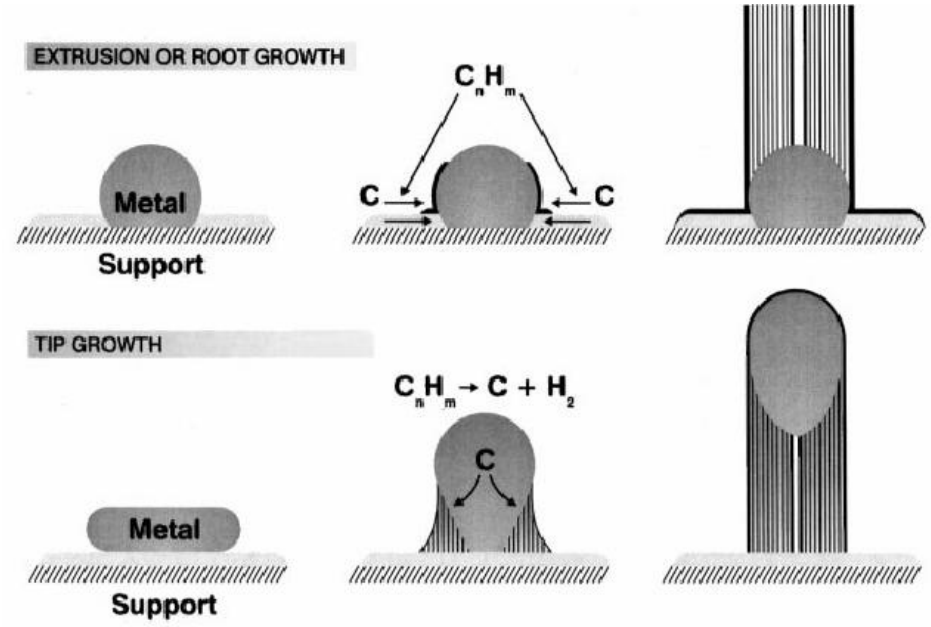

Figure 2.15 Growth models of CNT [55]

2.6.1-Base or Root growth model

In this growth model, the nanoparticles have a high adhesive force, allowing them to remain seated on the substrate during growth and the nanotubes remain open on the top end. C. J. Lee and J. Park reported the growth of CNTs by the base growth model by CVD [84]. In base growth model usually the as-grown CNTs are bamboo-shaped as shown in Figure 2.16 (a).

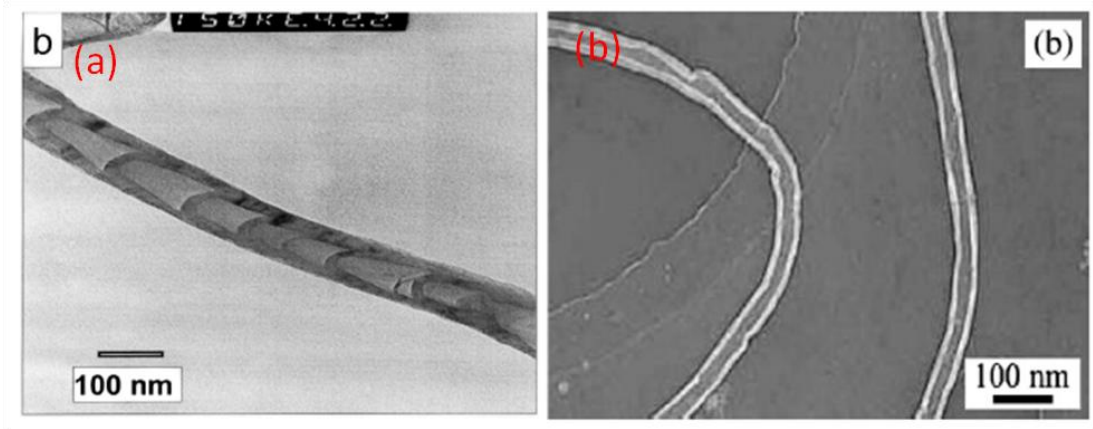

Figure 2.16 bamboo-shaped [84] and hollow CNTs [85]

2.6.2-Tip growth model

The CNTs grown by PECVD mostly follow the tip growth model. This model explains that if the interaction between catalyst and substrate is weak, the carbon atoms detach the particles and after growth of CNTs the particle remains on the tip. Mostly the as-grown CNTs are hollow as shown in Figure 2.16 (b)

2.7-Types of Defective CNTs

A CNT is straight by nature but insertion of some non-hexagonal defect in a perfect hexagonal network of atoms causes changes to the shape of the tube. These defects might be atomic dislocation, tube stress, change of aspect ratio and growth morphology of catalyst particles. After the discovery of CNTs by S. Iijima in 1991, different shapes of CNTs were theoretically predicted [86-91]. Models show that insertion of non-hexagonal defects in a hexagonal network of atoms is responsible for the CNT shape. The most common defects are pentagon-heptagon impurities in the hexagonal structure as shown in Figure 2.17.

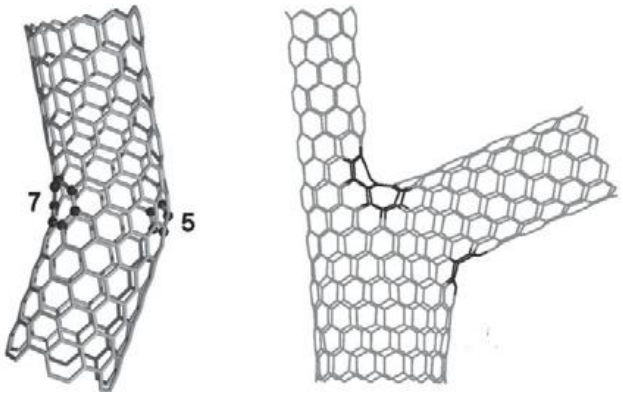

Figure 2.17 Pentagon-heptagon impurity in hexagonal network [92]

From the experimental results of different researchers, it has been observed that on the basis of experimental conditions we can grow CNTs of different shapes for different applications.

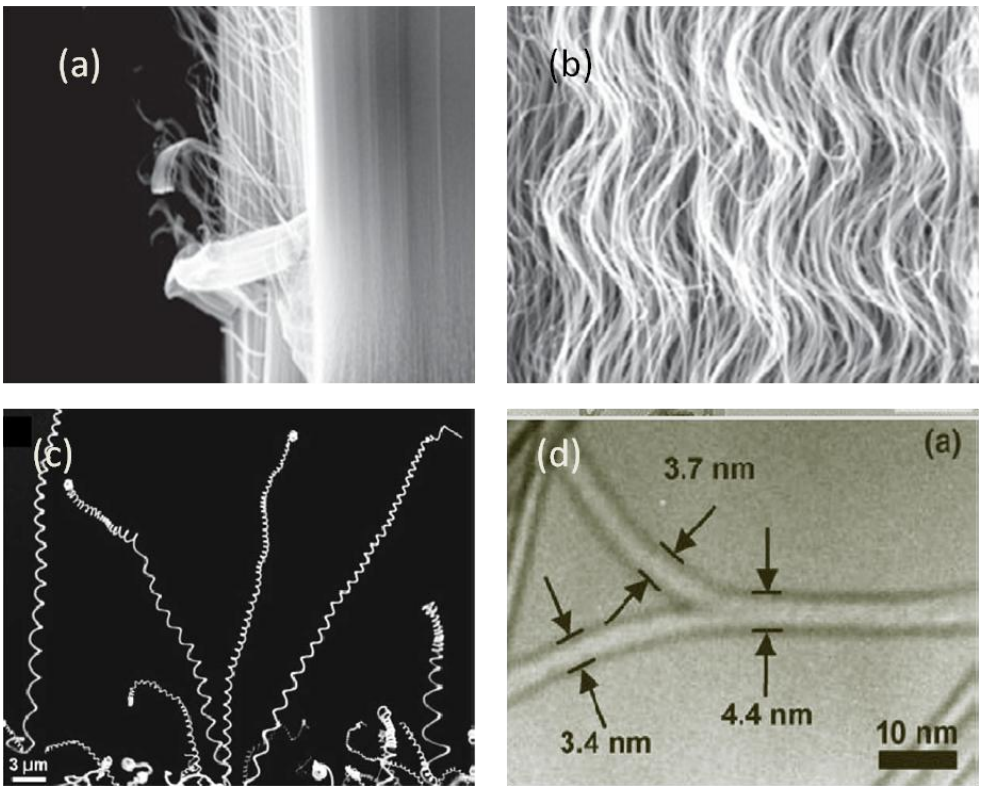

Figure 2.18 Different shapes of CNTs (a) vertically aligned (b) waved (c) coiled and (d) branched CNTs [92]

According to the theoretical models CNTs should be straight in their pure form but there are a lot of factors which make CNTs curved. In 1999 Fan et al. [93] produced

MWNTs on patterned porous silicon substrate with the help of electron beam evaporation through shadow masks. The tubes were perpendicular to the substrate as shown in Figure 2.18 (a). It is also possible to grow CNTs straight and perpendicular to the substrate with the help of external forces such as negative d.c biasing, selected gas flow direction and distribution of plasma in PECVD system. Morphology of catalyst nanoparticles is also a very important factor. If the shape of particle is uniform and their spacing controlled vertically aligned CNTs grow with the help of negative d.c biasing. Creation of completely spherical nanoparticles with uniform distribution is another objective which is only possible with electron beam lithography but is very time consuming and difficult. Cambridge University researchers reported vertically aligned CNTs growth in a CVD system by controlling carbon containing gas flow, pressure, plasma power, and by applying a d.c biasing. Applications of straight CNTs are in electron field emission, FETs and sensors [94-96].

A carbon nanotube bend because of its own weight, bending stress [97] or high aspect ratio is known as a waved or curved CNT. During growth, regular insertion of pentagon-heptagon pair defects in a hexagonal network can also give rise to waved CNTs as shown in Figure 2.18 (b). Non-uniform catalyst nanoparticles also responsible for waved structures. Growth with two groups of nanoparticles uniformly distributed over the substrate surface is the cause of regular bending. In these groups of particles, one shows a fast growth rate and the other is slow, making waved CNTs. These waved CNTs are believed to be helpful in CNTs yarn and Carbon clothes [98-100].

The third shape in CNTs produced due to the periodic insertion of pentagon-heptagon impurity pairs during growth is known as coiled CNTs. Coiled CNTs were predicted in the early 1990s and observed experimentally in 1994 by Amelinckx et al. [101]. Grobert et al. [102] explained the formation of coiled CNTs where growth depends upon the dimensions of small catalyst clusters. Applications of waved CNTs are in high performance electromagnetic wave absorbers, resonators, mechanical springs, electrical inductors and magnetic beam generators.

Branched CNTs are caused by insertion of non-hexagonal rings in hexagonal network where branches are joined. The branched CNTs were first observed in the arc-discharge method [103].

2.8-Applications of CNTs

The outstanding physical properties of CNTs made a versatile material in applications. The most common research areas for applications are electron field emission, thin film transistors, hydrogen storage, biomedical materials, AFM scanning tools and aerodynamics engineering.

A display device is a prominent and fast information sharing source which has attracted attention through the last decades. There are many different technologies of display devices such as the cathode ray tube (CRT), liquid crystal display (LCD), plasma technology, light emitting diode (LED) and field emission display (FED). The FED is based upon the electron emission from sharp cathodes by applying an electric field. The most common materials in FEDs are metals, silicon and CNTs. More recently, amorphous Si modified by laser processing has been researched in an attempt to resolve many future problems, and using conventional LCD display instruments and tools. Amorphous Si is commercially used for switching in thin film transistors (TFTs) for large area LCD display devices. Silva et al. [104] first observed that hydrogenated amorphous Si (a-Si:H) is a good electron emitter having threshold of less than 20 V/μm. Some more experiments have been conducted regarding the behaviour of a-Si:H after excimer laser irradiation. It has been observed that by laser irradiation a-Si thin films are converted into a new conducting material with a spike-like structure with good field emission capability [105-106]. Although a-Si is a novel material for display technology it has a relatively large threshold and low efficiency.

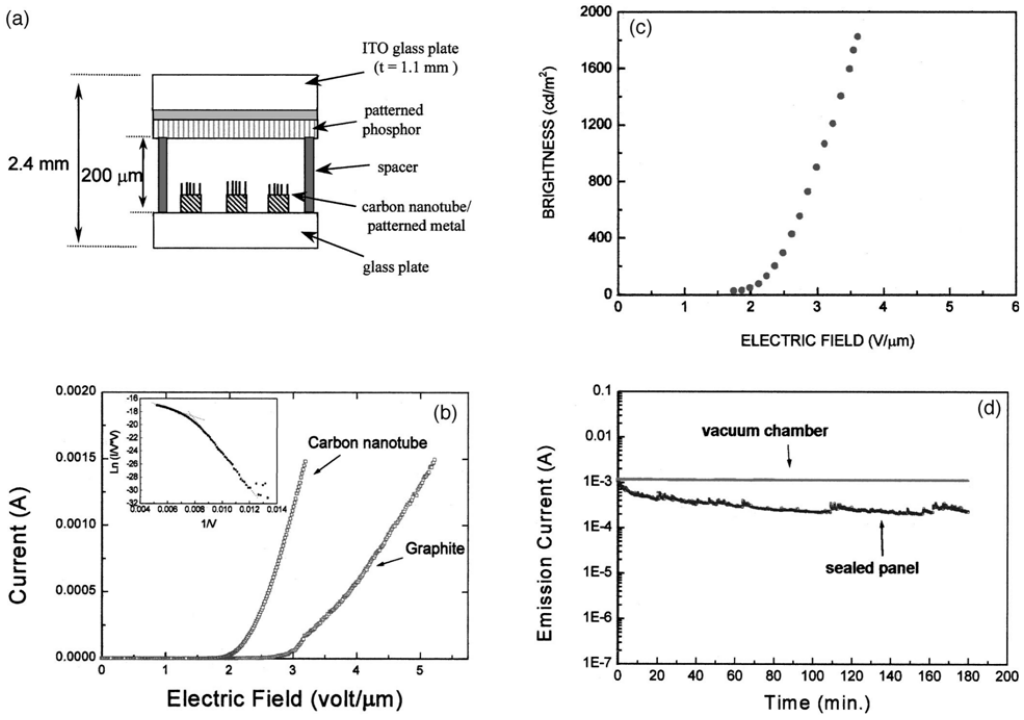

Figure 2.19 Schematic structure of CNTs flat panel display and emission current [107]

CNTs have excellent electron emission capability at low threshold. W.B. Choi et al. [107] fabricated a 4.5 inch sealed SWNTs field emission device which turns on at less than 1 V/μm with an emission current of 1.5 A at 3 V/μm as shown in Figure 2.19. Triode structure devices for field emission using CNTs were first developed by Y.S. Choi et al. [108] in 2004. They improved the field emission properties by using a patterned insulator.

Silicon based semiconducting devices attained prime importance in microelectronic technology with the birth of the first semiconducting transistor in 1948. From that time there has been an exponential growth in this industry and in device performance. The technological journey of devices from micro to nano made it possible to fabricate a large number of devices per unit area. After the discovery of CNTs, the physical properties of these tubes analysed and the unique electrical properties convinced researchers to design CNT-based electronic devices. The TFT is the backbone of flat panel display devices for pixel switching. Xiao et al. [109] prepared a TFT by fabricating aligned CNTs on a SiO_2 substrate and measured the electrical properties. Vaillancourt et al. [110] reported a flexible carbon nanotube

based TFT fabricated solely by using ink-jet printing technology on a polyimide. That device showed a high operating frequency of over 5 GHz. Recently, the world`s first sequential logic circuit using CNTs on plastic substrates was designed by Professor Yutaka Ohno at the University of Nagoya, Japan [111]. The complete logic gates are designed on plastic which opened doors to boost the plastic electronics industry by using CNTs.

A clean and environmentally friendly source of energy is hydrogen which can be used in fuel cells. As awareness is increasing, and turning to technologies we now demand safe energy production sources instead of nuclear and combustion, with alternatives such as fuel cells, wind and solar energy. Hydrogen is a source of energy with only water exhaust waste, so it is environmentally friendly and may be used in automotive applications as a fuel. The question is how to increase storage capacity of hydrogen for the new energy generation technologies. CNTs are good candidates for the storage of hydrogen. Dillon et al. [112] first observed by temperature programmed desorption (TPD) spectroscopy that SWNT cavities have hydrogen storage capacity of 5 to 10 wt%. They also predicted that SWNTs having diameters in the range of 1.6 to 2.0 nm would be more suitable for hydrogen storage. In 1999, Liu et al. [113] observed 4.2 wt% hydrogen storage in SWNTs at room temperature with high pressure (10 GPa). They explained that by increasing temperature, hydrogen could be released. In 2001 Lee et al. [114] investigated theoretically the mechanism of hydrogen storage in CNTs by using density functional calculations and predicted that hydrogen atoms could be absorbed and released through the nanotube wall with an activation barrier less than 2 eV.

The unique physical properties of CNTs made them a novel biocompatible material with potential in drug delivery [115], cancer therapy [116-117], biosensors [118], protein and DNA analysis [119-120]. This porous material is also good for the growth of cells in tissue engineering [121].

As the size of electronic devices decreases because of nano-materials, precise imaging is more important. AFM is a powerful instrument for measuring surface morphology of nano-materials. AFM tips are very fragile and need special care in

handling. After a number of scans, tips become rough and no good for further imaging. The high Young's modulus, better conductivity and excellent aspect ratio of CNTs enabled researchers to use them as probes in AFM for better resolution and high magnification. There are two ways to manipulate CNTs on the tip of cantilevers: manual attachment [122] and direct growth on the tip of cantilever [123-124]. Bunch et al. [125] observed that SWNT on an AFM tip could provide single molecule profile of a hydrated protein (RNA) with better resolution and reproducibility. They also suggested that tips may provide a general tip-surface reference standard for defining tip-surface interactions on molecular bonded organic surfaces.

References

1) Harvard University. "Chinese Used Diamonds To Polish Sapphire-rich Stone In 2500 BC."*ScienceDaily*, 13 Feb. 2005
2) Materials Research Science and Engineering Centre, University of Wisconsin Madison(http://mrsec.wisc.edu/Edetc/nanoquest/carbon/index.html)
3) L. Pauling, *The Nature of the chemical bond*, (Cornell University Press, 1948)
4) Sienko/Plane, Chemistry principle and Applications 1979
5) aBetterChemText.Com (http://abetterchemtext.com/Condensed/diamond.htm)
6) H.W. Kroto, J.R. Heath, S.C. O'Brien, R.F. Curl and R.E. Smalley, *Nature* **318**, 162(1985)
7) W. Kratschmer, L.D. Lamb, K. Fostiropoulos and D.R. Huffman, *Nature* **347**, 354(1990)
8) Carbon Technologies and Materials Russian Federation, St.-Petersburg (http://fulleren.com/index5_eng.php)
9) Fullerenes and Cosmic Carbon, *Science* **329**, 1159(2010)
10) C. Neto, F. Guinea, N.M.R. Peres, K.S. Novoseleov and A.K. Geim, *Rev. Mod. Phys.* **81**(1), 109(2009)
11) J.H. Chen, C. Jang, S. Xiao, M. Ishigami, and M.S. Fuhrer, *Nat. Nanotechnol.* **3**, 206(2008)
12) A. K. Geim and P. Kim, Carbon wonderland, *Sci. Am.* **298**, 90(2008)
13) K. S. Novoselov, A.K. Geim, S.V. Morozov, D. Jiang, Y. Zhang, S.V. Dubonos, I.V. Grigorieva and A.A. Firsov, *Science* **306**, 666(2004)
14) A. Reina, X. Jia, J. Ho, D. Nezich, H. Son, V. Bulovic, M. S. Dresselhaus, and J. Kong, *Nano Lett.* **9**, 30(2009)

15) P.R. Somani, S.P. Somani and M. Umeno, *Chem. Phys. Lett.* **430**, 56(2006)
16) Q. Yu, J. Lian, S. Siriponglert, H. Li, Y.P. Chen and S.S. Pei, *Appl. Phys. Lett.***93**, 113103(2008)
17) Z. Li, P. Wu, C. Wang, X. Fan, W. Zhang, X. Zhai, C. Zeng, Z. Li, J. Yang and J. Houet, *ACS Nano* **5**(4), 3385(2011)
18) Y.H. Wu, B.J. Yang, B.Y. Zong, H. Sun, Z.X. Shen, and Y.P. Feng, *J. Mater. Chem.* **14**, 469(2004)
19) Y.H. Wu, P.W. Qiao, T.C. Chong, and Z.X. Shen, *Adv. Mater.* **14**, 64(2002)
20) Y.H. Wu and T.C. Chong, 2001 MRS Spring Meeting, San Francisco, 16–20 April 2001, Abstract No. W8.3.
21) A.N. Obraztsov, A.A. Zolotukhin, A.O. Ustinov, A.P. Volkov, Y. Svirko and K. Jefimovs, *Diamond Relat. Mater.* **12**, 917(2003)
22) J.J. Wang, M.Y. Zhu, R.A. Outlaw, X. Zhao, D.M. Manos and B.C. Holoway, *Appl. Phys. Lett.* **85**, 1265(2004)
23) C. Berger, Z.M. Song, T.B. Li, X.B. Li, A.Y. Ogbazghi, R. Feng, Z.T. Dai, A.N. Marchenkov, E.H. Conrad, P.N. First and W.A. de Heer, *J. Phys. Chem. B* **108**, 19912(2004)
24) H. Zhang, Q. Fu, Y. Cui, D. Tan and X. Bao, *J. Phys. Chem. C* **113**, 8296(2009)
25) A.K. Geim and K.S. Novoselov, *Nat. Mater.* **6,** 183(2007)
26) M.A. Rafiee, J. Rafiee, Z. Wang, H. Song, Z.-Zhen Yu and N. Koratkar, *ACS Nano* **3**(12), 3884(2009)
27) L. Liao, Y-C. Lin, M. Bao, R. Cheng, J. Bai, Y. Liu, Y. Qu, K.L. Wang, Y. Huang and X. Duan, *Nature* **467**, 305(2010)
28) Z. Tang, H. Wu, J.R. Cort, G.W. Buchko, Y. Zhang, Y. Shao, I.A. Aksay, J. Liu and Y. Lin, *Small* **6**(11), 1205(2010)
29) T. V. Hughes and C. R. Chambers, Manufacture of Carbon Filaments, *US Patent No. 405*, **480**, (1889)
30) A. Oberlin, M. Endo, and T.Koyama, *J. Cryst. Growth* **32**, 335(1976)
31) White paper: Carbon nanotubes: Description and properties By Kai Schierholz, Chief Scientist Officer, Nanoledge Inc. April 2010
32) S. Iijima, *Nature* **354,** 56(1991)
33) T.W. Ebbesen and P.M. Ajayan, *Nature* **358**, 220(1992)
34) S. Iijima and T. Ichihashi, *Nature* **363,** 603(1993)
35) N. Hamada, S. Sawada and A. Oshiyama, *Phys. Rev. Lett.* **68**, 1579(1992)
36) R. Saito, M. Fujita, G. Dresselhaus and M.S. Dresselhaus, *Phys. Rev.B* **46**, 1804(1992)
37) J.W.G. Wildöer, L.C. Venema, A.G. Rinzler, R.E. Smalley and C. Dekker, *Nature* **391**, 59(1998)
38) T.W. Odom, J.L. Huang, P. Kim and C.M. Lieber, *Nature* **391**, 62(1998)
39) W.A. De Heer, A. Chatelain, D. Ugarte, *Science* **270**, 1179(1995)
40) M. Treacy, T.W. Ebbesen and J.M. Gibson, *Nature* **381**, 678(1996)
41) E.W. Wong, P.E. Sheehan and C.M. Lieber, *Science* **277**, 1971(1997)

42) M.R. Falvo, G.J. Clary, R.M. Taylor, V. Chi, F.P. Brooks Jr, S. Washburn and R. Superfine, *Nature* **389**,582(1997)
43) S. Frank, P. Poncharal, Z.L. Wang and W.A. de Heer, *Science* **280**, 1744(1998)
44) P.L. McEuen and J-Y. Park, *MRS Bulletin* **29**, 272(2004)
45) P. Kim, L. Shi, A. Majumdar and P.L. McEuen, *Phy. Rev. Lett.* **87**, 215502(2001)
46) J.P. Lu, *Phys. Rev. Lett.* **79**, 1279(1997)
47) E.W. Wong, P.E. Sheehan and C.M. Lieber, *Science* **277**, 1971(1997)
48) J.W.G. Wilder, L.C. Enema, A.G. Rinzler, R.E. Smalley and C. Dekker, *Nature* **391**, 59(1998)
49) R. Saito, M. Fujita, G. Dresselhaus and M.S. Dresselhaus, *Appl. Phys. Lett.* **60**, 2204(1992)
50) L.O. Biro, C.A. Bernardo, G.G. Tibbetts and Ph. Lambin, *Carbon Filaments and Nanotubes: Common Origins, differing Applications*, Kluwer Academic Publishers, Dordrechet, The Netherlands (2000)
51) T. Ando, *NPG Asia Mater.* **1**(1), 17(2009)
52) C. Journet, W.K. Maser, P. Bernier, A. Loiseau, M. Lamy de la Chapelle, S. Lefrant, P. Deniard, R. Lee and J.E. Fischer, *Nature* **388**(6644), 756(1997)
53) T.W. Ebbesen, H. Hiura, J. Fujita, Y. Ochiai, S. Matsui and K. Tanigaki, *Chem. Phys. Lett.* **209**, 83(1993)
54) R. Saito, M. Fujita, G. Dresselhaus and M.S Dreddelhaus, *Appl. Phys. Lett.* **60**(18), 2204(1992)
55) The Wondrous World of Carbon Nanotubes: a review of current carbon nanotubes technologies, Eindhoven University of Technology 2003
56) C.D. Scott, S. Arepalli, P. Nikolaev and R.E. Smalley, *Appl. Phys. A* **72**, 573(2001)
57) M. Endo, K. Takeuchi, S. Igarashi, K. Kobori, M. Shiraishi and H.W. Kroto, *J. Phys. Chem. Solids*, **54**(12), 1841(1993)
58) A.C. Jones and M.L. Hitchman, *Chemical Vapour Deposition: Precursors, Processes and Applications* (E-Book), Chapter1 (Overview of Chemical Vapour Deposition), Royal Society of Chemistry(2009)
59) K.B.K. Teo, C. Singh, M. Chhawalla, and W.I. Milne, *Encyclopedia of Nanoscience and Nanotechnology*, edited by H.S. Nalwa (American Scientific Publishers), **10**, 1-22(2003)
60) S. Kyung, Y.H. Lee, C. Kim, J.H. Lee, G.H Yeom, *Carbon* **44**, 1530(2006)
61) S. Hofmann, B. Kleinsorge, C. Ducati and J. Robertson, *New J. Phys.* **5**, 153.1(2003)
62) E.J. Bae, Y.S. Min, D. Kang, J.H. Ko, W. Park, *Chem. Mater.* **17**(20), 5141(2005)
63) Y.S. Choi, J.H. Kang, H.Y. Kim, B.G. Lee, C.G. Lee, S.K. Kang, Y.W. Jin, J.W. Kim, J.E. Jung and J.M. Kim, *Appl. Surf. Sci.* **221**, 370(2004)

64) R. Martel, T. Schmidt, H.R. Shea, T. Hertel, P. Avourisa, *Appl. Phys. Lett.* **73**(17), 122477.1(1998)
65) C. Liu, Y.Y. Fan, M. Liu, H.T. Cong, H.M. Cheng and M.S. Dresselhaus, *Science* **286**, 1127(1999)
66) B. Pérez, M. Pumera, M. Valle, A. Merkoçi and S. Alegret, *J. Nanosci. Nanotechnol.* **5**(10), 1694(2005)
67) T. Jutarosaga, S. Seraphin, S.M. Smith, Y. Wei, *Microsc. Microanal.* **12**(supp2), 662(2006)
68) P.B. Balbuena, J. Zhao, S. Huang, Y. Wang, N. Sakulchaicharoen and D.E. Resasco, *J. Nanosci. Nanotechnol.* **6**, 01(2006)
69) X.Z. Liao, A. Serquis, Q.X. Jia, D.E. Peterson, Y.T. Zhu and H.F. Xu, *Appl. Phys. Lett.* **82**(16), 2694(2003)
70) H. Cui, G. Eres, J.Y. Howe, A. Puretkzy, M. Varela, D.B. Geohegan, D.H. Lowndes, *Chem. Phys. Lett.* **374**, 222(2003)
71) W. Zhou, L. Ding and J. Liu, *Nano Res.* **2**, 593(2009)
72) B. Wang, X. Liu, H. Liu, D. Wu, H. Wang, J. Jiang, X. Wang, P. Hu, Y. Liu and D. Zhu, *J. Mater. Chem.* **13**(5), 1124(2003)
73) J.H. Han, J.E Yoo and C.J. Lee, *J. Korean Phys. Soc.* **39**, 116(2001)
74) T. Ižák, M. Veselý, T. Daniš, M. Marton, M. Michalka and M. Kadlečíková, *Vacuum* **82**, 134(2008)
75) I.T. Han, B.K. Kim, H.J. Kim, M. Yang, Y.W. Jin, S. Jung, N. Lee, S.K. Kim, J.M. Kim, *Chem. Phys. Lett.* **400**, 139(2004)
76) L. Xianming, K.H.R. Baronian and A.J. Downard, *Carbon* **47**, 500(2009)
77) J. Wei, K.P. Yung and B.K. Tay, *SIMTech technical reports* **10**(1), 1(2009)
78) Y. Wang, Z. Luo, B. Li, P.S. Ho, Z. Yao, L. Shi, E.N. Bryan and R.J. Nemanich, *J. Appl. Phys.* **101**, 124310.1(2007)
79) W. Zhou, Z. Han, J. Wang, Y. Zhang, Z. Jin, X. Sun, Y. Zhang, C. Yan and Y. Li, *Nano Lett.* **6**(12), 2987(2006)
80) C.C. Chuang, W.L. Liu, W.J. Chen and J.H. Huang, *Surf. Coat. Technol.* **202**, 2121(2008)
81) W.S. Choi, S-H. Choi, B. Hong, D-G. Lim, K-J. Yang and K-J. J-H. Lee, *Mater. Sci. Eng.* **C26**, 1211(2006)
82) Y. Wan, B. Li, S.H.Z. Yao and L. Shi, *Appl. Phys. Lett.* **89**, 183113.1(2006)
83) H. Sato and K. Hata, *New Diamond Front. Carbon Technol.* **16**(3), 163(2006)
84) C. J. Lee and J. Park, *Appl. Phys. Lett.* **77**(21), 3397(2000)
85) Z. Wang, D. Jia, S. Liu and M. Zhang, *Mater. Lett.* **62**, 3288(2008)
86) S. Ihara, S. Itoh and J. Kitakami, *Phys. Rev. B* **47**, 12908(1993)
87) B.I. Dunlap, *Phys. Rev. B* **46**, 1933(1992)
88) S. Ihara, S. Itoh and J. Kitakami., *Phys. Rev. B* **48**, 5643(1993)
89) A.L. Macky and H. Terrones, *Nature* **352**, 762(1991)
90) G.E. Scuseria, *Chem. Phys. Lett.* **195**, 534(1992)

91) L.A. Chernazatonskii, *Phys. Lett. A* **172**,173(1992)
92) M. Zhang and J. Li, *Mater. Today* **12**(6), 12(2009)
93) S.S. Fan, M.G. Chapline, N.R. Franklin, T.W. Tombler, A.M. Cassell and H. Dai, *Science* **283**, 512(1999)
94) S.J. Tans, A.R.M. Verschueren and C. Dekker, *Nature* **393,** 49(1998)
95) J. Kong, N.R. Franklin, C. Zhou, M.G. Chapline, S. Peng, K. Cho and H. Dai, *Science* **287,** 622(2000)
96) J.A. Misewich, R. Martel, Ph. Avouris, J.C. Tsang, S. Heinze and J. Tersoff, *Science* **300**, 783(2003)
97) S. Iijima, C. Brabec, A. Maiti and J. Bernholc, *J. Chem. Phys.* **104**, 2089(1996)
98) M. Zhang, K.R. Atkinson and R.H. Baughman, *Science* **306**, 1358(2004)
99) M. Zhang, S. Fang, A.A. Zakhidov, S.B. Lee, A.E. Aliev, C.D. Williams, K.R. Atkinson and R.H. Baughman, *Science* **309**, 1215(2005)
100) X. Zhang, K. Jiang, C. Feng, P. Liu, L. Zhang, J. Kong, T. Zhang, Q. Li and S. Fan, *Adv. Mater.***18**, 1505(2006)
101) S. Amelinckx, X.B. Zhang, D. Bernaerts, X.F. Zhang, V. Ivanov and J.B. Nagy, *Science* **265**, 635(1994)
102) N. Grobert, M. Terrones, S. Trasobares, K. Kordatos, H. Terrones, J. Olivares, J.P. Zhang, Ph. Redlich, W.K. Hsu, C.L. Reeves, D.J. Wallis, Y.Q. Zhu, J.P. Hare, A.J. Pidduck, H.W. Kroto and D.R.M. Walton, *Appl. Phys. A* **70**, 75(2000)
103) D. Zhou, and S. Seraphin, *Chem. Phys. Lett.* **238**, 286(1995)
104) S.R.P. Silva, R.D. Forrest, J.M. Shannon and B.J. Sealy, *J. Vac. Sci. Technol., B* **17** (2), 596(1999)
105) Y.F. Tang, S.R.P. Silva, B.O. Boskovic, J.M. Shannon and M.J. Rose, *Appl. Phys. Lett.* **80**(22), 4154(2002)
106) Y. Fan, M.J. Rose, S.K. Persheyev and M.Z. Shaikh, *Symposium on Photonics and Optoelectronics*, 1(2009)
107) W.B. Choi, D.S. Chung, J.H. Kang, H.Y. Kim, Y.W. Jin, I.T. Han, Y.H. Lee, J.E. Jung, N.S. Lee, G.S. Park and J.M. Kim, *Appl. Phys. Lett.* **75**(20), 3129(1999)
108) Y.S. Choi, J.H. Kang, H.Y. Kim, B.G. Lee, C.G. Lee, S.K. Kang, Y.W. Jin, J.W. Kim, J.E. Jung and J.M. Kim, *Appl. Surf. Sci.* **221,** 370(2004)
109) K. Xiao, Y. Liu, P. Hu, G. Yu, X. Wang and D. Zhu, *Appl. Phys. Lett.* **83**(1), 150(2003)
110) J. Vaillancourt, H. Zhang, P. Vasinajindakaw, H. Xia, X. Lu, X. Han, D.C. Janzen, Wu-Sh. Shih, C.S. Jones, M. Stroder, M.Y. Chen, H. Subbaraman, R.T. Chen, U. Berger and M. Renn, *Appl. Phys. Lett.* **93**, 243301(2008)
111) D. Sun, M.Y. Timmermans, Y. Tian, A.G. Nasibulin, E.I. Kauppinen, S. Kishimoto, T. Mizutani and Y. Ohno, *Nat. Nanotechnol.* **6**,156(2011)

112) A.C. Dillon, K.M. Jones, T.A. Bekkedahl, C.H. Kiang, D.S. Bethune and M.J. Heben, *Nature* **386**, 377(1997)
113) C. Liu, Y.Y. Fan, M. Liu, H.T. Cong, H.M. Cheng and M.S. Dresselhaus, *Science* **286**, 127(1999)
114) S.M. Lee, K.H. An, Y.H. Lee, G. Seifert and T. Frauenheim. *J. Korean Phys. Soc.* **38**(6), 686(2001)
115) A. Bianco, K. Kostarelos and M. Prato, *Curr. Opin. Chem. Biol.* **9**, 674(2005)
116) N. Wong, S. Kam, M. O'Connell, J.A. Wisdom and H. Dai, *PNAS* **102**(33), 1600(2005)
117) X. Yang, Z. Zhang, Z. Liu, Y. Ma, R. Yang and Y. Chen, *J. Nanopart. Res.***10**, 815(2008)
118) R.G. Compton, G.G. Wildgoose, and E.L.S. Wong, *Biosensing Using Nanomaterials,* Edited by Arben Merkoci, 2009 John Wiley & Sons, Inc.
119) S. Meng, P. Maragakis, C. Papaloukas, and E. Kaxiras, *Nano Lett.* **7**(1), 45(2007)
120) M. Zheng, A. Jagota, M.S. Strano, A.P. Santos, P. Barone, S. G. Chou, B.A. Diner, M.S. Dresselhaus, R.S. Mclean, G.B. Onoa, G.G. Samsonidze, E.D. Semke, M. Usrey and D.J. Walls, *Science* **302**, 1545(2003)
121) A. Abarrategia, M.C. Gutiérrez, C. Moreno-Vicente, M.J. Hortigüela, V. Ramos, J.L López-Lacomba, M.L. Ferrer and F.D. Monte, *Biomaterials* **29**, 94(2008)
122) R. Stevens, C. Nguyen, A. Cassell, L. Delzeit, M. Meyyappan and J. Han, *Appl. Phys. Lett.* **77** (21), 3453(2000)
123) J.G. Wen, Z.P. Huang, D.Z. Wang, J.H. Chen, S.X. Yang, Z.F. Ren, J.H. Wang, L.E. Calvet, J. Chen, J.F. Klemic and M.A. Reed, *J. Mater. Res.* **16** (11), 3246(2001)
124) T.S. Druzhinina, S. Hoeppener and U.S. Schubert, *Nano Lett.* **10**, 4009(2010)
125) J.S. Bunch, T.N. Rhodin and P.L. McEuen, *Nanotechnology* **15**, S76(2004)

CHAPTER 3 NANO-COMPOSITE MATERIALS

A multiphase solid material which has dimensions in the range of 100 nm is known as a nano-composite material. According to Ajayan et al. [1], one of its constituent materials must have at least one dimension on the nanometer scale. A nano-composite mat is good for the enhancement of electrical and mechanical properties of materials.

This chapter aims to explain the role of nano-composites in different fields such as displays, energy and the environment. The first section is dedicated to polymer materials: their conductivity, ballistic transport and mechanical strength. The role of CNTs in flexible devices is also discussed in that section. The second section is dedicated for PEMFCs. The current status of the PEMFC market, issues regarding catalyst material and problems related with the conventional membrane is discussed in this section. An important role of nanoparticles is photocatalytic ability. The third section explains briefly photocatalyst for self cleaning and water splitting activity in the generation of hydrogen for fuel cells.

3.1-Polymer and Nano-composite Material

Nanoparticles and nanotubes on polymer have great interest for researchers for the development of flexible nano devices. The conventional techniques for the creation of nanoparticles and tubes require high temperature, which reduces usability. Excimer laser processing makes this possible at room temperature. Now with excimer laser it is relatively straight-forward to modify plastic substrates. This offers

a number of potential applications in the field of flexible energy and biomedical devices. A detailed discussion about the formation of nanoparticles on plastic substrates will be given in Chapter 6.

3.1.1-Polymer

Polymer or plastic is a big class of natural and synthetic materials typically consisting of long chains of equivalent units (monomers) covalently bonded together [2]. Because of the long molecular chains in these materials, they can have softness, flexibility and can bear stress because of the strong bonding. Polymers are playing a very important role in human life. The human body contains different types of polymer such as DNA, amino acids and proteins. Because of the compatibility of polymers with the human body, researchers are trying to make devices on polymers which can be helpful in drug delivery, sensing and manmade organs with polymers which can perform the same task as natural organs in the body. Also, in the electronics industry, research is ongoing on flexible, cheap, lightweight and easy available material. Polymers have all of these properties. Because of the outstanding properties of polymer in the electronic, mechanical and biomedical industry, researchers are trying to make nano-composite materials. Although most polymers are not good conductors of heat or electricity, insertion of some nano materials could improve the conductivity in polymer composites. The role of CNTs in the preparation of transparent and flexible conductors is crucial. Also the mechanical properties of polymers could be improved with nano-fillers in solution based techniques. The problem with polymers is that they are not stable at higher temperature. The available polymers only tolerate temperatures up to 200°C. Research is going on in the polymers as there is a big class of materials from insulating to conducting and from soft plastic packing material to transparent PESPEX© sheets. The use of nano-materials in polymers is good to make it strong, catalytically active and conducting.

3.1.2-CNTs with polymers

The extraordinary mechanical properties of CNTs and carbon fibre make them attractive for the enhancement of mechanical properties of polymer materials [3]. The CNTs are ideal candidates as fillers in polymers to reinforce the polymer matrix for improvement in their shearing strength. There are different techniques to prepare CNTs-polymer composite material such as electrophoretic deposition, solution base deposition and direct growth of CNTs on polymer material.

To date there has been little work on the growth or transfer of CNTs on plastic materials. Direct transfer of as-grown vertically aligned CNTs on polycarbonate by heating up to the softening temperature was demonstrated by Tsai et al. [4]. They also checked the field emission capability of CNTs. The direct growth of CNTs on thick polyimide was reported in 2003 by Hofmann et al. [5]. They grew CNTs at 200°C by using a PECVD system. They also measured the field emission properties of as-grown CNTs on plastic and concluded that the result of field emission was same as from a Si substrate.

The use of CNTs and carbon nano fibres play an important role in the enhancement of mechanical properties of polymers. By using nano-fillers in polymer the tensile stress and shearing strain could be improved. A detailed study of CNTs-polymer composite materials has been carried out by Ciselli [6]. He prepared solution based nano-polymer composite and analyzed the mechanical properties of CNTs. The process of nano-composites by a solution based method has some disadvantages regarding dispersion and solvent contamination

Direct growth of CNTs on polymers and other substrates, provides novel materials for industrial and scientific applications. It could be a material for flexible sensors, a proton conductor in polymer membrane fuel cells or an active matrix for blood dialysis.

3.2-The Polymer Electrolyte Membrane Fuel Cell (PEMFC)

An aim of this research work is to develop a one step process to make a proton exchange device. A polymer electrolyte membrane fuel cell is a device in which the electrolyte is made of a proton conducting polymer. The first PEM fuel cell was invented by Thomas Grubb and Leonard in 1960 [7]. Initially, a polystyrene membrane was used as the electrolyte.

PEMFC was first used in NASA's Gemini V space program. In a PEM fuel cell hydrogen is used as a fuel which ionizes on the anode because of catalytic activity and decomposes into protons and electrons. The reactions at the anode and cathode are

Anode $H_2 \rightarrow 2H^+ + 2e^-$

Cathode $1/2O_2 + 2H^+ + 2e^- \rightarrow H_2O$

The main components of a PEMFC are

1. Hydrogen
2. Anode of nanoparticles on carbon
3. Polymer H^+ conducting electrolyte
4. Cathode of nanoparticles on carbon
5. Air (O_2/N_2)

In a PEMFC, the hydrogen molecules on the anode split into protons and electrons. The electrons are forced to go towards an external circuit for electricity and protons pass through the polymer membrane, reacting with oxygen supplied on the cathode resulting in water. The temperature required for the reaction is from 60 to 90°C as shown in Figure 3.1.PEMFCs are very popular in the renewable energy industry because of low temperature operation, high power density, compact system structure and ease of sealing.

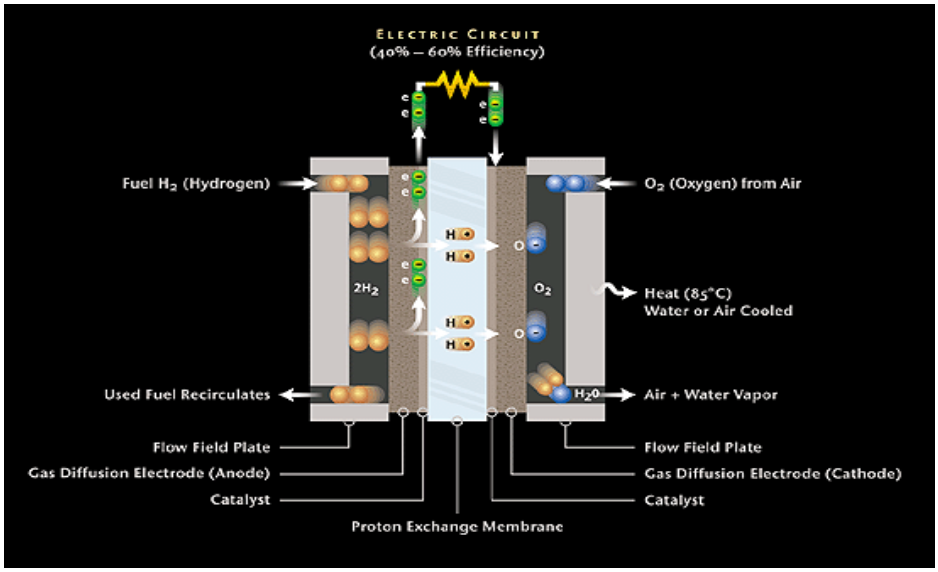

Figure 3.1 The schematic draw of fuel flow in PEM fuel cell

3.2.1-PEMFC market

Fuel cell technology is a new and fast growing energy technology. There are three main markets of PEMFCs: stationary power, transportation power, and portable power such as stationary power generators, fuel cell automobiles and portable devices such as calculators, laptops and mobile phones respectively.

According to the "2010 Fuel Cell Technologies market Report" Published by U.S Department of Energy [8], the fuel cell market is growing rapidly. In 2010 the American Recovery and Reinvestment Act (ARRA) provided a substantial boost to the U.S fuel cell industry by allocating $41.9 million for its commercialisation. Similarly a big increase in the sale of residential fuel cell units was observed in Japan and they aim to sell two million fuel cell vehicles by 2025. Table 3.1 shows the current worldwide hydrogen fuel cell products.

Table 3.1: ***Current commercially available PEMFC products [8]***

Manufacturer	Product Name	Application	Output
Ballard	FCVelo City 9SSL	Materials Handling Forklifts Classes I, II, and III	4.4 - 19.3 kW
	Gen 1030	Residential Cogeneration	1.2 kW
	FCGen 1020A CS	Back-up power	0.3 – 3.4 kW
	FCVelo City	Bus and Heavy Duty Trucks	75 and 150 kW
ClearEdge Power	CE5	Residential CHP	500 W
Horizon	H-100	Uninterrupted Power Supply	100 W
	H-1000	Uninterrupted Power Supply	1 kW
	H-3000	Uninterrupted Power Supply	3 kW
	GreenHub	Uninterrupted Power Supply	500 w – 2 kW
	MiniPak	Portable Battery Charger	100 W
Hydrogenics	HyPM XR Power Modules	Stationary	4, 8, 12 kW
	HyPM Rack	Stationary	Multiples of 10, 20, 30 kW
	FCXR System	Stationary	150 kW
	HyPM HD Power Modules	Mobility	4, 8, 12, 16 kW
	HyPX Power Packs	Class 1 Forklift Trucks	8 - 12 kW
IdaTech	ElectraGen™ 3	Backup Power for Telecom	3 kW
	ElectraGen™ 5	Backup Power for Telecom	5 kW
	ElectraGen™ H2-I	Backup Power for Telecom	2.5 - 5 kW
	iGen™	Portable, Backup Power for Telecom	250 W
	ElectraGen ™ ME	Backup Power for Telecom	2.5 - 5 kW
Morphic Technologies	Mira 6	Boats, Forklifts, APU	6 kW

	Max-E 3600	Battery Charger for RV	150 w
	Polaris TLC	Backup Power for Telecom	5Kw
	Polaris 5	APU	5 kW
	Orion5	APU	5 kW
	Orion1	Residential CHP	Unknown
Nuvera	PowerEdge CS25, CM25, CM32, RL25	Counterbalance Lift Trucks and Reach Trucks	25 kW – 31 kW
	PowerFlow PFV-5	Industrial Vehicles	5 kW
	Andromeda Fuel Cell Stack	Transportation	100 kW
	HDL-82 Power Module	Transportation	82 kW
Plug Power	GenDrive 160	Materials Handling Vehicles	8.7 kW
	GenDrive 170	Materials Handling Vehicles	10.1 kW
	GenDrive 240	Materials Handling Vehicles	10.5 kW
	GenDrive 312	Materials Handling Vehicles	2.6 kW
	GenCore® 5T Series	Backup -Telecom	5 kW
	GenCore® 5U Series	Backup -Utilities	5 kW
	GenCore® 5B Series	Backup - UPS	5 kW
	GenSys 6U48	Residential CHP, Backup Power	6 kW
Protonex	M300-CX	Portable Battery Charger	300 W
	UAV-C250	UAV Power Source	250 W
	UGV-C250	UGV Power Source	250 W
Relion	T-1000	Backup	600 - 1200 W
	T-2000	Backup	600 W - 2kW
	I-1000	Backup	1 kW
Trulite	KH4 Power System	Portable	150 W - 250 W
UTC Power	PureMotion® 120 System	Transportation	120 kW
	PureCell® System Model 5	Backup	5 kW

3.2.2-Catalyst Issues

The catalyst in a fuel cell plays a very important role in the separation of protons and electrons at the anode. The platinum-group metals are popular for catalytic reactions in fuel cells, but they are very expensive and research is ongoing to replace Pt with cheaper metal to reduce the cost of fuel cells. The other drawback is the control of water flow. With the flow of water in the fuel cell the Pt nanoparticles also segregates and slowly the performance of the fuel cell decreases. The acidic solution of water sometimes dissolves nanoparticles. It is possible to reduce the cost of PEMFC by replacing platinum with CNTs and other metal nanoparticles. CNTs have good storage capability of hydrogen fuel and by direct growth with catalyst Ni on the top could be helpful for the stability of nanoparticles.

3.3-Photocatalytic Activity of Nanomaterials

Another interesting activity of nanoparticles is photocatalysis. When the photons of UV light with energy equal to or greater than the band gap of a semiconductor catalyst are incident on it, an electron can be promoted to the conduction band and a positive hole remaining behind results in free radicals which are efficient oxidizers of organic matter, as illustrated in Figure 3.2. Photocatalysis could be important in water purification. Environmental friendly hydrogen gas can also be produced by water hydrolysis. The quality of drinking water is always very important because there are number of diseases caused by organic pollutants in water. Zeltner et al. [9] developed a technique to degrade water contaminants using photocatalysis. This process detoxifies waste water through sun light and heterogeneous catalysts [10]. TiO_2 is a good candidate as a photocatalyst for the purification of water and air [11].

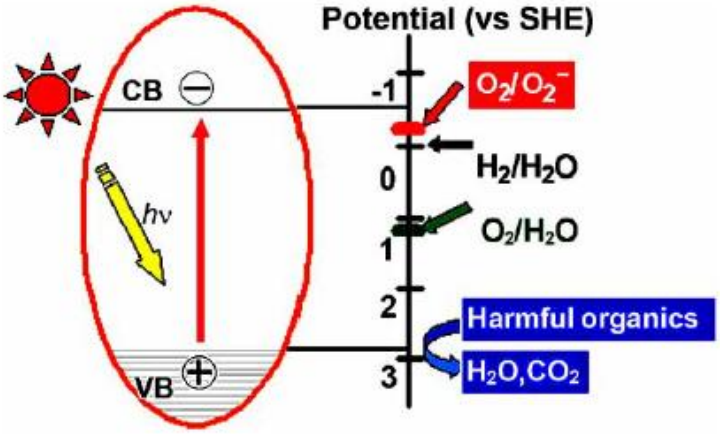

Figure 3.2 Schematic drawing of the possible Photocatalytic reaction mechanism [12]

Excellent mechanical properties and large surface area of CNTs made it possible to use them in the enhancement of photocatalytic activity of semiconducting materials. The photocatalyst-CNTs composite works as a semiconductor-metal junction Schottky barrier which increases the recombination time of electron hole pairs by the depletion layer between them which maintains charge separation [13]. This Schottky barrier absorbs more amounts of pollutants. The property of CNTs which may increase recombination time is its electron storage capacity which accepts more photon excited electrons and increases photocatalytic efficiency [14]. Lee et al. [15] prepared TiO_2-MWNTs nano composites photocatalyst by a sol-gel process. They observed that the large surface area of CNTs could provides more binding surfaces for charge carrier trapping for more efficient photo catalytic degradation.

3.3.1-Photocatalytic activity and water splitting

One application of photocatalyst is the production of hydrogen by water splitting as shown in the reaction below.

$$H_2O + 2h^+ \rightarrow 1/2O_2 + 2H^+ \qquad \text{(Oxidation)}$$

$$2H^+ + 2e^- \rightarrow H_2 \qquad \text{(Reduction)}$$

$$H_2O + h\upsilon \rightarrow H_2 + 1/2O_2 \qquad \text{(Overall Reaction)}$$

When UV light of suitable wavelength is incident on the photocatalyst, it produces an electron-hole pair. Before recombination, a redox reaction splits water into hydrogen and oxygen. A number of materials have been studied as photocatalysts such as TiO_2, ZnO, ZnS, $SrTiO_3$ and some nano composites are the most thoroughly investigated in the literature [16-17].

3.3.2-Amorphous silicon for water splitting

Amorphous silicon has been actively researched as an electronic material for over thirty years. The outstanding performance of this material allowed its use for conformal and large scale coating on a variety of substrates at a low temperature [18]. It is widely used in the electronics industry for applications such as thin film transistors, solar cells and photoreceptors [19]. The low electron mobility of this material due to micro-strutcral defects made it unsuitable for the high speed display devices. Poly crystalline Si is a better option to meet the demands of high speed diplay devices. Zhu et al. [20] fabricated a photoelectrochemical (PEC) cell by using hydroened amorphous silicon carbide (a-SiC:H) for water splitting. They concluded that high quality a-Si:H with the addition of carbon not only increased its band gap ($\geq$ 2.0 eV) but also improved its corrosion resistance in the equeous electrolyte. By utilizing the density functional theory (DFT) calculations Zang et al. predicted that silicon nano-wires terminated with suitable hydrogen and chlorine surface coverage should be a promisingphotocatalytic for water splitting [21].

There are some techniques to convert amorphous Si into conducting Si such as thermal annealing and excimer laser irradiation. Thermal annealling require high temperature which is not suitable for flexible (polymer) substrates. On the other hand excimer laser is a low temperature technique of converting smooth surface of a-Si into conducting crystalline silicon with higher electron mobility. The excimer laser pulses of nanometer wavelength only absorbed by Si and modify it with minimum effect on the substrate. The low temperature processing made it possible to fabricate electronic devices on flexible (plastic) substrates [22]. The detailed discussion about the deposition of a-Si:H film and surface modefication by excimer laser irradiation will be described in Chapter 6.

References

1) P.M. Ajayan, P. Redlich and M. Rühle, *J. Microscopy* **185**(2), 275(1997)
2) Chapter1 by R.G. Linford 'Applications of Electro active polymers' edited by B. Scrosati Published by Chapman& Hall London (1993)
3) S. Bal and S.S. Samal, *Bull. Mater. Sci.* **30**(4), 379(2007)
4) T.Y. Tsai, C.Y. Lee, N.H. Tai, and W.H. Tuan, *Appl. Phys. Lett.* **95**, 013107(2009)
5) S. Hofmann, B. Kleinsorge, C. Ducati and J. Robertson, *New J. Phys.* **5**, 153.1(2003)
6) Paola Ciselli, PhD Thesis Eindhoven University of Technology Italy (2007)
7) X-Zi Yuan and H. Wang, PEM fuel cell fundamentals: PEM fuel cell electrocatalysts and catalysts layers by Zhang, Jiujun 1st edition 2008 Springer
8) 2010 Fuel Cell Technologies Market Report, compiled by the staff of the Breakthrough Technologies Institute, Inc., in Washington, DC. U.S. Department of Energy
9) W.A. Zeltner and M.A. Anderson, The use of nanoparticles in environmental applications. In: Pelizzetti E. ed. Fine Particles Science and Technology. Kluwer Academic Publishers, 643(1996)
10) Y. Zhang, J.C. Crittenden, D.W. Hand and D.L. Perram, *Environ. Sci. Technol.* **28**, 435(1994)
11) M.R. Hoffmann, S.T. Martin, W. Choi and D. Bahnemann, *Chem. Rev.* **95**, 69(1995)
12) D. Chen, *Recent Patents on Nanotechnology* **2**, 183(2008)
13) A.L. Linsebigler, G.Q. Lu and J.T. Yates, *Chem. Rev.* **95**, 735(1995)
14) A. Kongkanand and P.V. Kamat, *ACS Nano* **1**, 13(2007)
15) S.H. Lee, G. Pyrgiotakis and W. Sigmund, *Journal of the European Academy of Science* **1**(1), 2011
16) R.F. Howe, Dev. *Chem. Eng. Mineral Process.* **6**(1), 55(1998)
17) S.T. Aruna and K.C. Patil, *J. Mater. Synth. Process.* **4**(3), 175(1996)
18) C.R. Wronski, J.M. Pearce, R.J. Koval, A.S. Ferlauto and R.W. Collins, *RIO 02 - World Climate & Energy Event,* 68(2002)
19) P.G**.** LeComber, *Phys. Scr.* **45**, 22(1992)
20) F. Zhu, J. Hu, I. Matulionis, T. Deutsch, N. Gaillard, E. Miller and A. Madan, *Philos. Mag.* **89**(28), 2723(2009)
21) R.Q. Zhang, X.M. Liu, Z. Wen and Q. Jiang, *J. Phys. Chem. C* **115**, 3425(2011)
22) N.D. Young, D.J. McCulloch and R.M. Bunn, *Digest of Technical Papers AM-LCD* **97**, 47(1997)

CHAPTER 4 EXPERIMENTAL TECHNIQUES

This chapter aims to provide a description of the experimental techniques adopted in this research from sample preparation to the growth of CNTs and graphene. The characterization techniques used to explain surface features and growth results of CNTs is also explained.

The first section of this chapter is about the thin film preparation techniques (deposition techniques) on solid substrates such as Si wafer, eagle glass and polymers (PEN and Nafion). Additionally, the PECVD system for the deposition of a-Si films on different substrates is discussed. The second section briefly explains the PECVD system used for the growth of the CNTs and graphene in this research. All the components of the PECVD system are explained here. The final section is covering characterization and measurement techniques utilized in this research.

4.1-Deposition Techniques

Two techniques, d.c sputtering and thermal deposition were used to prepare thin metal films on different substrates such as glass, Si wafer and polymers. PECVD was used to prepare a thin layer of amorphous silicon on different substrates.

4.1.1-d.c sputtering

Sputtering is a technique to deposit a thin layer of material on a substrate. It is a very important tool in material engineering and in the electronic industry. Sputtering techniques replaced thermal deposition systems which required heating system to

evaporate material. The thin films prepared by sputtering are smooth, uniform and precise in thickness up to nanometres. The process occurs due to the bombardment of energetic ion particles on the target.

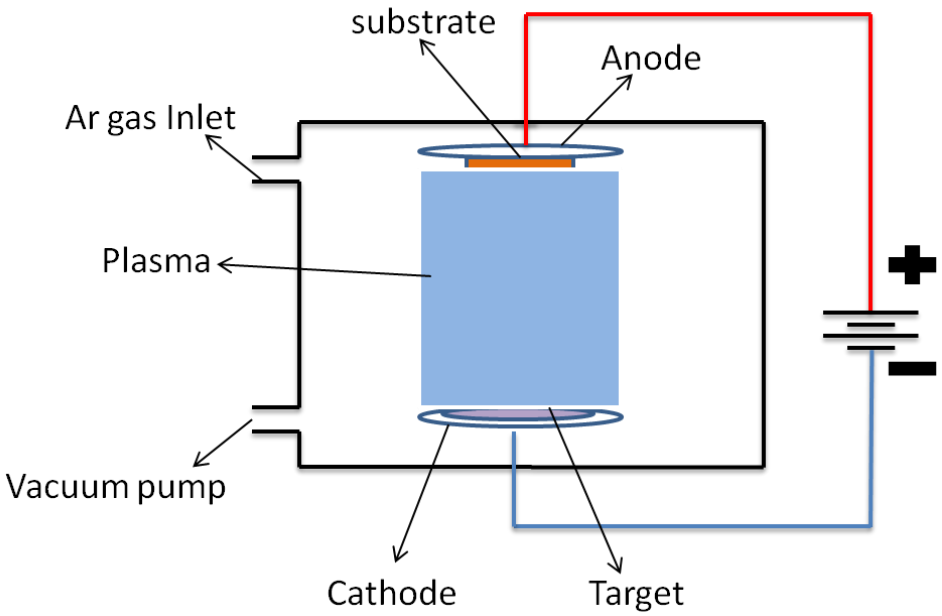

Figure 4.1 Schematic diagram of d.c sputtering

A sputtering system consists of a vacuum chamber with two electrodes as shown in Figure 4.1. After creating a base pressure vacuum, argon gas is supplied to the chamber with a gas pressure of 4.0×10^{-3} Torr. A negative potential between electrodes is applied to accelerate argon ions towards the target to dislodge material particles from the target and deposit them on a substrate in the surrounding area. In our research experiments, d.c sputtering was used frequently to deposit thin layer of catalyst Ni on the Si substrate and other metallic support layers for CNTs.

4.1.2-Thermal evaporation

Thermal evaporation is a simplest technique to deposit a thin layer of material on the substrate. In this technique, high current on a resistor is applied to produce high temperature. This high temperature evaporates the target placed on the resistor. The most commonly used materials as resistances are tungsten, tantalum and molybdenum as shown in the schematic diagram in Figure 4.2.

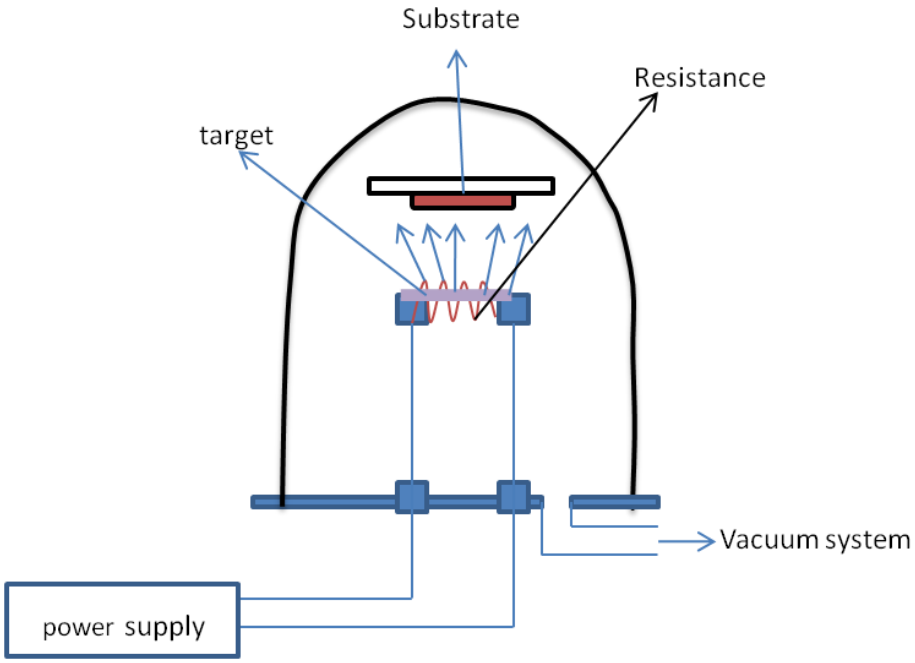

Figure 4.2 Schematic diagram of thermal evaporator

In this work thermal evaporation was used for some special materials which were not available as d.c sputtering targets.

4.1.3-Plasma enhanced chemical vapour deposition for a-Si:H

PECVD is a technique for the deposition of high quality a-Si films on substrates. The process involves the decomposition of silane (SiH_4) with other doping and alloying gases. Heating and radio frequency power provides energy to disassociate SiH_4 molecules. Hydrogen gas can also be introduced in the chamber to produce hydrogenated a-Si film. The system consists of a vacuum chamber with heating and cooling system, mass flow controllers, induction coil radio frequency generator with matching network and a heated stage to place substrate samples. A schematic drawing is shown in Figure 4.3.

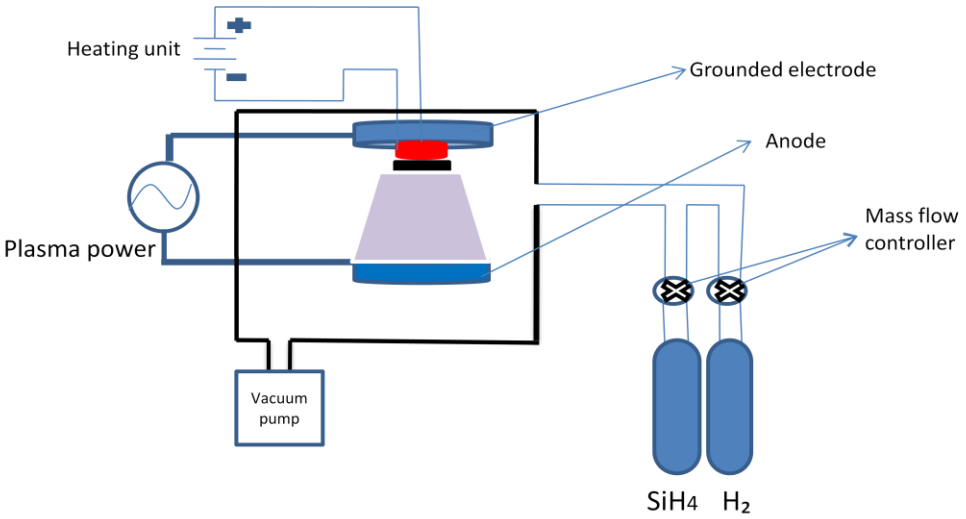

Figure 4.3 Schematic diagram of PECVD system for a-Si:H

Dundee University has a PECVD system for the deposition of a-Si:H. The PECVD system has a gas inlet, regulated by electronic mass flow controllers. The pumping system evacuates the chamber to 10^{-5}Torr and regulates pressure. Feedstock gases silane and hydrogen at the pressure 150 mTorr were used for the deposition of thin films of a-Si:H. In this research, some a-Si samples were prepared for the growth of CNTs.

4.2-PECVD System for CNT Growth

The PECVD system is renowned for high yield and relatively low temperature growth of CNTs. The purification rate is better than other growth techniques but the only problem associated with using this technique is that the nanotubes grown are mostly multiwalled. Since PECVD is a modified form of CVD it has nearly the same design except for the plasma control unit.

Every PECVD system has basically four units such as

1. Temperature control unit
2. Gases flow control unit
3. Vacuum and pressure control unit
4. Plasma control unit

The design and fabrication of a new PECVD system used for the growth of CNTs in this research was a major part of this research work, and the system had to be optimised for growth of CNTs and modified for graphene. Significant thought was given to the design and characterisation of the heating unit. This was the first unit for carbon deposition to be developed at Dundee. The aim of the system was to develop novel integrated carbon and silicon structures for renewable energy applications. This demanded careful design and optimisation of the system for carbon nanotube growth.

4.2.1-Chamber details

The chamber of the PECVD system is made from 316 LN stainless steel material fitted with CF type flanges for window, electrical feed-through, gas inlet and pumping ports. The chamber lid and base has rubber O rings. The inner dimensions of the chamber are:

Diameter	: 200 mm
Height	: 120 mm
Electrodes diameter	: 170 mm
Electrodes gap	: 120 mm

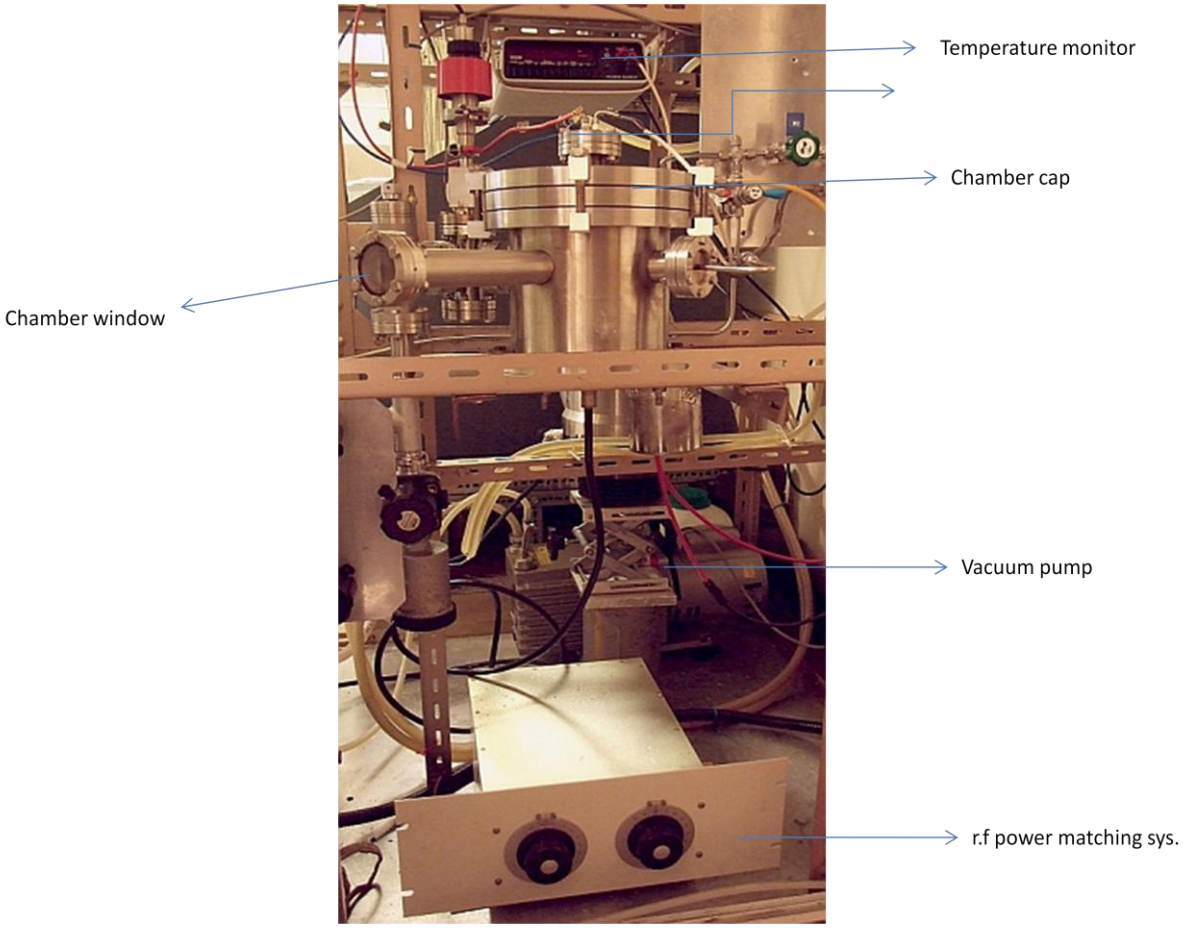

Figure 4.4 PECVD chamber for the growth of CNTs

The chamber has four side windows and one on the top. Two side ports are used for gas flow and vacuum pressure connections, one window to view the plasma and the remaining port can be used for d.c biasing. The upper part of the stainless steel chamber is moveable with a window cap for the heater, thermocouple and substrate holder as shown in Figure 4.4. This part of chamber also works as the grounded electrode.

4.2.2-Temperature control unit

The heating unit of the system was designed for high temperature carbon deposition by designing a ceramic spiral heater permanently fixed with clips on the upper lid of the chamber. Ceramic plates were placed underneath the heater to control the heat conduction. Heater electrodes and thermocouple wires were covered with ceramic beads and quartz tubes to stop heat conduction and shorting as shown in Figure 4.5.

The design of the heating unit allowed loading and unloading (sample exchange) in an effective manner.

Ceramic heater model number GAXP-85-IPL-QS (by Micropyretics Heaters International Inc. U.S.A) with power of 85 Ws and 6.4516 cm^2 in dimensions was used in PECVD system for the growth of CNTs and graphene. The power supply operating the heater has a Monson model number EP-925. The thermocouple used for the measurement of temperature was made by spot welding of chromel and alumel wires together. It was directly connected to a DVM for read-out in mV and the values calibrated by a chart.

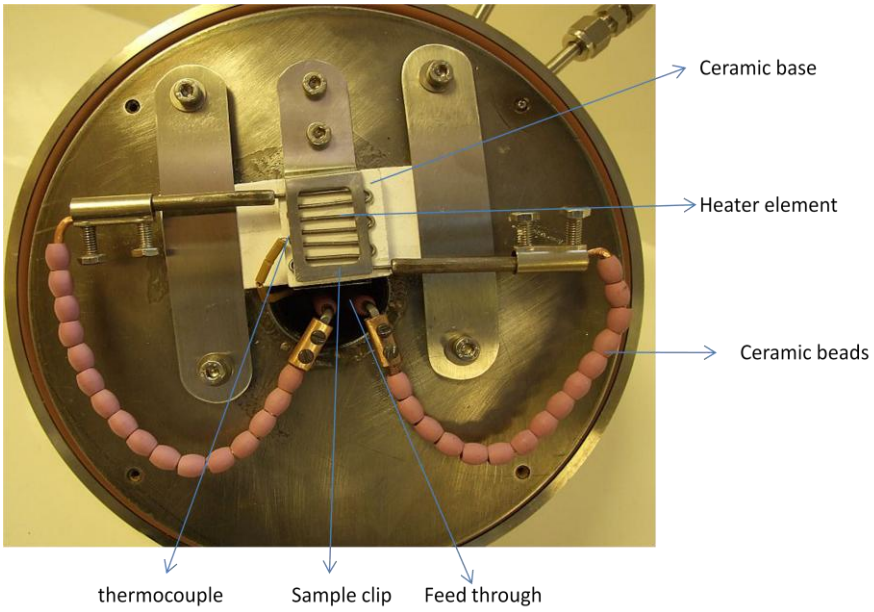

Figure 4.5 Upper lid of the PECVD chamber with heater

The 4-pin feed-through for the heater and thermocouple (model number EFT0541093 by Kurt J Lesker Co.) was used for electric supply and thermocouple connections.

4.2.3-Gas flow controlling unit

The mass flow controllers used in the PECVD system were by Vacuum General and the range of 0-100 scm^3min^{-1}as shown in Figure 4.6. All the gases were supplied by BOC (British Oxygen Company).

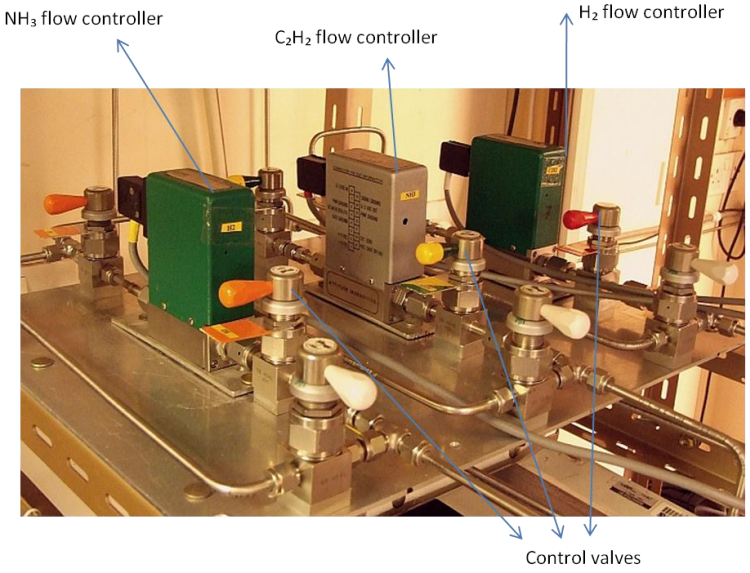

Figure 4.6 Gases flow control panel with inlet and outlet valves

4.2.4-Vacuum and pressure control unit

The vacuum and pressure control unit consisted of two rotary pumps, one turbo molecular pump and two gauge meters. An Edwards's turbo molecular pump model number EXT500C was used to create a high vacuum and an Edwards E2M18 rotary pump was used for the running conditions. Collectively, these two pumps created high vacuum quickly. There was another powerful rotary pump (Edwards E2M40) designed for high pressure inside the chamber.

In order to read the high vacuum created by the pumps, an Edwards penning gauge model number CP25-K was used and the process vacuum read by a Vacuum General Baratron type gauge known as a CML.

4.2.5-Plasma creation unit

The plasma creation system consisted of a radio frequency (R.F.) power supply, by ENI Power System Incorporated, which gave a 13.56MHz fixed frequency. This power supply was connected to the lower electrode of the chamber via a matching network taken from an old sputtering system made by RFA Co. By matching network we can control the output of the R.F. power applied on the electrode.

4.3-Characterization and Measurement Techniques

The techniques used to study the growth of CNTs, graphene and amorphous materials were SEM, AFM, STM, TEM, and optical microscope..

Electron microscopy techniques (SEM, TEM) were used frequently in this research to characterize CNTs, graphene and laser processed a-Si. These techniques are more valuable for the surface morphology and elemental analysis of as-grown CNTs and laser processes a-Si:H. In electron microscopy, an electron beam of fixed energy exhibits wave-like properties and by using high voltage it is possible to achieve a consistent resolution of the order of the inter-atomic spacing in a crystal. In these instruments, a high energy beam of electrons generated by an electron gun, either thermionic or field emission, is accelerated by a high voltage through electrostatic and electromagnetic lenses. These lenses are used to focus the beam on the specimen to analyze. A high vacuum is required in these instruments to avoid electron scattering by residual gas.

4.3.1-Scanning electron microscope (SEM)

A surface morphology study of nanoparticles and CNTs in this research was conducted by SEM which is an efficient and quick tool for analysis. In SEM, a powerful beam of electrons (typically 5-20 keV) produced by an electron gun interacts with the surface of the substrate and loses its energy by inelastic scattering. The secondary electron beam produced is detected by a number of detectors for imaging. Scanning coils, back scatter detector and secondary electron detector helps to build up an image and x-rays for elemental analysis. The two most commonly

used modes in SEM imaging are SEI (secondary electron image) and BEI (back scattered electron image). SEI, the most frequently used mode in SEM makes an image by secondary electrons emitted from the excited surfaces of the substrate. High magnification is achieved by this mode. BEI uses high energy electrons emitted by the collision of incident beam with an atom in the specimen.

Two type of SEM were used in this research

1. Philips XL30 HRSEM
2. Jeol JSM-7400F HRSEM

The Philips XL30 was used frequently for determination of the surface structure of nanoparticles and CNTs. Loading, tilting and imaging were easy in that machine, only resolution was limited. The Jeol 7400 is a powerful tool for high resolution imaging. It can produce high quality images even at low voltage. This machine was used for imaging of surface features, CNT diameter measurements and study of nanoparticles.

4.3.2-Transmission electron microscope (TEM)

TEM is a powerful tool for the investigation of the internal structure of nano-materials, especially CNTs. In this microscope the refined beam of electrons passes through the ultra thin specimen and an image is formed due to the interaction of un-scattered electrons through the specimen on a phosphor screen. In TEM, an electron in a crystalline sample is scattered according to Bragg's law which means that at certain critical angles, the incoming beam is diffracted from the axis while on the other angles the beam is transmitted largely. This diffraction of electron beam allows us to get a diffraction pattern of a material. This machine can also be used as an elemental analysis tool. Diffraction pattern of a material is helpful to determine defects, impurities and dislocations.

A JEM 2011 HRTEM was used for the detailed study of CNTs in this research work. The machine was equipped with an EDX system for elemental mapping and spectral analysis. It also had a GATAN CCD camera for direct imaging on a computer.

4.3.3-Atomic force microscope (AFM)

AFM is a probe scanning high resolution microscope for surface scanning, first invented by G. Binning et al. [1]. This machine can detect atomic scale features of nano-materials by measuring the variation of the forces between the cantilever and sample substrate. The imaging in AFM is very easy, and no vacuum is required which saves energy and time. It is possible to generate three dimensional images with the help of this tool. This machine can easily analyse conducting and non-conducting surfaces.

The morphology of catalyst nanoparticles, created for the growth of CNTs, was studied with the help of Digital Instruments Dimension 3000 scanning probe microscope (SPM).

References

1) G. Binnig, C.F. Quate and Gerber, *Phys. Rev. Lett.* **56**, 930(1986)

CHAPTER 5 GROWTH OF CNTS AND GRAPHENE

The growth of CNTs in a PECVD system mostly depends on the formation of nanoparticles; their shape, size, morphology and contact of the particles with the substrate. So, the formation of nanoparticles is the first step towards growth of CNTs. The second thing is the catalytic efficiency of nanoparticles. Mostly transition metals are good catalysts but all are not suitable for the growth of CNTs and graphene. It was experimented to determine which catalysts were more suitable in our experimental conditions. So all the details regarding substrate material, catalyst nanoparticles, growth controlling parameters in PECVD system is discussed in this chapter. The experimental results about the growth of CNTs and graphene are analysed.

The first section of this chapter explains how the samples were prepared and the choice of substrate. The second part covers the sample preparation mechanism and the process of nanoparticle creation as well as all state variables for the creation of nanoparticles. The role of the buffer layer in the creation of nanoparticles is also discussed.

The third part explains the growth process of CNTs and all its parameters. The role of the catalyst and buffer layer in the reduction of growth temperature of CNTs is also analysed. Growth time, chamber pressure and plasma power , which affect the growth are also described. Additionally, the results were analysed by using instruments such as scanning electron microscope (SEM), transmission electron

microscope (TEM) and atomic force microscope (AFM), which are described briefly in this chapter.

Although growth of graphene was not in the direct scope of this research, some experiments were conducted to grow a few layers of graphene that were used to stabilise surfaces. The growth mechanism of graphene and two techniques of growth are discussed in the final section.

5.1-Preparation of the Samples

The growth of CNTs on substrate in the predetermined positions is only possible with the help of CVD and PECVD. CNTs Substrates can be patterned for different applications such as field emission, electronic devices, solar cells and many applications in medical devices as well. Different types of sample substrates can be used to grow CNTs, such as glass, silicon wafer and quartz. Growth of CNTs on glass is a little hard, because glass melts at the higher temperature of the thermal annealing stage, inducing deformation. Also oxidation is difficult on sputtered Si on glass which performs the role of buffer layer. On the other hand Si wafers are stable at very high temperature; oxidation can easily be achieved in a high temperature furnace.

Oxidized n-type and p-type wafers were preferred for the growth of CNTs to avoid amorphous carbon deposition during the growth of CNTs at low temperature. The oxidized layer was between 100 nm to 500 nm thick. To make nano catalysts for the growth of CNTs, a thin layer of catalyst was prepared because it is compulsory in PECVD growth of CNTs. A catalyst nanoparticle provides nucleation for the growth of CNT.

5.2-Creation of Nanoparticles

One of the key features of this work is to make catalytic nanoparticles for both CNT nucleation and growth and for an active catalyst for the anode and cathode of a fuel cell membrane. Nanoparticles were made by thermal annealing, but also by a new process of confined ultrathin films on plastic with laser ablation. This method has far reaching implications for large area processing and for one step electrode formation for energy devices. The nanoparticle creation process obeys the Volmer-Weber Model. According to this model, the growing layer on the substrate wants to minimize surface energy and try to 'ball up' on the substrate [1]. In other words, the difference in thermal expansion of two metals allows the thin layer on top of the substrate to convert into two-dimensional islands during thermal annealing.

Figure 5.1 Schematic representation of nanoparticles formation because of mismatch of thermal expansion

In the PECVD technique, growth of nanotubes depends upon the nature of the catalyst nanoparticles; type of catalyst material, substrate-surface interaction and dimension of catalyst particles. Also the diameter of the catalyst particle directly affects the size of the carbon nanotube. So, it is very important to create nanoparticles. There are a number of techniques available and reported in the literature to create nanoparticles. The most common are:

1. Liquid based nanoparticles
2. Electron beam lithography
3. Nanoparticles by thin layer

Liquid based nanoparticles are nanoparticles in organic or inorganic compounds which can easily spinout on the substrates. Patterning the growth of CNTs in liquid based nanoparticles is somewhat difficult. Electron beam lithography enables the growth of CNTs at particular locations such as at catalyst particles on the tip of an

AFM cantilever. Electron beam lithography is a dedicated job which takes time and requires special expertise.

There are two ways to create nanoparticles in thin layers.

i. Thermal annealing of thin layer
ii. Laser ablation of thin layer

The thermal annealing of a thin layer of metal to make nanoparticles is the easier and cheaper technique. The thickness of the metal layer determines the diameter of the nanoparticles. Laser ablation also converts a thin layer of catalyst into particles. Excimer laser processing works well because it only affects the upper surface of the substrate [1].

It has been observed that the particles created by the techniques mentioned above were not complete spheres. To refine and reduce the size of nanoparticles, the plasma plays a very important role and optimising the plasma power is essential to create uniform spherical nanoparticles [2].

Three techniques used for the creation of nanoparticles in this research study were:

1- Liquid based nanoparticles

2- Laser ablation

3- Thermal treatment

It has been found that thermal ablation is the easiest, most powerful and cheapest technique. It is straight-forward because it is possible to complete the whole process from creation of nanoparticles to growth of CNTs in the same chamber. Also by reducing the thickness of catalyst layer, the size of the nanoparticles can be reduced.

5.2.1-Liquid-based nanoparticles

A solution of nickel nanoparticles in organic solvent was used to grow CNTs. The spin coating technique was used to deposit nanoparticles on the silicon substrate. Heating and plasma treatment was also conducted in the chamber on some samples. The morphology and structure of particles was observed by SEM.

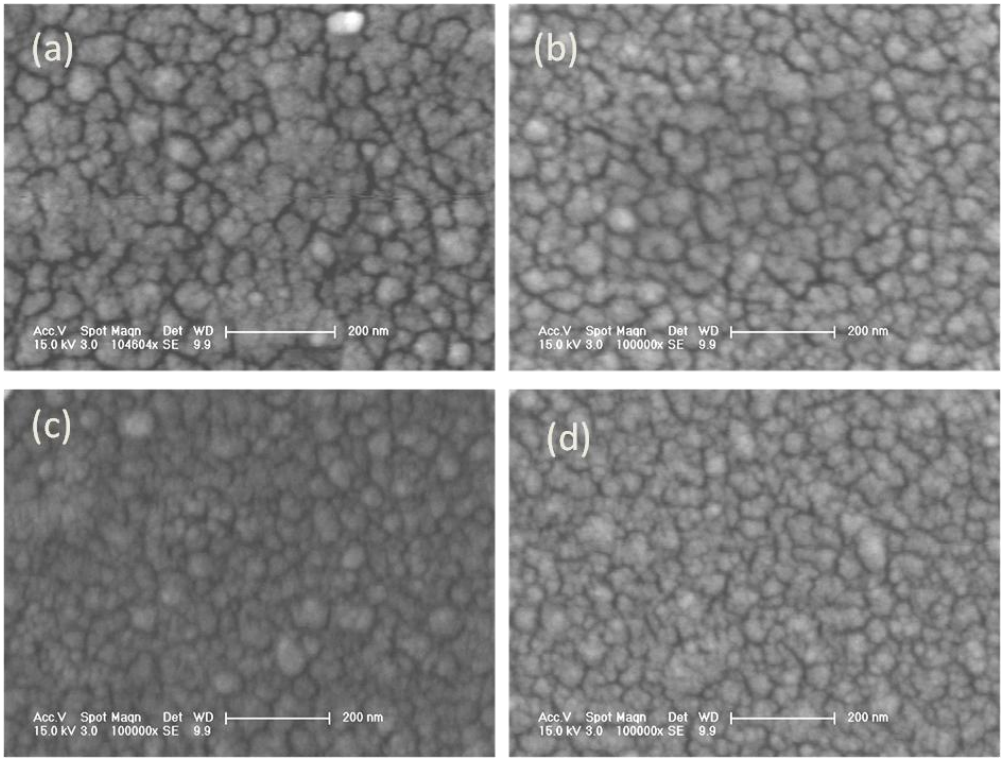

Figure 5.2 Solution based nanoparticles (a) after 10 minutes heating, (b) 5 minutes plasma treatment, (c) 10 minutes plasma treatment and (d) 15 minutes plasma treatment. Plasma treatment was applied after 10 minutes heating

Figure 5.2(a) shows the surface of the substrate after 10 minutes heating at 550 °C. The nanoparticles formed clusters with each other and the surface was completely disordered. There was a little improvement in the shape of particles after plasma treatment but they were not separated into small uniform spheres, as shown in Figure 5.2 (b-d). It has been observed that after the heating and plasma treatment, the particles were still meshed and surface was not suitable for the growth of CNTs.

5.2.2-Thermal ablation and plasma treatment

To study the formation of nanoparticles and the effect of plasma treatment in thermal evaporation of thin solid films, four samples were prepared with an 8 nm thick Ni catalyst layer on an oxidized Si wafer. The first sample was only heated and the rest of the samples were heated and plasma treated as well.

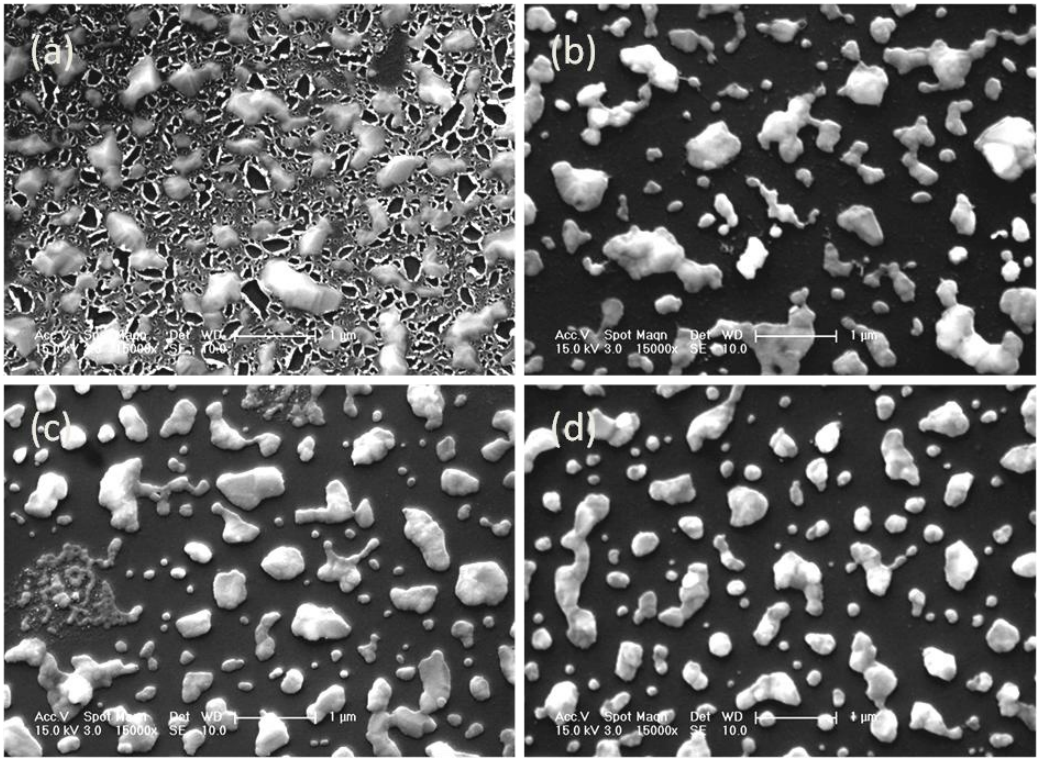

Figure 5.3 SEM images after thermal evaporation and plasma treatment a) After heating for 20minutes in NH3 at 575 °C b) 3 minutes NH_3 plasma after heating c) 6 minutes plasma treatment after heating d) 10 minutes plasma treatment after heating. Temperature during plasma treatment was 550 °C and plasma power was 160 W

After thermal evaporation

The first sample was heated for 20 minutes at a temperature of 575 °C in the presence of 30 scm^3min^{-1} NH_3 at a pressure of 1.5 Torr. Figure 5.3(a) shows the SEM image of the sample. It can be seen that the thin layer was divided into big clusters and started peeling off the surface. It has been observed from imaging of particles that with only heating of the sample substrate in the presence of ammonia gas it is not enough to convert a thin layer of catalyst into nanoparticles. Plasma treatment is necessary to make the refined small sized spheres which are responsible for the growth of nanotubes.

After plasma treatment

By the application of NH_3 plasma, the surface morphology of the thin metal was totally changed. Although the particles were different in their shape and structure the peeled surface and big clusters now disappeared and the surface was divided into

particles. By changing the plasma treatment time, the structure and size of particles was studied. In the first test, after heating the sample was treated in NH_3 plasma for three minutes at 550 °C, and the sample was divided into nanoparticles. The size of particles was quite big and particles were not completely spherical, as shown in Figure 5.3 (b). After six to ten minutes of plasma treatment, the size of the particles was reduced, the structure evolved towards a sphere and the sizes of the big clusters were also reduced, as shown in Figure 5.3 (c-d). As we observed the small particles, they were adhered to the surface and the angle of contact with the surface was large. By increasing the plasma treatment time up to 10 minutes, the particle size was reduced and particles were completely spherical with a low angle of contact, as shown in Figure 5.3 (d).

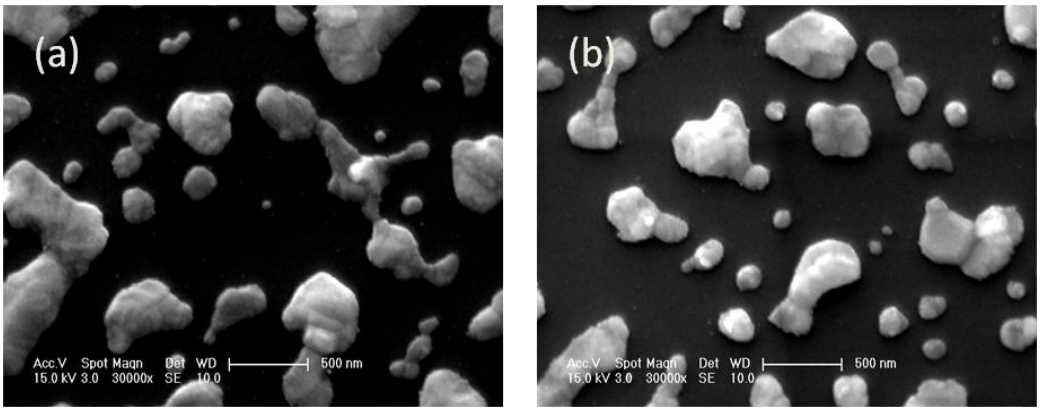

Figure 5.4 Nanoparticles after Plasma treatment (a) 6 minutes and (b) 10 minutes plasma treatment

These highly magnified SEM images of nanoparticles after 6 minutes and 10 minutes plasma treatment show the size of nanoparticles in Figure 5.4. It is clear from the images that after six minutes plasma treatment the particles were not complete spheres. After 10 minutes plasma treatment, the number of small spheres was increased but some small spheres present after 6 minutes treatment had disappeared.

5.2.3-Creation of nanoparticles by excimer laser

It is possible to create nanoparticles by excimer laser processing. The detailed discussion on how to create nanoparticles through laser interactions is given in the next chapter.

5.2.4-The role of the buffer layer in the formation of nanoparticles

A big variation in the size of as-grown CNTs on different buffer layers suggested experimentally to check the role of buffer layer in the formation of nanoparticles. For this purpose a piece of Si wafer was coated one half with Ta and other with Ti transition metals. The thickness of the buffer layers was 15 nm, and a 4 nm thin layer of Ni catalyst was also deposited on the top of the buffer layer. After cleaning the sample was loaded into the PECVD chamber and heated for 20 minutes at 600 °C in the presence of ammonia gas. To refine the nanoparticles, NH3 plasma at 160 W was applied for 6 minutes in the same chamber. The surface morphology of the sample was observed using AFM and SEM.It was observed that the substrate was full of nanoparticles on the buffer layer support, as shown in the AFM micrographs in Figure 5.5. There was a big difference in the morphology of the nanoparticles on each of the buffer layers. The nanoparticles created on the titanium buffer support were smaller in size with an entangled structure as shown in Figure 5.6 (a). The surface was fully covered but the particles were not completely spherical on the Ti support. The particles created on the tantalum support were completely spherical and nearly uniform in shape, but the sizes were a little larger as shown in Figure 5.5 (b).

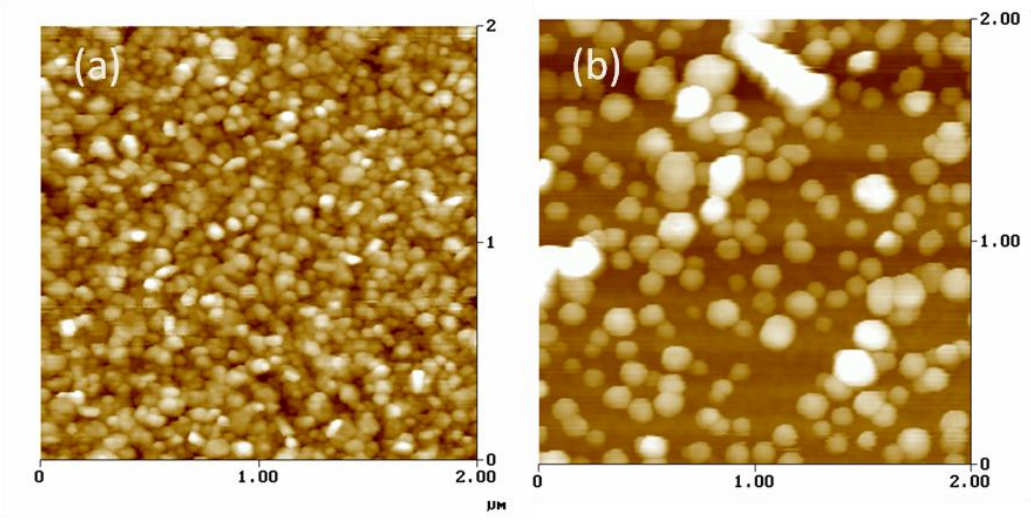

Figure 5.5 (a) Nanoparticles of Ni on Ti buffer layer and (b) Ni nanoparticles on Ta buffer layer. The substrate was Si wafer.

To verify the results of AFM imaging, some new samples were prepared and SEM used for imaging. This time three types of samples were used: Ni on oxidized Si, Ti and then Ni on oxidized Si and a Ta buffer layer with Ni on it. The nanoparticle creation procedure was the same as described above. It has been observed with SEM imaging that the nanoparticles created on oxidized Si sample were not actually nanoparticles but rather clusters on the substrate as shown in Figure 5.6 (a). The particles formed with the Ti buffer layer were smaller in size but meshed on the substrate as shown in Figure 5.6(b). The nanoparticles created with the help of the Ta buffer layer were completely spherical, bigger in size, and separated as shown in Figure 5.6 (c). The production of uniform and complete spherical nanoparticles on Ta support suggested a check on the behaviour of a Ta thin layer with thermal annealing. For this purpose a thin layer of Ta was deposited on a piece of oxidized Si wafer and annealed this sample half an hour at 600 °C. It was observed that the substrate was stable after heating as shown in Figure 5.6 (d).

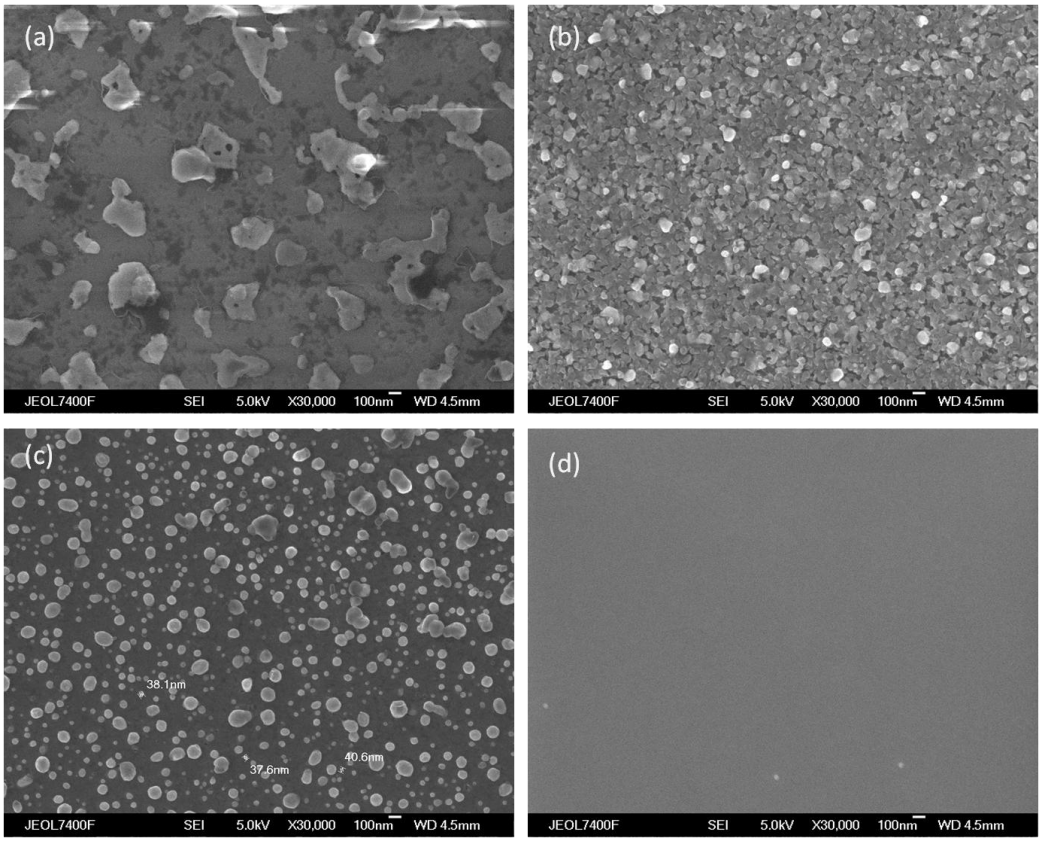

Figure 5.6 SEM images of nanoparticles on different support layers (a)4nm Ni only on oxidized Si wafer, (b)15 nm Ti and 4 nm Ni on oxidized Si, (c) 15 nm Ta and 4 nm Ni on oxidized Si and (d) 15 nm Ta only without catalyst on oxidized Si

The conclusion of these experiments is that the use of a buffer layer in the creation of nanoparticles is beneficial. A buffer layer improves the shape of particles and stops the interaction of Si substrate with catalyst particles. Additionally Ta is a good candidate for a buffer layer because of its stability at temperature.

5.3-Growth of CNTs

The vapour-liquid-solid model (VLS model) explains the growth of CNTs [4]. According to this model, nanotube growth starts on particular sites where the interaction energy between the metal catalyst particle and substrate is weaker. In PECVD system the feedstock gas decomposes on the catalyst particles and makes a compound of solid-liquid at higher temperature. After reaching super-saturation the excess carbon makes organised tube structures. It is a well known technique for the

growth of CNTs at low temperature. It also facilitates completion of all the steps of growth in the single run. Some of the parameters used to control the growth of CNTs in PECVD system are tabulated in Table 5.1.

Table 5.1: CNTs growth parameters in PECVD system

Parameters	**Variation**
Catalyst	Ni, Fe, Ni-chrome and Ni-Fe alloy
Buffer layer	Si, SiO_2, Ta, Ti, Al, Cu and Cr
Plasma power	50 W to 250 W
Temperature	140 °C to 600 °C
Gases	C_2H_2:NH_3 (20%:80%)
Pressure inside chamber	4 Torr to 6.5 Torr
Catalyst thickness	0.5 nm to 8 nm

5.3.1-Role of catalyst

To observe the role of the catalyst on the growth of nanotubes, initially four transition metal catalysts were selected, they were: nickel, iron, nichrome and nickel-iron alloy. In the sample preparation, p-type Si (100) wafers were first oxidized by thermal oxidization (500 nm) to prevent interaction between Si and catalyst in forming silicide. This silicide prevents the growth of CNTs by creating amorphous carbon on the surface. d.c sputtering was used to deposit a thin layer (4 nm) of nickel catalyst at a base pressure $3.6x10^{-5}$ Torr and the other three catalysts were deposited by thermal evaporation.

Before loading the sample into the PECVD chamber, it was cleaned using cleaning solution B, washed in deionised water and dried in a nitrogen gas flow. After cleaning, the sample was fixed on the ceramic heater placed at the grounded electrode of the R.F power supply. The sample was first heated to create nanoparticles and after that R.F plasma was used to refine sphericity of

nanoparticles. The growth time was only five minutes in a 180 W plasma at a temperature of ~500 °C.

The growth of CNTs was observed using the Philips XL30 scanning electron microscope at an accelerating voltage of 15 keV. Further analysis and imaging was performed using a 5 keV electron beam in a Jeol 7400F series HRSEM, with an Oxford EDX analysis system. The features of interest were observed in both SEI and BEI detector modes.

Figure 5.7 shows the growth results of CNTs on different catalysts: (a) shows the surface of substrate after the growth of nanotubes on nickel catalyst. The average size of particle was 150 nm and there were only a few tubes on the whole surface of the substrate. When iron was used as the catalyst, on pre-treatment it did not divide into uniform nanoparticles, producing only big clusters of iron of non-uniform shape. The average size of cluster was more than 200 nm with amorphous carbon on the top. Figure 5.7 (b) is evidencing that there was not even a single tube on this run with iron catalyst.

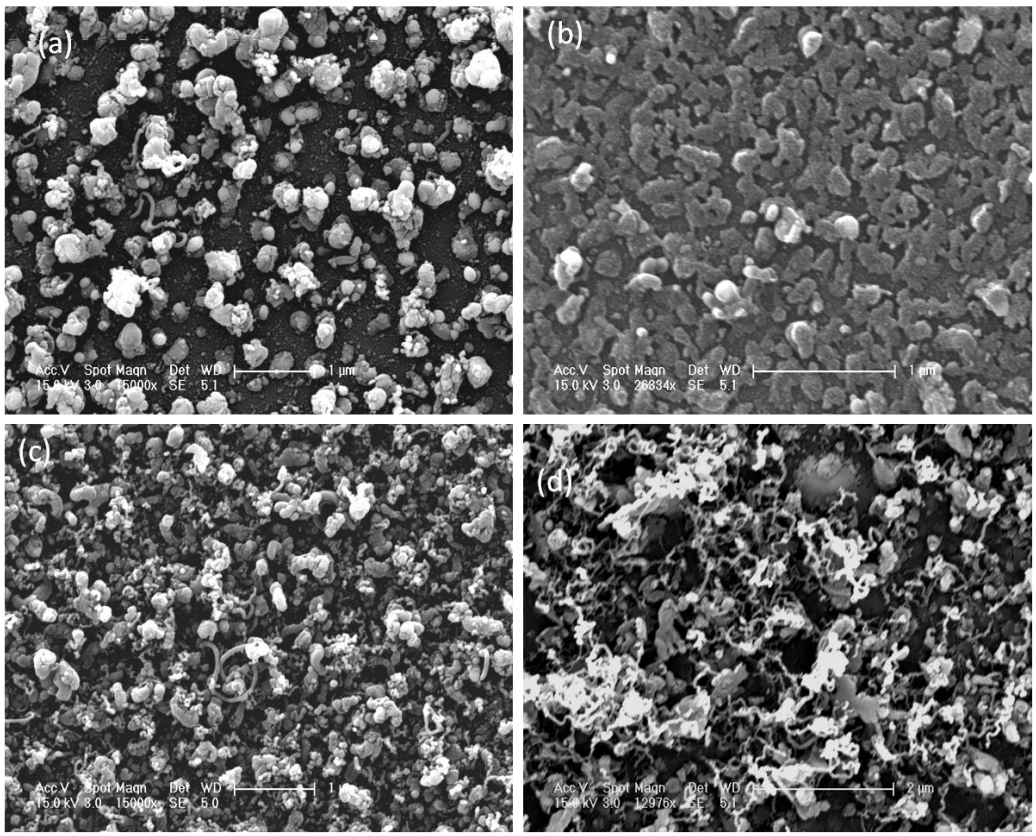

Figure 5.7 SEM photographs of CNTs grown on different (d.c sputtered) catalyst layers (a) 4 nm Ni,(b) 4 nm Fe,(c) 4 nm Nichrome and (d) 4 nm Ni-Fe . Underneath all the catalysts was 500 nm thermally grown SiO_2

Two samples of metallic alloys were also prepared: the first was nichrome and the second, Ni-Fe. The SEM results of the alloy of nickel and chromium (4 nm nichrome) showed that the size of nanoparticles was reduced and in the range of 60 nm to 80 nm. Growth was improved and there were lumps of a few CNTs on some particular areas as shown in 5.7 (c). In the fourth sample, iron and nickel were mixed in thermal evaporation and deposited to a 4 nm thin layer. The as-grown CNTs on Fe-Ni alloy were better than the other three samples. The average diameter of the CNTs was 45 nm and surface area was more than 50% covered with tubes. The CNTs were curved rather than straight with some big lumps covered with amorphous carbon as shown in Figure 5.7 (d).

It has been concluded from these growth results that it is very difficult to grow CNTs on SiO_2, and it is not completely overcoming the interaction between Si and catalyst during growth. On all the samples, the surface was very unusual, with big lumps of

amorphous material, non uniform particle size and few tubes with Ni and Ni related alloys. The sample with the iron catalyst showed no nanoparticles and the surface was fully covered with amorphous carbon.

5.3.2-Role of metallic support layer

The growth of CNTs on samples without a metal buffer layer was not good in the sense of effective nanoparticles and nanotube production. The literature also supports the use of a buffer layer in the growth of CNTs by PECVD [1, 5]. Therefore, experiments were carried out with a support layer underneath the catalyst. Initially four samples were prepared with support metals; aluminium, tantalum, titanium and copper. The thickness of the metallic layer was 20 nm and the catalyst used on all samples was only nickel. d.c sputter was used to deposit metallic layers and catalysts on the substrates.

The growth was conducted in the same process described above. The growth results on some metals were excellent though some were not wholly satisfactory. On each sample, small variation in growth parameters such as temperature, surface morphology of sample and plasma stability was present. To overcome this problem, it was decided to prepare one sample with four metallic support pads on it and grow CNTs during the same run. A homemade shadow mask was used to deposit metallic pads by d.c sputtering and the thickness of pads was kept 16 nm. The metals used for the pads were aluminium, tantalum, titanium and copper. The Ni catalyst with thickness 4 nm was used on the top of all pads. The schematic diagram in Figure 5.8 shows the layered structure of the pads and the thin film of catalyst.

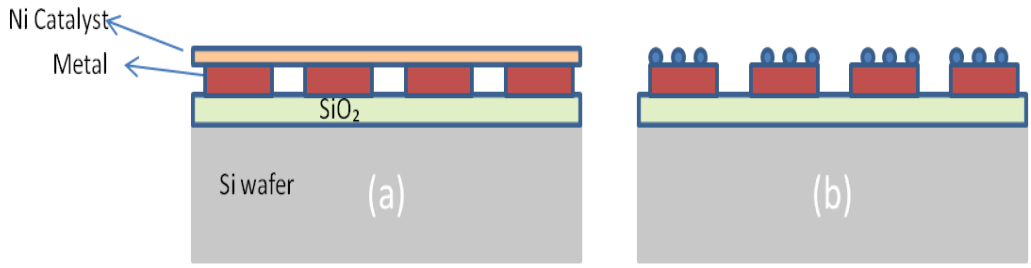

Figure 5.8 Schematic diagram of sample with different metallic pads (a) a thin layer of Ni on metallic pads and (b) after thermal annealing the thin film was converted into nanoparticles on the pads

Before the growth of CNTs, thermal annealing and plasma treatment was conducted to create completely spherical nanoparticles on the pads. Imaging was performed on the Philips XL30 scanning electron microscope with an accelerating voltage of 15 keV. Figure 5.9 shows the result of as-grown CNTs on metallic pads.

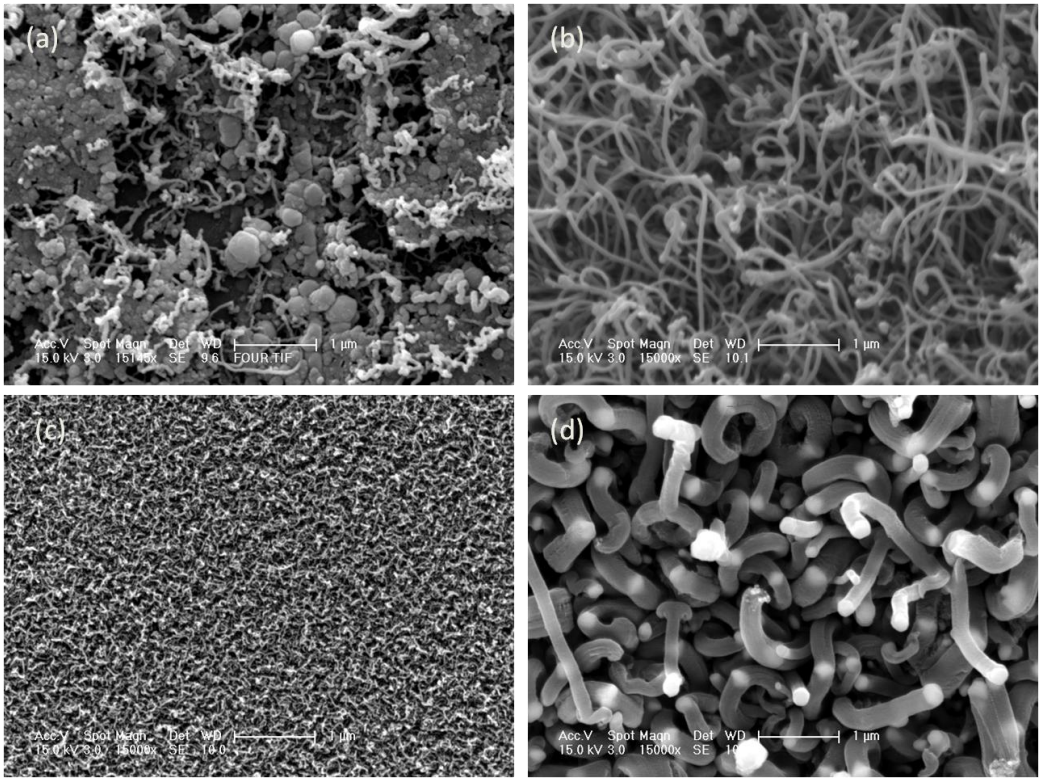

Figure 5.9 SEM photographs of grown CNTs on different buffer layers, (a) 4 nm Ni on 20 nm Al, (b) 4 nm Ni on 20 nm Ta, (c) 4 nm Ni on 20 nm Ti and (d) 4 nm Ni on 20 nm Cu.

The first material used as a support layer for the CNTs growth was aluminium (Al). Al is very prevalent for CNTs growth in the literature but when it was tried to grow CNTs on the Al support, the results proved unpredictable, as shown in Figure 5.9 (a).

The growth density was very low and the tubes were curled, with lumps of amorphous carbon on the surface of substrate. The growth of CNTs on the Ta support layer on the other hand was absolutely fine; straight and long tubes were grown on the Ta buffer layer as shown in Figure 5.9 (b). The tube diameter was in the range of 25 nm to 35 nm with a height of about 8 μm in five minutes growth. The third material used as a buffer metal was titanium (Ti). Thin tubes with a curled structure were grown on it as shown in Figure 5.9 (c). Growth of tubes was roughly the same as for the Ta support and the density was very high. The fourth metal was Cu; growth was found to be very sparse, with lumps of big fibre like structures deposited as shown in Figure 5.9 (d).

In these experiments, it was observed that a support layer is essential for the growth of nanotubes and SiO_2 is not enough to prevent the interaction of amorphous carbon on the surface. It was also observed that a support layer of Al was not suitable for the growth of CNTs because melting temperature of Al (650 °C) is very close to that of the growth temperature of CNTs. Therefore, during the creation of nanoparticles, Al was mixed with Ni making the surface non uniform and unfavourable for CNTs growth.

The growth of CNTs on Ta and Ti support layers was very much encouraging because both materials are physically hard with a very high melting temperature. As described earlier that the particles created on these buffer metals were spherical because of weaker interaction between catalyst and them. The interaction of substrate and catalyst is crucial in the formation of nanoparticles and depends upon two factors.

The first factor is the melting point of materials. If the melting point of the catalyst is nearly the same as for the buffer layer, the materials will interact with each other during thermal annealing and resultant nanoparticles will be bigger in diameter and this will also affect the efficiency of catalyst in the growth of CNTs. The best examples of such buffer layers are Al and Cu which have nearly the same melting range as catalyst Ni.

The second and most important factor is the surface energy of the substrate. We know that a liquid droplet always wants to minimize its surface area because of surface tension and cohesive forces. During thermal annealing and plasma treatment, the thin layer of catalyst cracks in different places and tries to minimise to "ball up". This process depends upon the interaction between catalyst and buffer material.

The surface energy of thin films and their interfaces plays a dominant role in the formation of nano-spheres. There are various models for the growth of thin films in which the most well-known are shown in the schematic drawing in Figure 5.10. The first model is favourable for layer by layer growth of substrate films. If the surface energy of the substrate is greater than the over layer and interface surface energies combined, the growth will be layer by layer. The other two models (Stranski-Krastanov and Island Growth) explain island growth of thin films with lower surface energies [3]. To convert a thin film of metal into nanoparticles we need to see in reverse direction which means higher surface energy of buffer layer can easily convert a thin catalyst layer into nanoparticles.

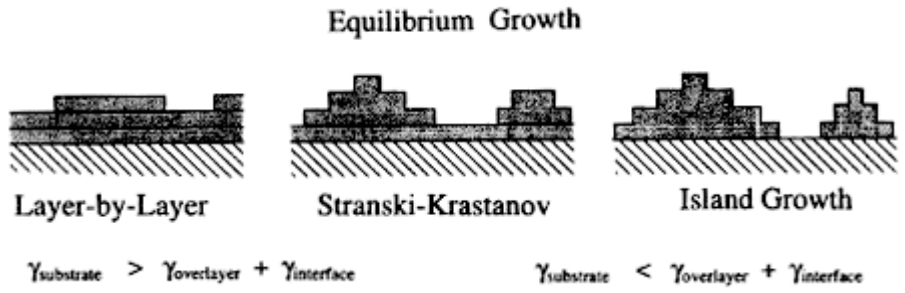

Figure 5.10 Schematic drawings of thin film growth models and surface energies [6]

During the formation of nanoparticles there are three forces exerted on it:

1- Surface energy of substrate material (γ_{sub})

2- Surface energy of catalyst material (γ_{cat})

3- Interface between buffer layer and catalyst (γ_{int})

The interaction between the buffer layer and catalyst depends upon the difference between catalyst and buffer layer material surface energies plus their interface energy.

If $\gamma_{sub} \geq \gamma_{cat} + \gamma_{int}$ ---------- (5.1)

The catalyst will ball up and convert into nanoparticles.

If $\gamma_{sub} < \gamma_{cat} + \gamma_{int}$ ---------- (5.2)

The interaction energy will be higher and particles will remain in clustered structure.

The balance of surface energies also explains the angle of contact for the islands i.e.

$$\cos\theta = (\gamma_{sub} - \gamma_{cat}) / \gamma_{int} \text{ ---------- (5.3)}$$

if

the angle is acute and surface energy of buffer layer is greater than their interface energy. The thin layer will ball up on the buffer layer and convert into nanoparticle. On the other hand,

if $-1 < -\cos\theta < 0$

the angle is obtuse and there is large interaction between catalyst and buffer layer. Nanoparticle formation will be difficult in this condition. Table 5.2 shows the surface energies of different materials.

Table 5.2: ***Surface energies of selected metals [7,8]***

Material	Surface energy J/m^2	Temperature °C	Mineral Hardness
Ni	2.4	1455	4.0
Cu	1.8	1084	3.0
Al	1.1	660	2.75
Ti	2.6	1668	6.0
Ta	3.0	3017	6.5
Fe	2.9	1538	4.0
Si	1.1	1414	6.5
SiO_2	0.5 - 1.0	1584	No details
Cr	2.3	1907	8.5

If the surface energy of the buffer layer (substrate) is greater than the surface energy of the catalyst and their interface, the catalyst will be more easily ball up and convert into nano-spheres. If the interaction is higher the catalyst will be in clusters. It has been observed in this research that because Ta has a higher surface energy than Ni which helps in the formation of spherical nanoparticles and Ti with slightly high surface energy than Ni made it hard to convert Ni into complete spherical nanoparticles. So, in our experiments it has been observed that on Ti the nanoparticles entangled with each other. The other materials used in this research as buffer layers were Al, Cu and SiO_2. These have lower surface energies and were not favourable materials for the formation of nanoparticles. Table 5.2 shows surface energy and other parameters.

It was observed during the growth of CNTs on Ta buffer layer that the production of nanotubes was high and alignment was good. When the sample was scratched, the CNTs on the surface, was smooth and uniform as shown in Figure 5.11.

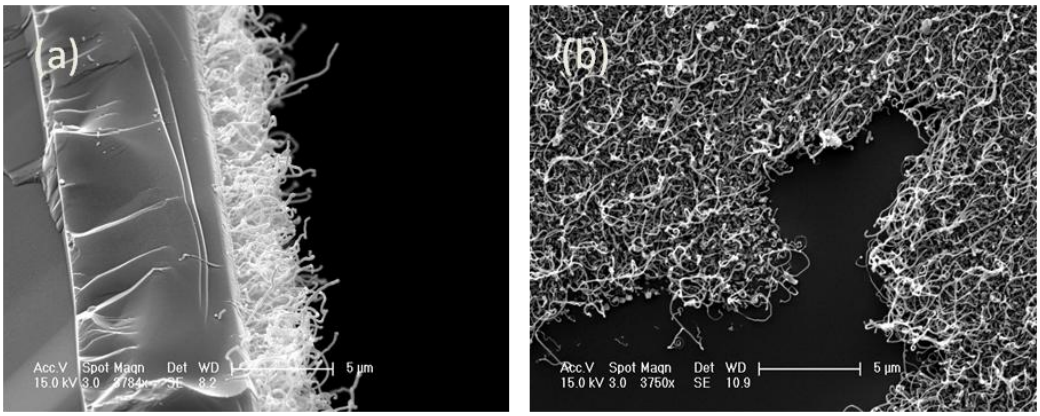

Figure 5.11 Different SEM images of grown CNTs with Ni catalyst on Ta support layer (a) cross sectional view, (b) scratched portion shows uniform Ta surface

Further structure and diameter of tubes grown on Ta and Ti buffer layers were analysed in HRSEM Jeol 7400F with an Oxford EDX analysis system. Figure 5.12 shows the diameters of nanotubes on Ti and Ta pads.

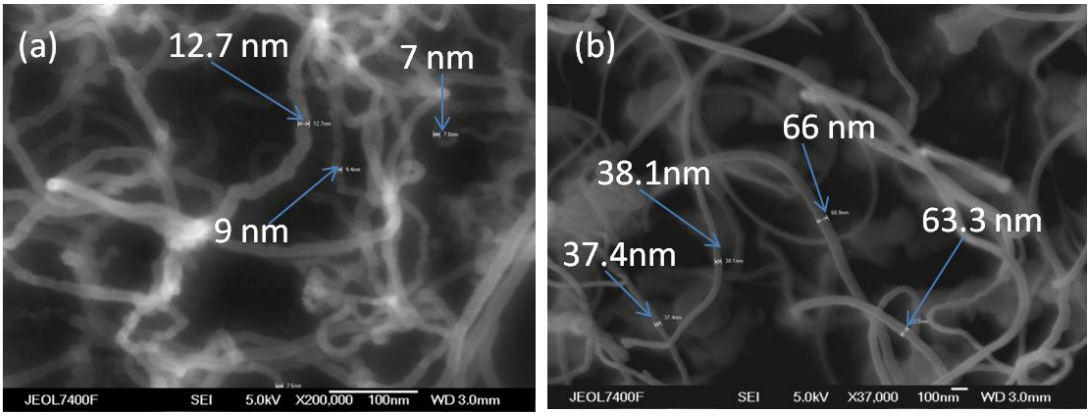

Figure 5.12 HRSEM images of CNTs (a) CNTs on Ti with tube diameters from 7 nm to 10 nm and (b) CNTs on Ta with tube diameters from 35 nm to 65 nm

It was also observed in the imaging of the shapes that CNTs grew on that particular area of Ti metal pad where the metallic layer peeled off as shown in Figure 5.13.

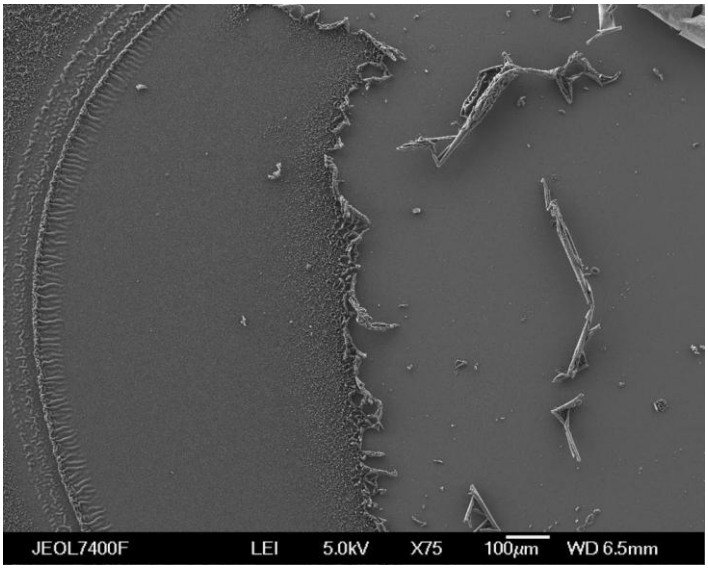

Figure 5.13 peeled off area on Ti buffel layer

The diameters of the nanotubes were in the range of 7 nm to 10 nm with tangled structures. On the other hand, the growth of tubes on a Ta support pad showed that metal was still present and visible on the surface. The diameter of tubes grown on the Ta support was relatively large, in the range of 35 nm to 65 nm, but the tubes were long and straight. Also there were big sphere like structures under the CNTs on the Ta pad of the samples as shown in Figure 5.14.

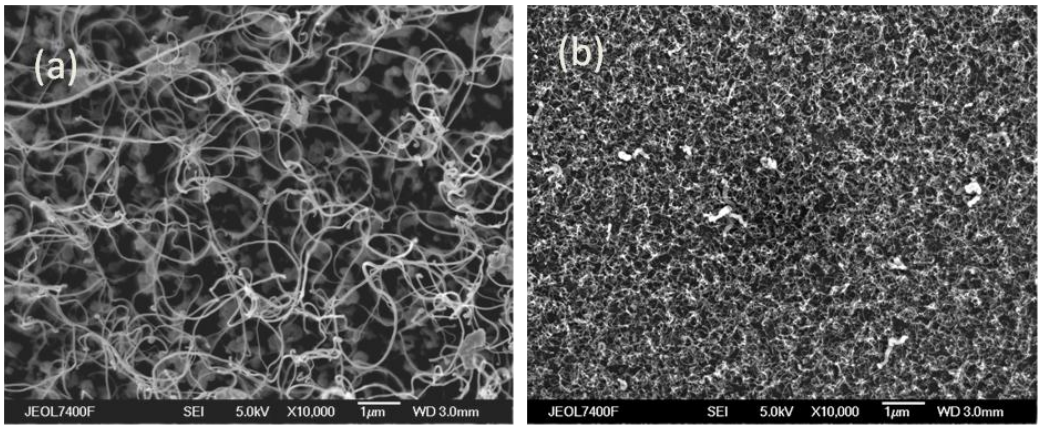

Figure 5.14 SEM images of (a) sphere like structures on Ta support underneath the tubes and (b) plane sample underneath the Ti pad

5.3.3-Internal Structure Analysation of CNTs

For the investigation of the internal structure of the CNTs, a transmission electron microscope (Jeol JEM 2011 HRTEM) was used. The machine was equipped with an EDX system for elemental mapping and spectral analysis. It also had a GATAN CCD camera for direct imaging on the computer. Two types of samples were prepared for TEM analysis; 1- CNTs grown on Ta buffer layer and 2- CNTs on Ti buffer layer. To transfer CNTs on TEM grids, the nanotubes were removed from Si samples with the help of an ultrasonic bath in ethanol.

The CNTs solution was dropped on carbon coated Cu TEM grids with the aid of a syringe and left for 24 hours to dry out the ethanol. The following things were observed in TEM analysis.

1- Diameter of CNTs
2- Number of walls
3- Spacing between walls
4- X-ray analysis

With the help of high magnification it was observed that the CNTs grown on Ta buffer layer have 20 to 30 walls. The tubes were straight and hollow with Ni nanoparticle on the tip as shown in Figure 5.15. The diffractrogram facility of the TEM machine allowed calculation of the spacing between the walls. It has been observed that the spacing between the tubes was 0.35 nm, exactly the same as graphite atomic layer spacing which confirmed the growth of CNTs in this research.

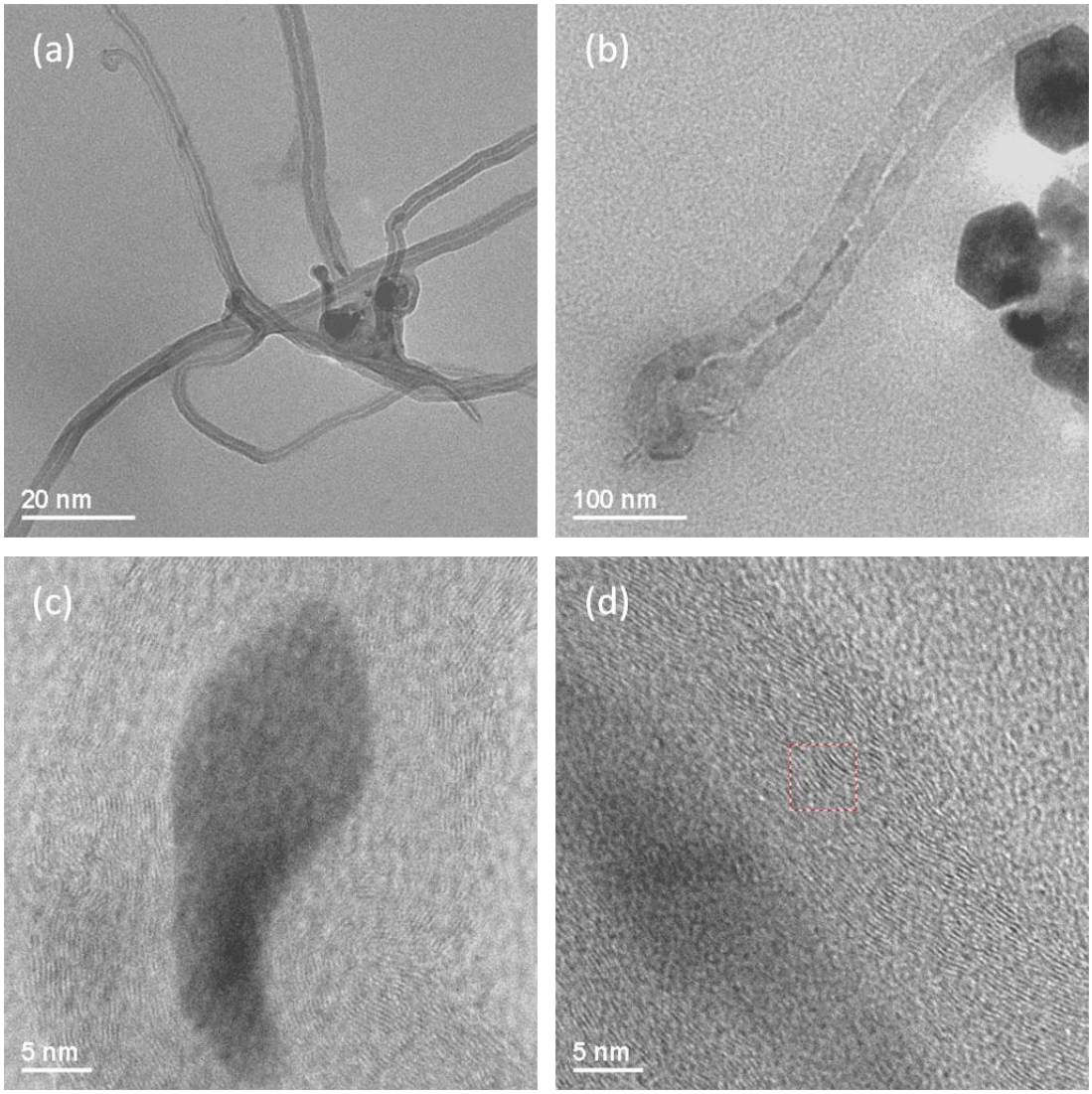

Figure 5.15 HRTEM images of CNTs grown on Ta support buffer layer with Ni catalyst. (a) shows the hollowness in the tubes, (b) shows that tubes are closed with catalyst on the tip, (c) shown the shape of catalyst on the tip and (d) shows number of walls in the tube.

A similar analysis was conducted with the nanotubes grown on Ti buffer layers. There were only six to seven walls in these tubes, as shown in Figure 5.16. The tubes were hollow and straight. The diffraction fringes pattern had 0.358 nm spacing, confirming the graphite (carbon) material.

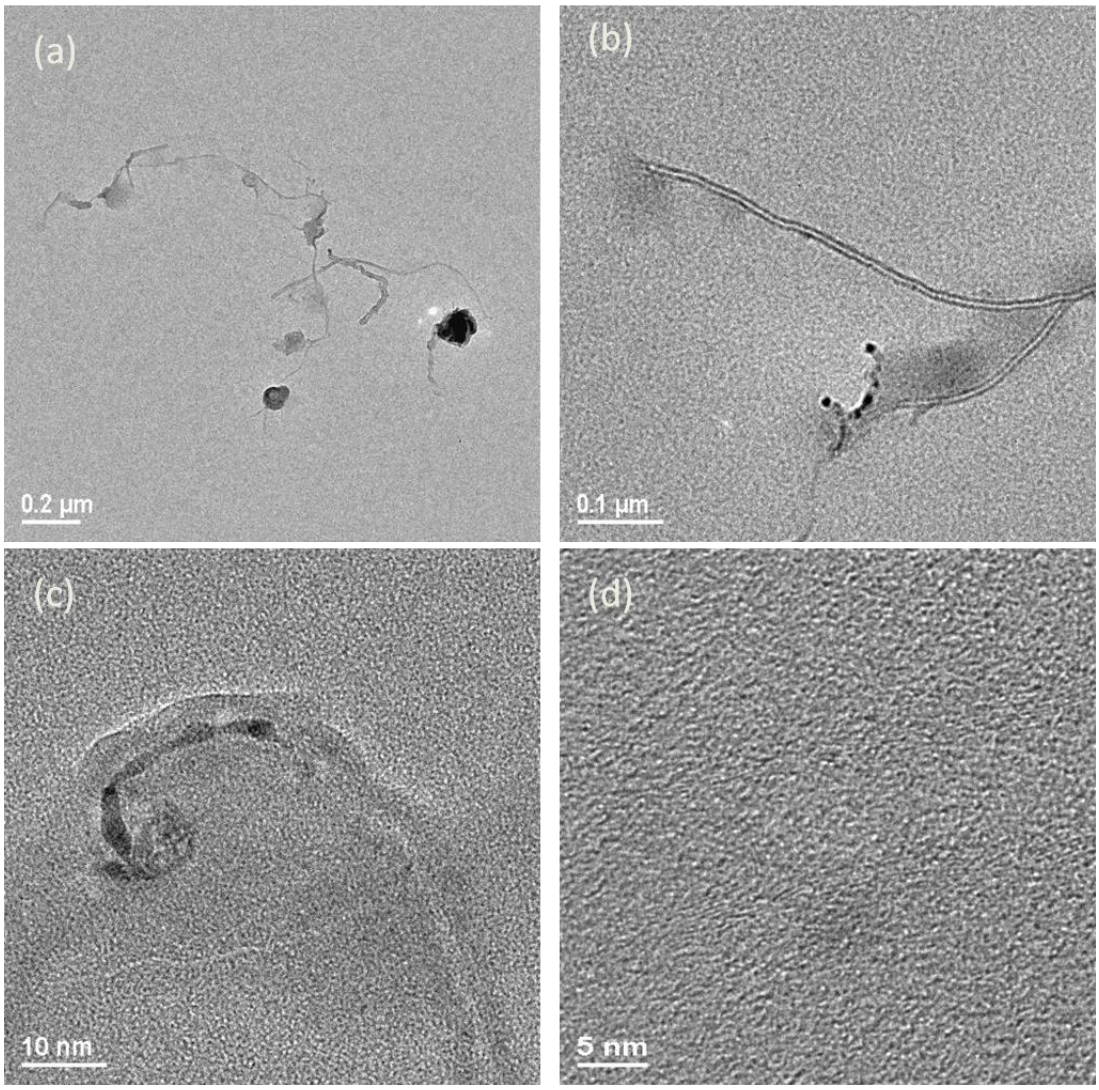

Figure 5.16 HRTEM images of CNTs grown on Ti support buffer layer with Ni catalyst. (a) shows the size of the tubes, (b) shows that tubes are closed with catalyst on the tip, (c) shown the shape of catalyst on the tip and (d) shows number of walls in the tube.

X-ray Analysis of the tip of CNTs

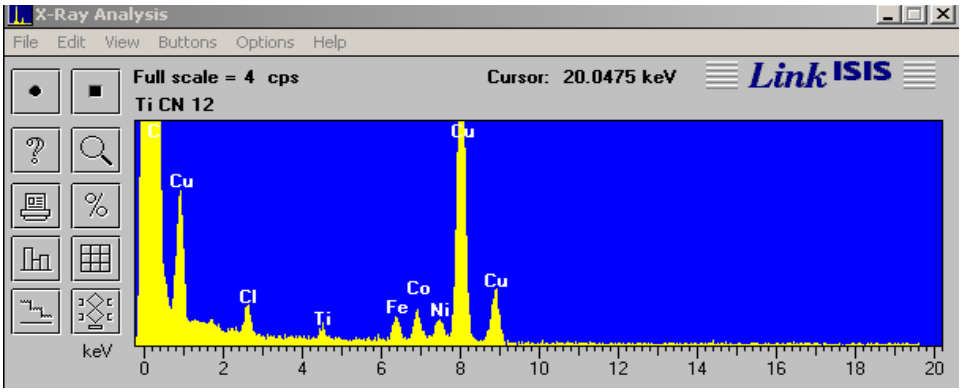

Figure 5.17 EDX analysis of CNTs on Ti support

The diameter of the tubes was less than 8nm with nanoparticle on the tip of tubes at the end of the process. X-ray analysis was also conducted on the tubes which confirmed the presence of carbon, nickel and titanium as shown in Figure 5.17.

It was observed in the spectroscopy of CNTs with TEM that as-grown CNTs were multiwalled followed by tip growth model. Ti was good for small diameter and Ta was good for bigger tubes. The as-grown tubes were straight and hollow.

5.3.4-Role of R.F plasma power

The effect of plasma power on the growth of CNTs in the PECVD system was also analysed. For this purpose, five samples were prepared with a 10 nm buffer layer of Ti and an 8nm thin layer of Ni catalyst. Both metals were deposited on Si wafer by d.c sputter at a base pressure of 4.2×10^{-5} Torr in Ar plasma. The growth procedure of CNTs was the same as described above. The growth temperature was 525 °C and the time of growth was 5 minutes. The only variable in this set of experiments was plasma power. The first experiment was done with 50 W plasma, the second with 100 W, the third 150 W, the fourth 200 W and the last with 250 W plasma. Again SEM was used to analyse the growth of CNTs as shown in Figure 5.18.

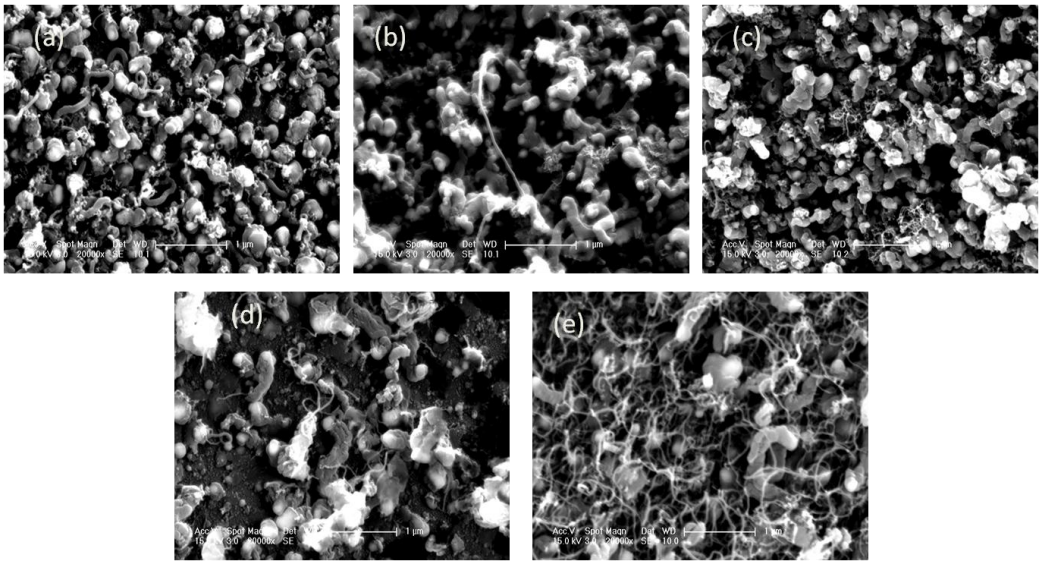

Figure 5.18 SEM images of as- grown CNTs (a) 50 W plasma, (b) 100 W, (c) 150 W, (d) 200 W and (e) 250 W plasma power. The buffer layer was Ti (10 nm) and catalyst was Ni (8 nm) on Si wafer.

The growth of CNTs with 50 W plasma was very poor because the plasma was weak and the sample was fully covered with meshed nanoparticles as shown in Figure 5.18(a). As the power of plasma was increased, the growth rate was also increased as shown in Figure 5.18 (b-e). CNT growth with the 250 W plasma was encouraging, with production of long tubes as shown in Figure 5.18 (e).

5.4-Role of Temperature in the Growth of CNTs

Temperature is a key factor in the growth of CNTs; it provides enough energy for carbon atoms to dissociate the catalyst nanoparticle from the surface of the substrate and makes a hexagonally arranged tube of its atoms. Initially the growth was only possible at quite high temperature but with the help of the plasma in CVD is now possible at low temperature. Some experiments were carried in the PECVD system to find the lowest possible temperature for the growth of CNTs. It was observed in other experiments that a Ta buffer layer is very helpful in the low temperature growth of CNTs. The samples were prepared with a 10 nm Ta buffer layer and a 4 nm nickel catalyst on the top. The nanoparticles were created first by thermal annealing and plasma treatment. Growth of CNTs was done as described above by changing the deposition temperature as defined in Table 5.5.

Table 5.3: ***Temperature variation table for the growth of CNTs***

Sample	Pressure (Torr)	Temperature (°C)	R.F Plasma (W)	Growth time (min)
1	5.5	545	200	5
2	5.5	300	200	6
3	5.5	145	200	5

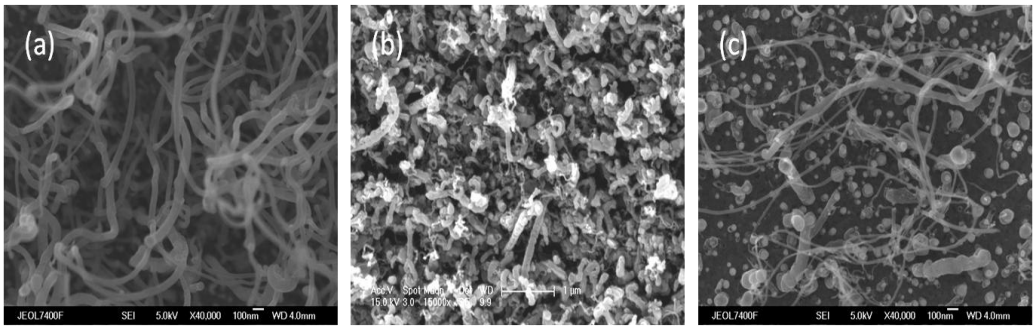

Figure 5.19 HRSEM images of CNTs with variation of temperature (a) 545 °C, (b) 300 °C and (c) 145 °C. buffer layer was 10 nm Ta and catalyst Ni 4 nm

HRSEM was used to observe the growth of CNTs. It has been observed in the three different temperature runs that growth of CNTs is possible at low temperature in a PECVD system but for high density and uniform growth more than 500 °C is required for MWNTs, as shown in Figure 5.19.

5.5-Role of Catalyst Layer Thickness on the Growth of CNTs

A catalyst is a main character in the growth of CNTs in the PECVD technique and growth of nanotubes and it is not possible without it. It was also noted that the catalyst particles should be nano-sized spherical to play the role of seeds in the growth of tubes, as described earlier. The literature is full of evidence that the catalyst film thickness explains the size of nanoparticles which are ultimately responsible for the size and growth of CNTs. As the thickness of the catalyst layer

decreases, the diameter of the nanotubes decreases. By reducing the thickness of catalyst film to atomic level, growth of SWNTs could be possible at low temperature in PECVD. Experiments were conducted to observe the effect of catalyst film thickness on the diameter of the nanotubes. Three type of samples were prepared: 1) 5 nm thin layer of catalyst Ni, 2) 1.0 nm and 3) 0.5 nm catalyst Ni. The catalyst was deposited by d.c sputtering on buffer layers of Ti and Ta. SEM was used to analyse the surface structure of CNTs.

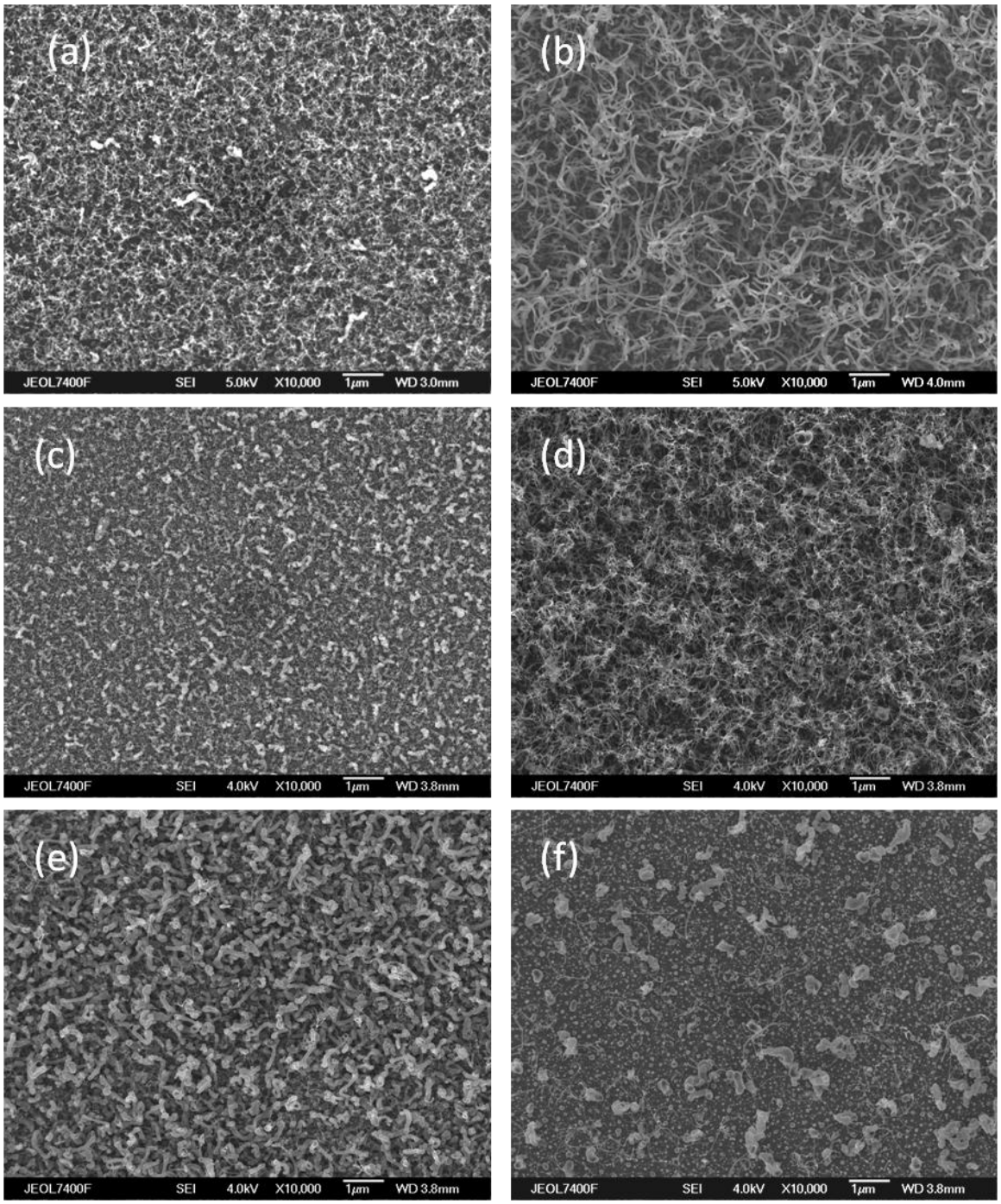

Figure 5.20 SEM micrographs of CNTs on different catalyst thickness, (a, b) 4 nm Ni catalyst, (c, d) 1 nm Ni and (e, f) 0.5 nm Ni. (a, c, e) has 15 nm Ti buffer layer and (b, d ,f) has 15 nm Ta buffer layer

The CNT growth conditions were the same as previously described. Figure 5.20 presents low magnification images of CNTs for an overall view and Figure 5.21 shows a magnified view.

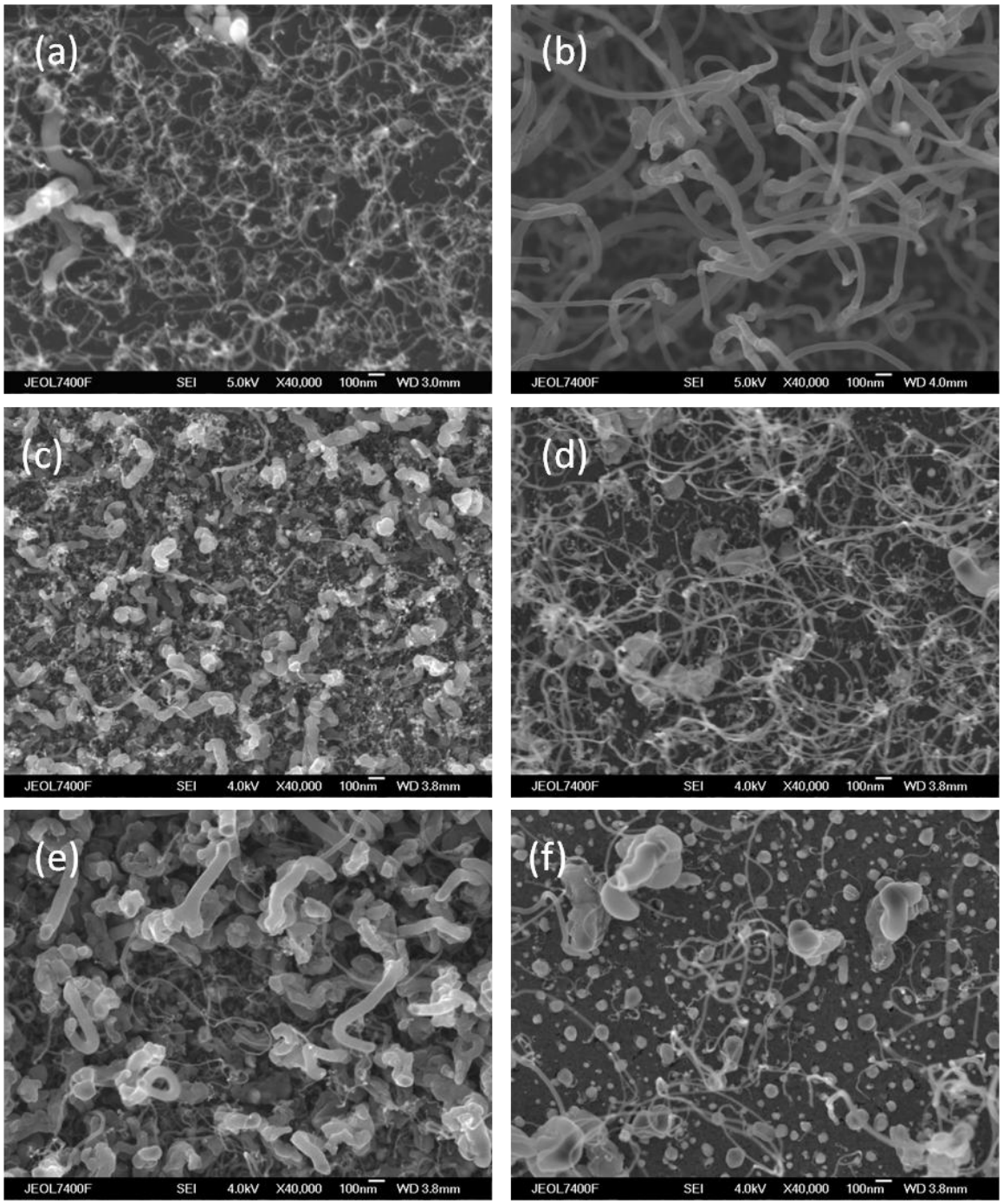

Figure 5.21 Magnified SEM micrographs of CNTs on different catalyst thickness, (a, b) 4 nm Ni catalyst, (c, d) 1 nm Ni and (e, f) 0.5 nm Ni. (a, c, e) has 15 nm Ti buffer layer and (b, d ,f) has 15 nm Ta buffer layer

Two things are commonly observed in these experiments

1. Diameter of CNTs
2. Production density

On both buffer layers, the diameter of nanotubes was definitely reduced by decreasing the thickness of catalyst film. The reduction in the diameter of CNTs was prominent using the Ta buffer layer as shown in images (b, d, f) in Figures 5.20 & 5.21. With a 5 nm thick catalyst, the diameters of tubes were between 25 nm to 30 nm, and by reducing it to 0.5 nm the as-grown CNTs were under 8 nm in diameter. The diameter of tubes grown on a Ti buffer was also reduced by reducing the thickness of the catalyst and there was some evidence of SWNTs growth on it. The measured diameter of nanotubes on 5 nm catalyst film on Ti buffer was less than 8 nm. By reducing the thickness of the catalyst the diameter was reduced as shown in Figure 5.21 (a, c& e). There are very tiny nanoparticles on the tips of tubes presenting some SWNTs.

The production density of CNTs was definitely decreased by reducing the thickness of catalyst film because the active number of nanoparticles was reduced. There is quite a big decrease in the number of nanotubes on Ta buffer supports through decreasing the thickness of the catalyst. On Ti buffer layers apparently the surface of the substrate was covered with carbon nano fibre (CNF) and tiny tubes were under them. It was also observed that as the thickness of the catalyst decreases the fibre like structure was more prominent on Ti buffer layer substrates.

From these experiments it is concluded that the thickness of catalyst film is also responsible for the diameter of as-grown CNTs. If thickness is on an atomic level, we could grow SWNTs at low temperature in PECVD system. Moreover, production decreases by reducing the thickness of the catalyst which results in fewer nanoparticles. A Ta buffer layer is suitable for MWNTs and a Ti buffer layer support is good for the growth of single walled CNTs.

5.6-Growth of Graphene

The outstanding electrical and transport properties of graphene as discussed in the literature review attracted us to prepare some single layer graphene samples for applications in a PEN fuel cell. For this purpose two routes for the growth of graphene were selected.

1. PECVD System
2. Exfoliation (or Scotch Tape cleaving method)

5.6.1-PECVD System for graphene

Growth of bi-layer graphene was conducted in the PECVD system with Ni and Cu catalysts. The procedure for sample preparation was the same as described earlier in the growth of CNTs. In CNTs, a thin metallic film up to a few nanometres was sufficient to convert metal into nanoparticles with thermal annealing and plasma treatment. In the growth of graphene case is different; a thick layer of metal is required to absorb carbon and precipitate on cooling. So the catalyst film thickness was kept in hundreds nanometres.

For the growth of graphene in the C-gear system argon carrier gas equipment was installed for cooling purposes. Growth steps and controlled parameters are given in Table 5.6

Table 5.4: Steps for graphene growth in PECVD system

Steps	**1**	**2**	**3**	**4**
Gas	Ar	H_2	C_2H_2:H_2	Ar
Flow (scm^3min^{-1})	20	20	4:20	80
Pressure (Torr)	0.5	0.5	0.5	1.0
Plasma (W)	No	No	200	No
Time (min)	15	2	10	15

1- Argon annealing

2- Hydrogen annealing

3- Growth Process

4- Fast cooling

The growth mechanism of graphene in CVD and PECVD could be explained in three steps.

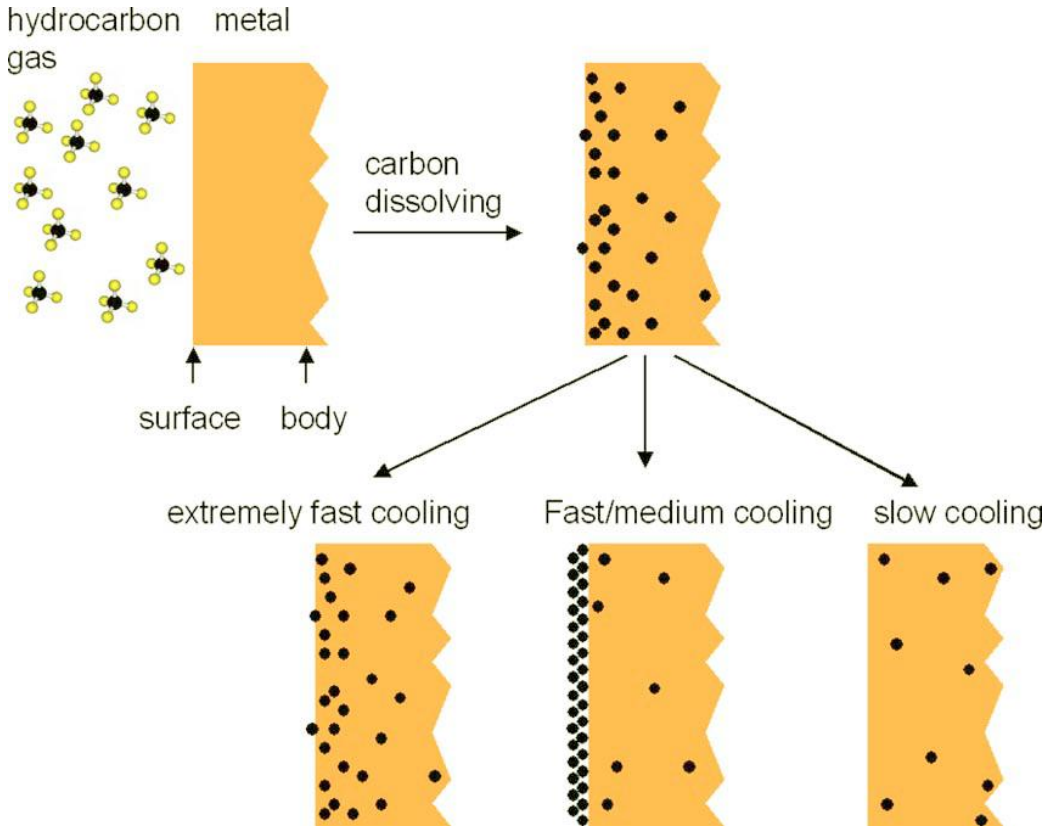

Figure 5.22 Growth mechanism of graphene [9]

1- The carbon atoms from hydrocarbon precursors dissociate on the surface of catalyst Ni on high temperature.

2-The solubility of carbon atoms in Ni makes carbon dissolution in the catalyst.

3- On fast cooling the dissolved atoms precipitate at the surface of the catalyst.

The growth mechanism is also explained in Figure 5.22. Initially two type of catalysts Ni and Cu were used in the growth of graphene film.

Graphene growth on Cu

When it was tried to grow graphene on the Cu thick film the results were not good, as shown in Figure 5.23. During the process of growth the thick film of Cu was ablated and evaporated and there was no evidence of graphene growth.

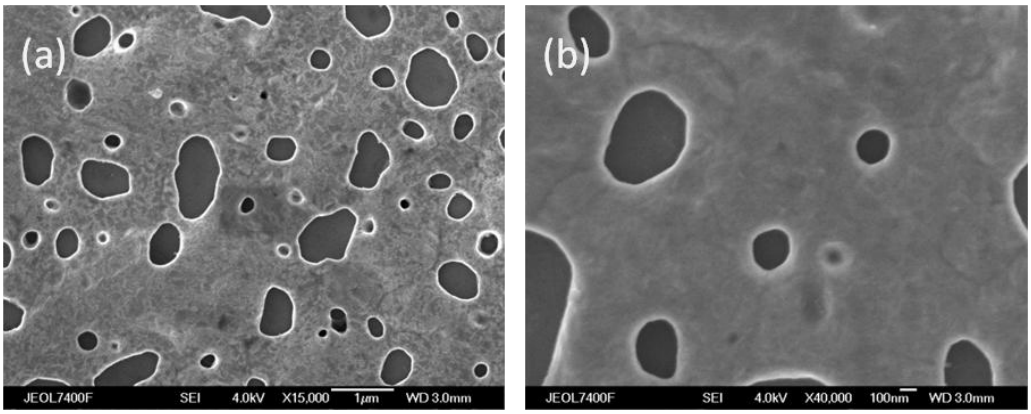

Figure 5.23 Graphene growth results on Cu in PECVD. The thickness of the film was 200 nm

Graphene growth on Ni

When it was attempted to growth graphene on a thick film of Ni, the results were also poor. The SEM images of as-grown graphene are showing that there are some layers of graphene on the top of metal Ni as shown in Figure 5.24. By chemically etching Ni it could be possible to observe a number of layers of graphene.

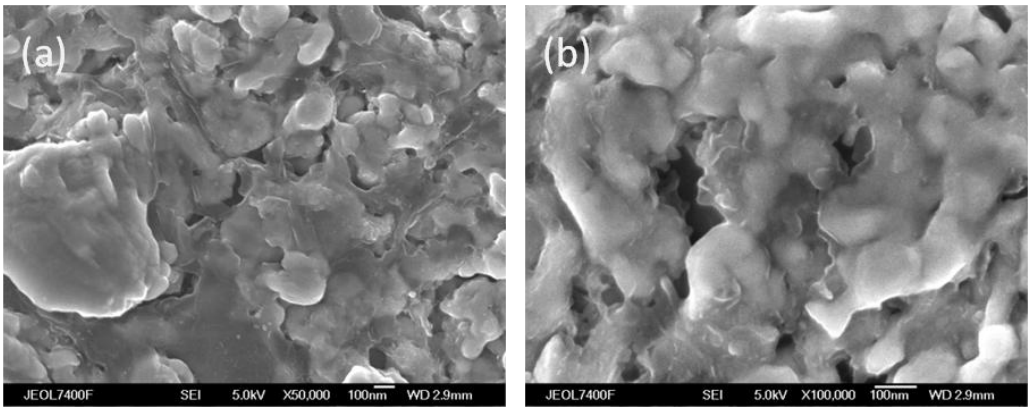

Figure 5.24 Graphene growth on 200 nm thick Ni film

5.6.2-Graphene by exfoliation or cleaving method

The weak Van der Waals forces between different stacks of graphite made it possible to separate these layers into single layer graphene. In this research the exfoliation technique was learned from the A.K. Geim research group at Manchester University. It was learned how to prepare single layer graphene and observe in an optical microscope. In this technique a small flake of graphite was peel off repeatedly on different places of an adhesive scotch tape. Peeling was performed in such a way that planes remained unbroken. Graphene was then transferred on properly cleaned oxidized silicon substrate. The prepared graphene sample was then washed with acetone, which dissolved the tape leaving only graphene. Optical microscopy and AFM were used observe the number of layers and thickness of the graphene layers. The optical microscope images are shown in Figure 5.25. From the graphene optical contrast paper [10] it is easy to determine the number of layers of graphene.

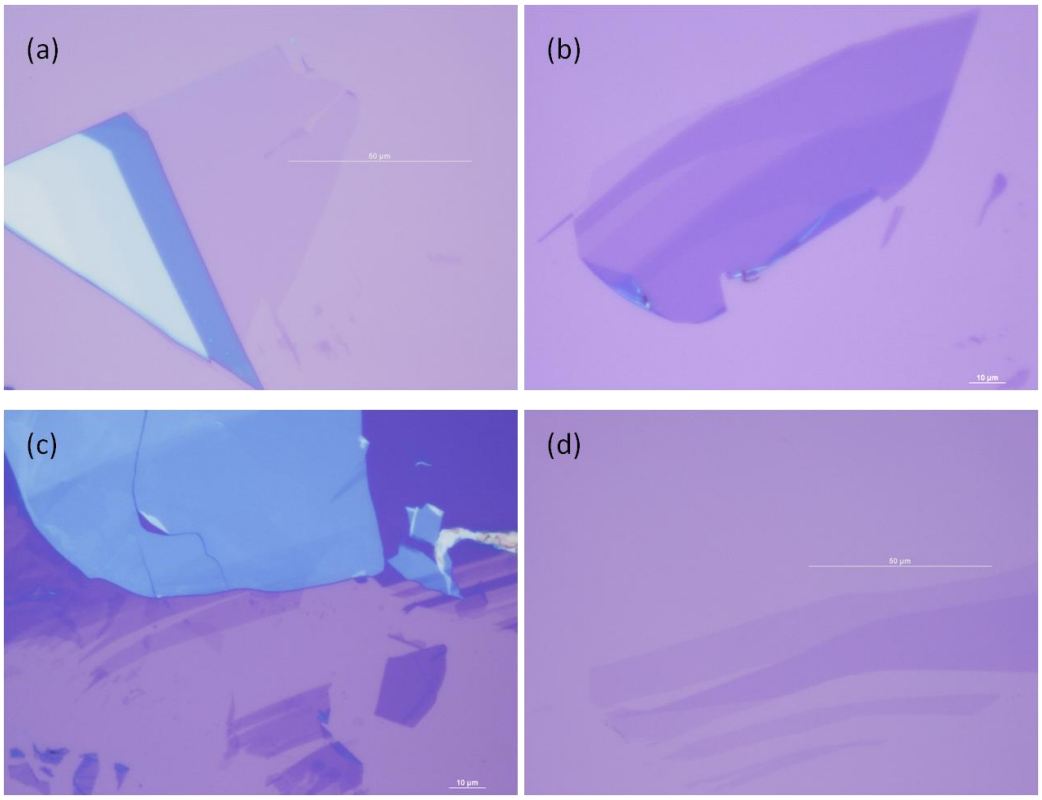

Figure 5.25 Graphene from single layer to many layers

The AFM was used to measure the thickness of the graphene film, as shown in figure 5.26.

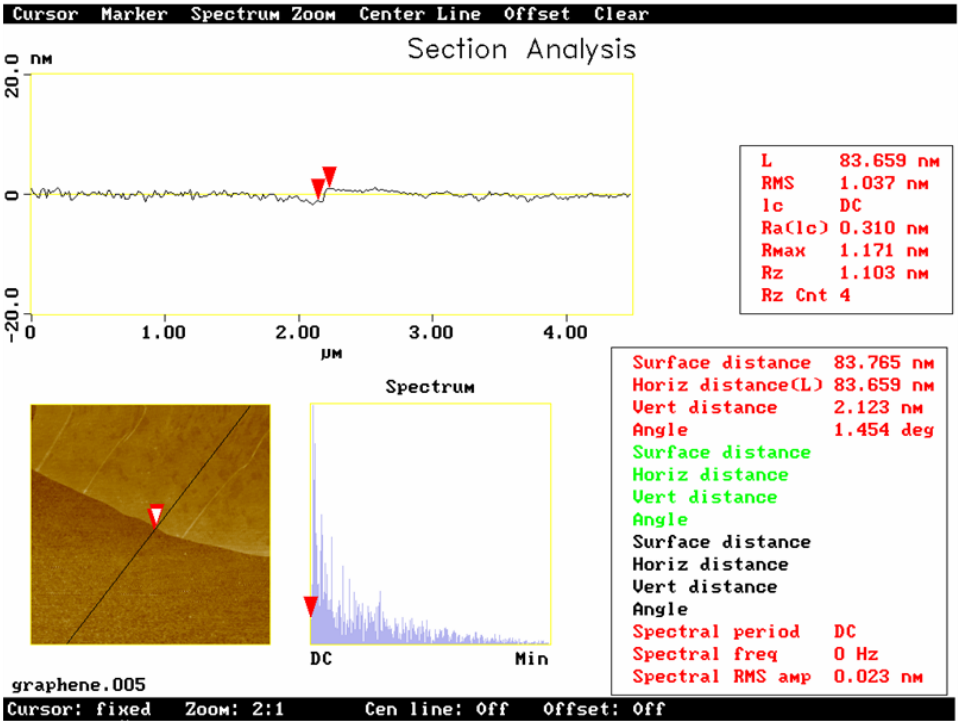

Figure 5.26 AFM overall surface image of graphene shows the thickness of graphene film

5.7-Discussion and Conclusions

In the growth of CNTs it was observed that a catalyst plays a key role. Its size, surface adhesion and interaction with the substrate effect the growth of CNTs. Thermal annealing and plasma treatment is the best technique to create nanoparticles. With this technique size of particles could be controlled. With single-step process is required to create nanoparticles and to growth CNTs in PECVD system. This single-step process protects the sample form oxidisation and other contaminations.

A detailed study about the role of buffer layer underneath the catalyst was conducted in this chapter and it was observed that a buffer layer is beneficial. The size and shape of nanoparticles could be controlled with a buffer layer. Among the different materials Ta and Ti gave encouraging results. Ta surface was smooth and particles were uniformly spherical. The growth of CNTs on Ta was observed even at 140°C. The diameters of the nanotubes were from 30 nm to 70 nm because the size of

particles was big on Ta buffer layer. Whilst Ti is good buffer layer for thin nanotubes 7 nm to 10 nm in diameter. A detailed study was also conducted about the role of catalyst in the creation of nanoparticles and growth of CNTs. It has been observed that Ni is best for low temperature growth in PECVD system. The growth parameters such as temperature, plasma power and thickness of catalyst layer were analysed in this research. It was observed that the size of particles also depends upon the thickness of catalyst film. If the thickness of metal film is in the range from 0.5 nm to 1 nm the particles will be 1nm to 5 nm and growth of SWNTs may be possible in a PECVD system at low temperature. Moreover, production decreased by reducing the thickness of the catalyst. Growth of FLG was conducted in the PECVD system and it was observed that there may be some graphene 2-dimensional films on the Ni particles.

5.8-Summary

In this section of the thesis we briefly researched the following:

- Nanoparticles were created with three techniques. Thermal annealing and plasma treatment was good to create spherical nanoparticles.
- H_2 plasma improves particle quality
- The buffer layer and type of catalyst plays important role in the sphericity of particles.
- It was observed that the materials such as Ta and Ti with higher surface energy are good buffer layers.
- During growth of CNTs it was observed that PECVD system is good for the growth of CNTs at low temperature. Growth is possible even at 140°C.
- The growth of CNTs was conducted for the first time in Dundee University during this research.
- The surface adhesion and interaction energy for the catalytic activity was discussed. It was briefly explained that buffer layer and type of catalyst affects the growth density and diameter of CNTs.

- It is explained that Ta buffer layer is good for low temperature growth of CNTs. Small diameter (7-10 nm) CNTs are possible with Ti buffer layer
- Few layers of graphene were prepared with the help of A.K. Geim research group (Condensed Matter Research Group) at Manchester University. by chemical exfoliation. PECVD system was also used to grow graphene but low temperature of system temperature did not give good results

References

1) Y. Wang, Z. Luo, B. Li and P.S. Ho, *J. Appl. Phys.* **101**, 124310(2007)
2) C.E. Giusca, S.J. Henley, C.H.P. Poa, A.A.D.T. Adikaari, J.D. Carey, and S.R.P. Silva, *Appl. Phys. Lett.* **84**, 4035(2004)
3) W.P. Wang, H.C. Wen, S.R. Jian, J.Y. Juang, Y.S. Lai, C.H. Tsai, W.F. Wu, *Appl. Surf. Sci.* **253**, 9248(2007)
4) Carbon Nanotubes: Synthesis, Structure, properties and applications by M.S. Dresselhaus, G. Dresselhaus and H. Avouris published by Springer 2000
5) J. Wei, K.P. Yung and B.K. Tay, *SIMTech technical reports* **10**(1), 1(2009)
6) J. A. Venables, *Introduction to Surface and Thin Film Processes*. Cambridge University Press, 2000
7) Web elements "Home of the periodic table" Web Elements Ltd, U.K (http://www.webelements.com/)
8) Materials Research Science and Engineering Centre, University of Wisconsin Madison (http://mrsec.wisc.edu/Edetc/nanoquest/carbon/index.html)
9) Q. Yu, J. Lian, S. Siriponglert, H. Li, Y.P. Chen and S. Pei,, *Appl. Phys. Lett.* **93**, 113103(2008)
10) Z.H. Hi, H.M. Wang, J. Kasim, H.M. Fan, T. Yu, Y.H. Wu, Y.P. Feng and Z.X. Shen, *Nano Lett.* **7**(9), 2758(2007)

CHAPTER 6 LASER PROCESSING AND NANO-MATERIALS

Pulsed laser irradiation of solid thin films has great importance in the world of nanotechnology. It can convert amorphous silicon into conducting crystalline structures for many technological applications in the field of TFTs, electron emission, bio-conducting materials, and sensors. Laser irradiation is also suitable for the creation of nanoparticles on thin films which can enhance catalytic efficiency in the growth of CNTs, and photo-catalysts for water purification and other applications. Laser ablation of targets at higher temperature can also produce nanotubes and nano-wires such as CNTs, CNF, silicon nano-wires, boron nitride nanotubes (BNTs).

The main focus of this chapter is to develop a single step process to prepare a catalytically active proton conducting polymer material by laser irradiation. The first section of this chapter is devoted to understand excimer laser. The optical system for beam profile modification is described. The subsequent section covers PEN and Nafion polymers. The details about the creation of nanoparticles with laser for the growth of CNTs, PEM fuel cell membrane and photo-catalysis are then discussed. It is also explained how laser irradiation of a film of amorphous silicon can be used to convert it into new material with different external and internal morphology.

6.1-Excimer Laser

Excimer ultraviolet (UV) lasers are frequently used in industrial and scientific applications. It is prevalent for the photolithography of micro and nano-electronic devices, surgery of eyes and dermatological treatment. Excimer laser with high pulse energies is also a novel tool for the modification of thin films on a variety of substrates at room temperature [1]. The most important part of excimer laser is its optical system which transforms a raw rectangular beam into coherent modified beam (shape and intensity) as shown in Figure 6.1. This optical system allows the reshaping of beam according to the needs of the process. There are four type of lenses used in excimer laser.

1. Telescope lenses
2. Homogenizer lenses
3. Slope lenses
4. Condensing lens

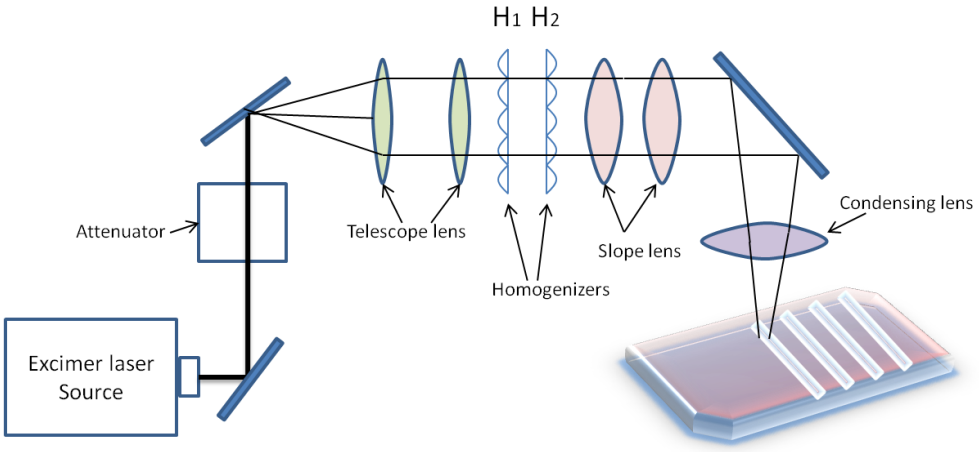

Figure 6.1 Schematic diagram of excimer laser

A set of telescope lenses are responsible for converting the raw laser beam into a uniformly parallel beam. The homogenizer lenses are a group of cylindrical micro-lenses based homogenizers which produce a very flat intensity beam profile for

uniform processing. The homogenization of the incident beam depends on the Fresnel number defined as

$$F_N \approx P_{LA}.D_{FT}/4\lambda.f_{FL} \quad \text{------ (6.1}$$

where

P_{LA} = pitch of the micro-lens array

D_{FT} = size of the flat top in the plane of homogenization

f_{FL} = focal length of micro-lens

λ = wavelength

Simply put, a high Fresnel number will increase uniformity in the intensity of beam [1]. Mostly there are two groups of homogenizers in an excimer laser; one group is responsible for intensity uniformity along the long axis and other for the short axis. If we use one group of homogenizers the top hat uniformity will be produced along the short axis and with both groups of homogenizers the beam intensity will be uniform along the short and long axis. In this research only one group of homogenizers was used to make the Gaussian beam profile (top hat along long axis and Gaussian along short axis). The third set of lenses are slope lenses which are responsible for the division of the full beam into two halves and overlap each other to make the Gaussian beam semi-Gaussian. The beam profiles are illustrated in Figure 6.2. Each beam profile has its own importance regarding the applications. A top hat beam profile with same energy fluence is good for MEMS photo masking. A semi-Gaussian or sloped beam profile has maximum energy at the edge of the beam shape and energy of beam varies ascending or descending order (low to high or high to low leading edge). This beam profile is good to modify a-Si:H thin film into spike-like structures.

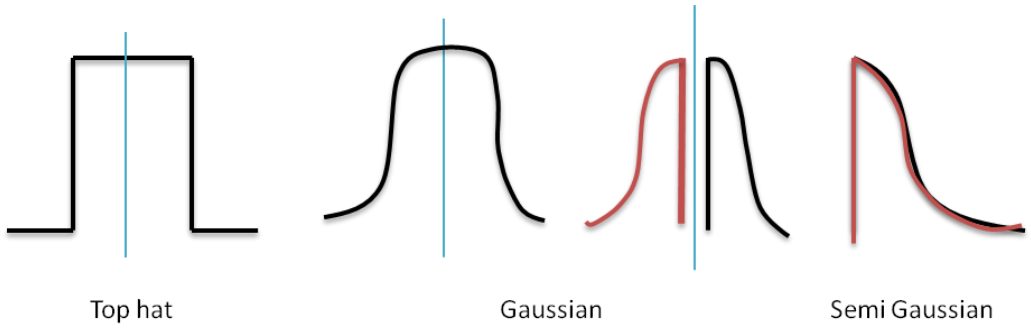

Figure 6.2 Beam profile of excimer laser

The excimer laser used in this research was a LPX Pro 210F from Coherent GmbH Germany. This KrF excimer laser has a wavelength of 248 nm and energy from 100 mJ to 400 mJ.

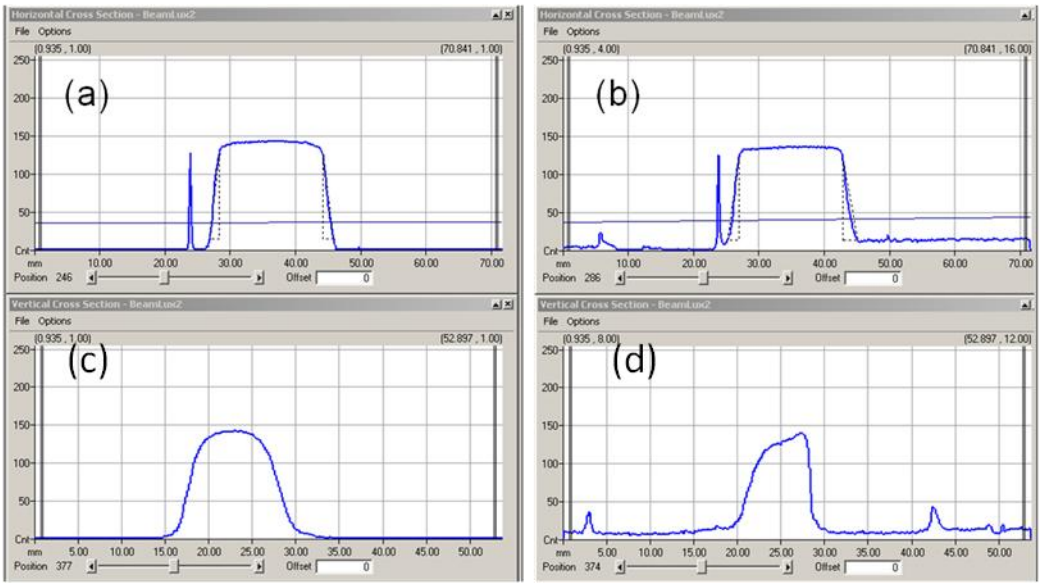

Figure 6.3 Live images of laser beam profiles both in horizontal and vertical axis (a, b) Top-Hat beam profile, (c) Semi-Gaussian beam profile and (d) Sloped beam profile.Y-axis shows energy intensity while X-axix is the beam length

A computer controlled substrate stage allowed the movement of samples in two dimensions and the scanning speed was also handled by this. The detailed parameters of the laser are given below.

Excimer Laser parameters

Pulse profile : Top hat, Gaussian, and Semi-Gaussian

Pulse area : 4x8 mm^2

Wavelength : 248 nm

Laser beam energy : 100-400 mJ

Pulse length : 10-25 ns

Sample scan speed : 1-5 mms^{-1}

6.2-PEN and Nafion

Polymers are ubiquitous organic materials with large molecular chains. Some polymers have excellent electrical and mechanical properties. Biocompatibility of some polymers may make it possible to grow human organs in future, and its proton transport capability across the material through atomic level holes makes it a promising material in renewable energy application areas.

The polymer polyethylenenaphthalate (PEN) used in this research was from Teonex. It is a good material for insulation and is a flexible substrate. These films with some superior barrier properties have been used in electrical and electronic applications including FED, thermal transfer ribbon, capacitors, motors, transformers, flexible printed circuits, solar batteries and high density long play magnetic tapes [3]. The chemical formula of this flexible film is shown in Figure 6.4.

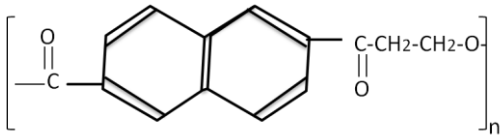

Figure 6.4 Chemical formula of PEN

We have been looking for a way to make a one step process that fabricates a robust mesoporous carbon that conducts electrons, whilst depositing the catalyst.

In PEMFC technology, protonic transport across the membrane is required to generate electricity. For this purpose proton exchange membranes were designed. Nafion is a well-known proton exchange membrane. It is a hydrated soft polymer with fixed charge sites and free volume (small-pore structures) for transport. The fixed charge sites should be of opposite charge compared to moving H^+ for the balance across the polymer. These fixed charge sites provide temporary centers for the moving charges. The vibrations of polymer segments induce physical transfer of ions from one charged site to another. The mechanism of proton transport is shown in Figure 6.5.

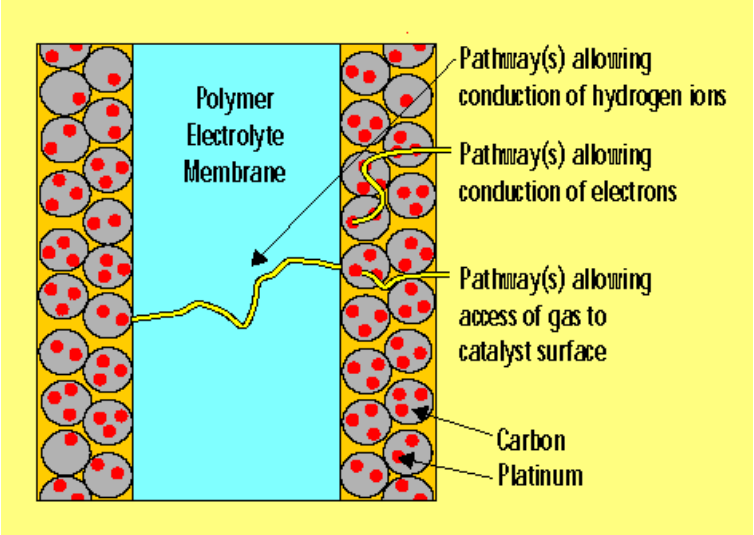

Figure 6.5 Schematic drawing of the mechanism of conduction across the membrane

Nafion is a copolymer of Teflon and perfluoro-3, 6-dioxa-4-metyl-7-octene-sulfonic acid. The Teflon backbone provides the mechanical strength whilst the sulfonic acid

group provides sites for the proton transport across the membrane. The chemical structure of Nafion is given in Figure 6.6.

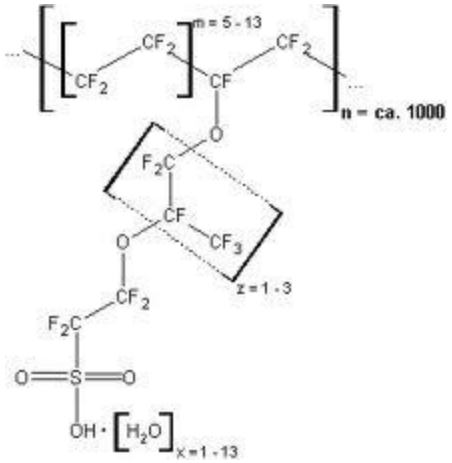

Figure 6.6 Structural formula of Nafion [4]

6.3-Laser for Nanoparticles Creation

Laser processing is an excellent tool for the fast and large area production of nanoparticles. The laser irradiation enables the creation of nanoparticles on a thin film of metal on many substrates such as polymer, glass, ceramic, and Si wafer. The nanometer scale wavelength of the pulse laser only ablates the top thin film of metal without affecting the underlying substrate. The fast melting and cooling system in laser converts a thin film of a material into nanoparticles. This capability made laser prevalent tool for the creation of nano-materials.

6.3.1-Nano-dots on Si wafer

In this work it has been determined that the low profile excimer laser is a proficient tool for the creation of nanoparticles. For this purpose a thin layer of Ni (10 nm) was deposited on a Si wafer and a low energy beam of laser light used to convert the thin film into nanoparticles. It was observed that there was a very small band of energy for irradiation because very low energy does not modify the surface and high energy evaporates thin film. The particles created by laser irradiation were completely spherical but size was a bigger as shown in Figure 6.7.

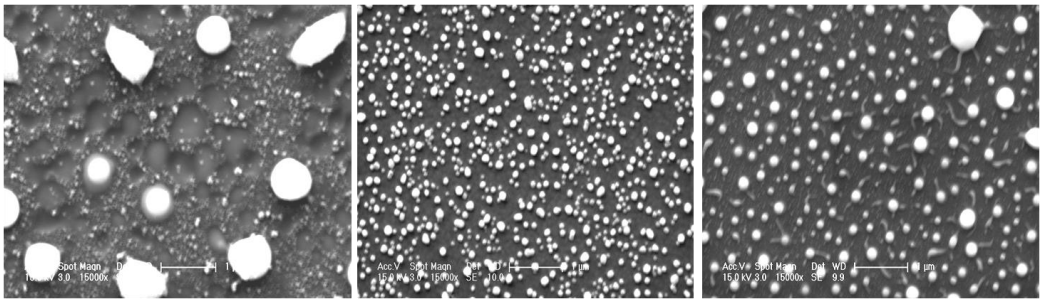

Figure 6.7 Laser processed nanoparticles on Si substrate (a) 125 mJ laser energy, (b) 155 mJ and (c) 125 mJ. Samples a and b were in IPA solution during laser processing

6.3.2-Nanoparticles on PEN

Excimer laser irradiation was used to develop a novel single step process for the modification of surface with carbon and nanoparticles for potential applications in proton exchange membrane for PEMFC. This material has a layered structure and on the top of both sides there is a barrier layer which provides enhanced adhesion, winding and handling properties. This layer also absorbs UV light and helps in the modification of structure of PEN during excimer laser irradiation.

A study of the creation of nickel nanoparticles on PEN was conducted with the help of the excimer laser and a unique confinement process. The idea behind the creation of nanoparticles on PEN was to make it possible to grow CNTs on plastic materials in PECVD system with the help of catalyst nanoparticles. The difficulty in the creation of nanoparticles on plastic is that plastic is very soft, with a very low melting temperature. A rise in temperature up to 100°C could deform plastic.

A 50 µm thick PEN sheet from Teijin DuPont Films Japan was used to create nanoparticles in this research. The sheet was cleaned using IPA and dried in a flow of N_2. The d.c sputtering was used to deposit thin layers of Ni (10 nm) and Cr (20 nm). Use of Cr as a buffer layer underneath the catalyst Ni on PEN increased thermal strength without poisoning the catalyst.

Excimer Laser with different energies from 60 mJ to 90 mJ was used to ablate thin layer into nanoparticles. The frequency of laser pulses was 25 Hz with sample speed 2 mm/s. The Philips XL30 SEM was used to observe the surface structure of PEN after laser irradiation. ImageJ was used to measure the width of clusters and diameters of nanoparticles.

Figure 6.8 shows the SEM images of PEN samples after laser ablation. Laser irradiation created a clustered structure. It is clear from images that the metals were peeled off due to laser. It is observed in SEM images that with laser ablation process the thin layer of metal divide into clusters because of low softening temperature of polymer.

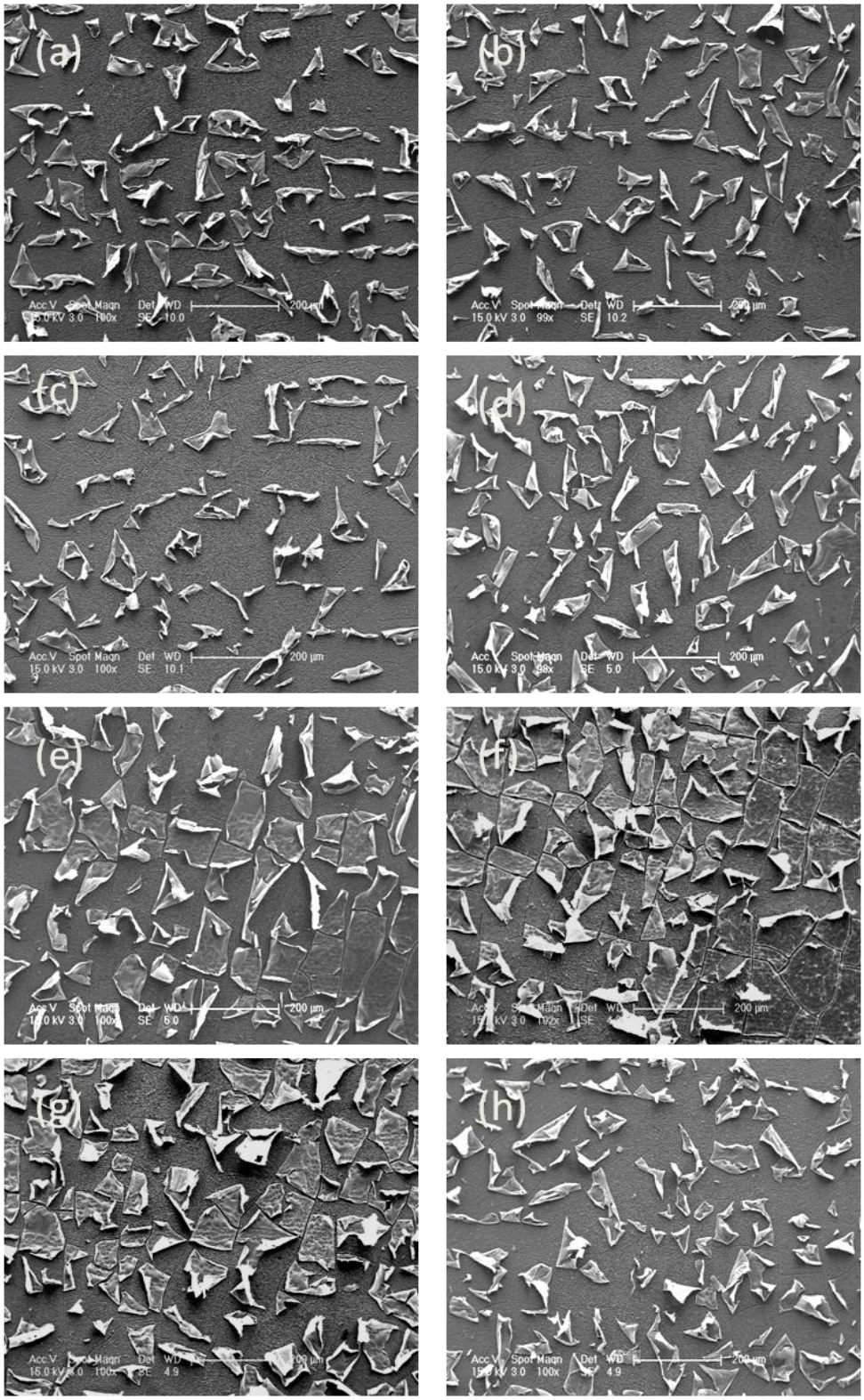

Figure 6.8 Metallic clusters produced with different laser energies (a) 60 mJ, (b) 66 mJ, (c) 75 mJ, (d) 78 mJ, (e) 81 mJ, (f) 84 mJ, (g) 87 mJ and (h) 90 mJ. In all runs the frequency of laser pulses was 25 Hz and 2 mm/s sample speed.The thickness of Ni was 10 nm

The size of cluster also depends upon the energy of laser beam. The average size of clusters was increased by increasing laser beam energy from 66mJ to 84mJ after that the width of clusters started to reduce. The graph between laser beam energy and average width of clusters is showing the variation in clusters size.

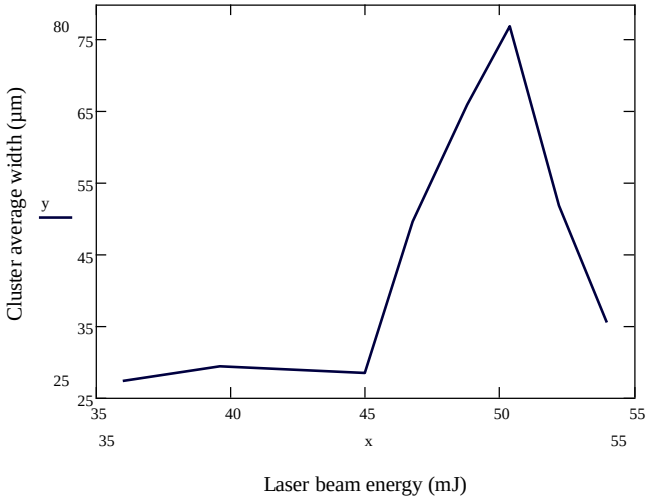

Figure 6.9 Variation in the size of clusters with laser beam energy

The nanoparticles on the clusters were observed at high magnification in SEM (XL 30K). Mostly, the nanoparticles were entangled with each other. However, the clusters which were created with laser energy from 81 mJ and 84 mJ had separate nanoparticles as shown in Figure 6.10.

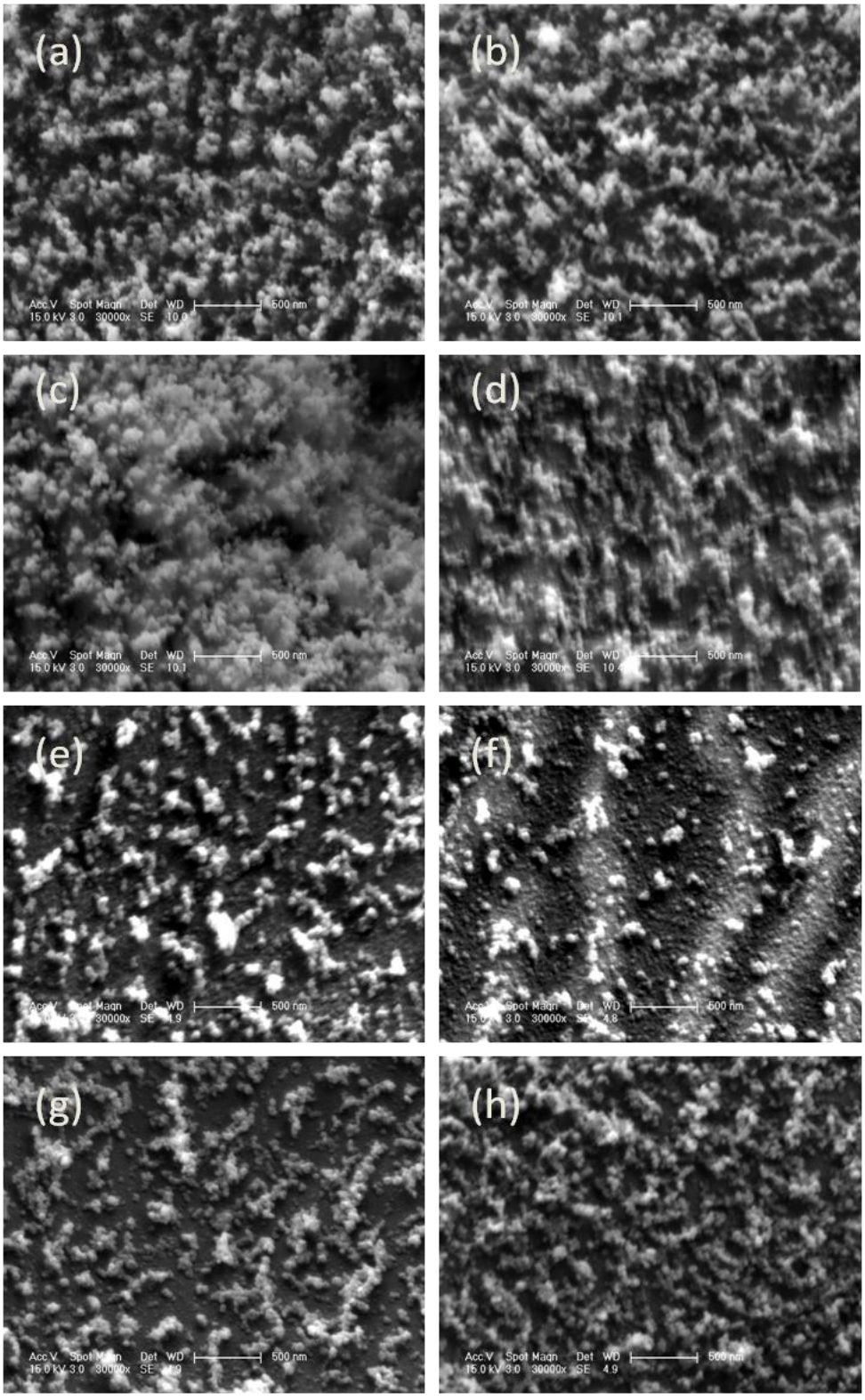

Figure 6.10 SEM images of nanoparticles produced on clusters with different laser energies (a) 60 mJ, (b) 66 mJ, (c)75 mJ, (d) 78 mJ, (e) 81 mJ, (f) 84 mJ, (g) 87 mJ and (h) 90 mJ. In all runs the frequency of laser pulses was 25 Hz and 2 mm/s sample speed. The thickness of Ni was 10 nm.

It was observed in the variation of energy of laser that optimum energy for the creation of nanoparticles was in the region from 81 mJ to 84 mJ. With 84 mJ laser pulses, the nanoparticles were small separate and rounded, with average size of particles around 20 nm, as shown in Figure 6.11.

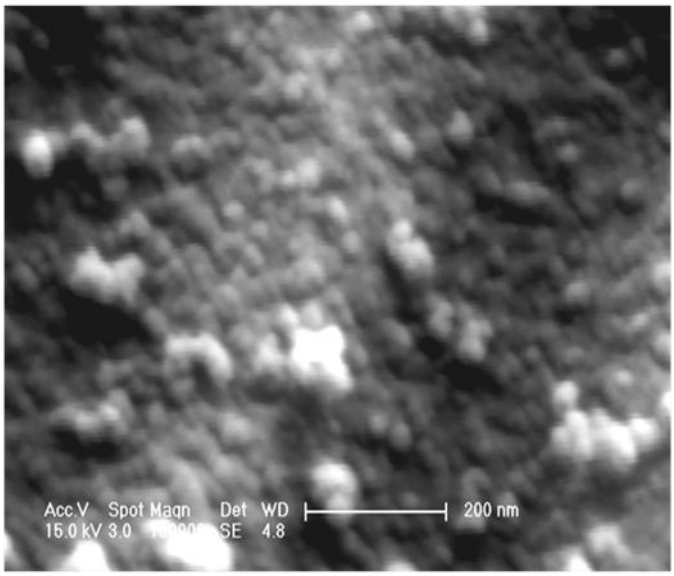

Figure 6.11 Magnified SEM image of nanoparticles of Ni on PEN with 84 mJ laser beam energy

In conclusion, it is possible to create catalyst nanoparticles with the help of laser ablation. The small variation in laser beam energy causes a big change in surface structure. With 86mJ laser energy nanoparticles were separate and may be helpful in the growth of CNTs.

6.3.3-Nanoparticles on Nafion

To observe the behavior of Nafion by excimer laser irradiation a thin film (30 nm) of Ni was deposited by using d.c sputtering on Nafion. Different energies of excimer laser were used to observe the effect of laser energy on the size of nanoparticles. Imaging was conducted by SEM.

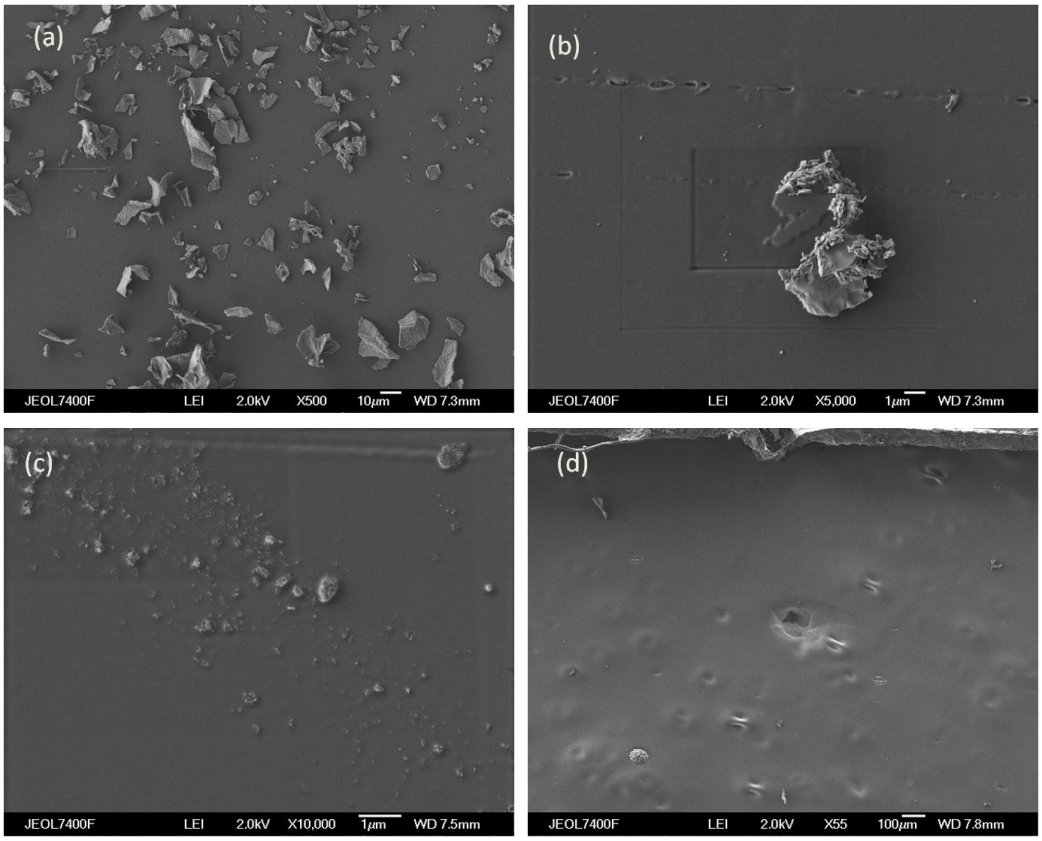

Figure 6.12 Laser irradiated of Ni on Nafion substrate (a) 60 mJ laser energy, (b) 75 mJ, (c) 90 mJ, and (d) 105 mJ laser energy

Laser irradiation mostly ablated the metal Ni on higher energies, and only at low energy (60 mJ) there was some evidence of clusters of metal as shown in figure 6.12. With high energy laser processing, the film of Ni totally disappeared and the surface of the Nafion was smooth.

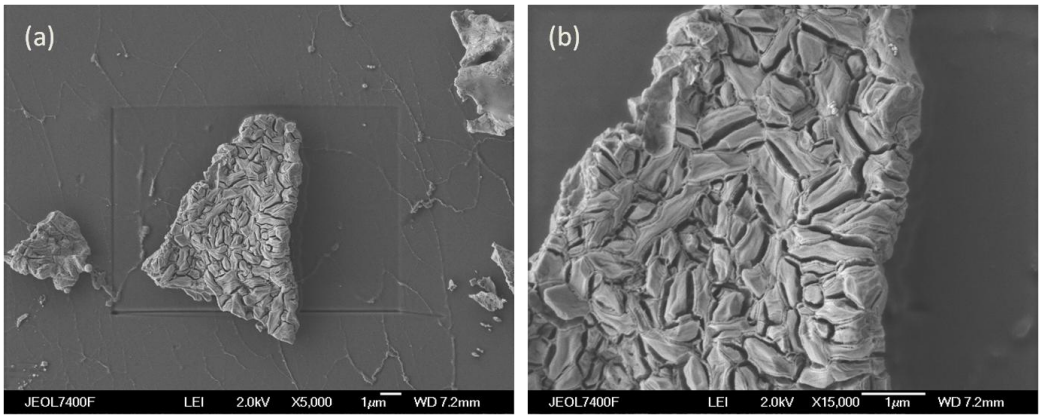

Figure 6.13 Low energy laser (60 mJ) change thin layer of metal into crystalized metal cluster

The fast charging during imaging suggests that there was moisture on the Nafion sheet which did not allow the thin film of metal to convert into nanoparticles by laser irradiation, as shown in Figure 6.13. It was decided to dry Nafion more vigorously before metal film deposition and laser processing. For this purpose some pieces of Nafion were placed in an oven at 80°C for more than seven days.

After drying, a thin film of Ni 50 nm was deposited by d.c sputtering. A 66 mJ excimer laser (lowest energy possible) was used to modify the surface of the Nafion. The SEM images in Figure 6.14 show the surface of the Nafion after laser irradiation. Laser irradiation made metal film into flakes and there were some particles as well.

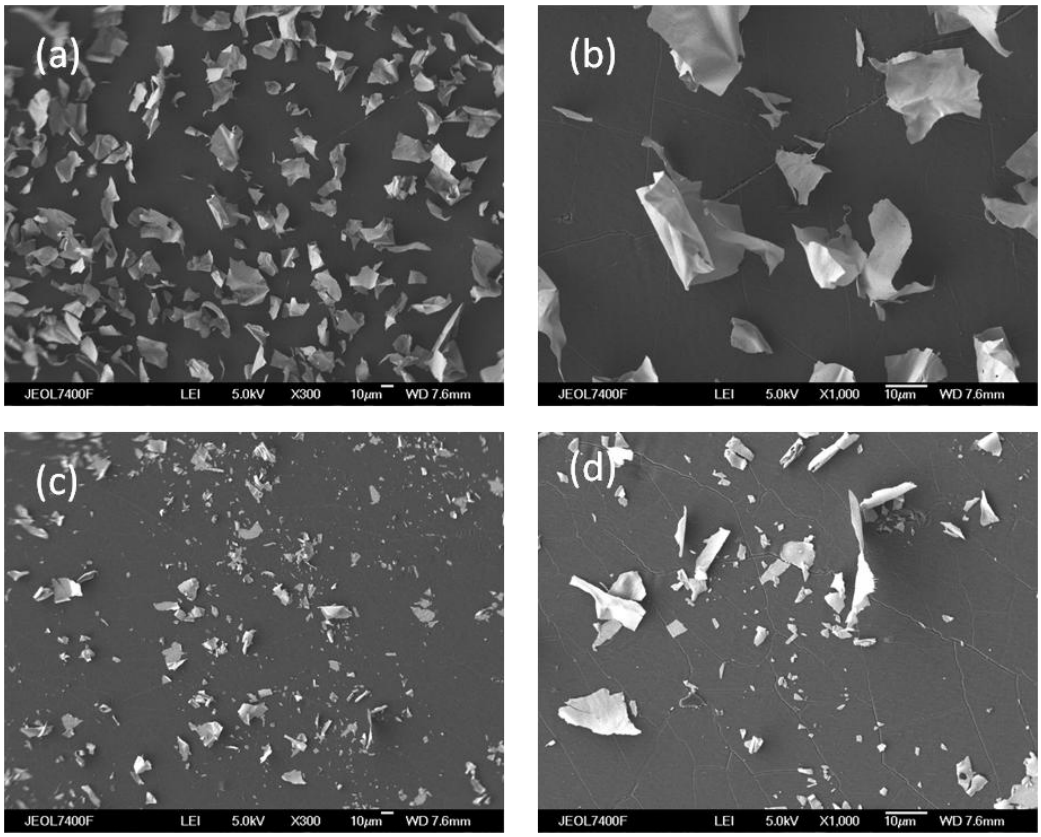

Figure 6.14 SEM images of dry Nafion after laser irradiation. 30 nm Ni was on the top of Nafion

It has been also observed during laser irradiation that Nafion is transparent to UV light (like quartz) which means that surface absorption is very low and transmission high. This effect was observed during laser irradiation when exposed metal on one side of Nafion and the other side was modified as well.

In conclusion, although Nafion is a widely used material for fuel cell applications it does not seem feasible to develop a one step process to convert it as electrolyte and electrode by laser irradiation. UV light transmission and the hydrophilic nature of Nafion do not allow the creation of nanoparticles on it.

6.4-Laser Processed Silicon and CNTs

Amorphous silicon is a very actively exploited electronic and optical material. Outstanding performance of this material allows it for conformal and large scale coating on a variety of substrates at low temperature [5]. It is widely used in the electronics industry for such devices as thin film transistors, solar cells and photoreceptors [6]. Amorphous silicon is also a good electron emitter at higher threshold from 15 to 20 V/µm. The problem with this material is that it is not a stable emitter and after couple of uses material efficiency decreases. Higher threshold of this material shows that it is not an energy efficient material for display devices.

CNTs have excellent electrical, thermal and mechanical properties. These tubes are good electron field emitters at low threshold from 2 to 5 V/µm and are very stable. To improve the material properties of amorphous silicon, it was attempted to make a composite material of a-Si and CNTs. For this purpose a multi-step technique employing a lift-off method has been used to deposit a buffer layer and Ni catalyst on the tips of laser processed silicon (LPS). Figure 6.15 shows a schematic diagram of the multi-step technique to create CNTs on the tips of LPS. A p-type silicon wafer was used as a substrate for the deposition of a:Si. The wafer was first oxidised to avoid interaction between the Si and the amorphous material. A thin layer of Mo (120 nm) was coated on top to grow amorphous silicon. The hydrogenated amorphous silicon of thickness 500 nm was deposted in a PECVD system at 220 °C and 100 mTorr gas pressure. SiH_4 was used as a feedstock gas with a flow rate of 75 scm^3min^{-1}.

To create LPS microstructure spikes on the sample, an excimer laser (LPXpro210F Coherent GmbH Germany) was used. Laser energies from 210 mJ to 240 mJ was used to irradiate the a-Si:H thin films. The sample were placed on the computer controled translation stage and scanned along the x-direction. Because the beam profile was sloped, the laser fluence suddenly increases to its maximum and then gradually reduces to zero producing a spike-like structure on the substrate.

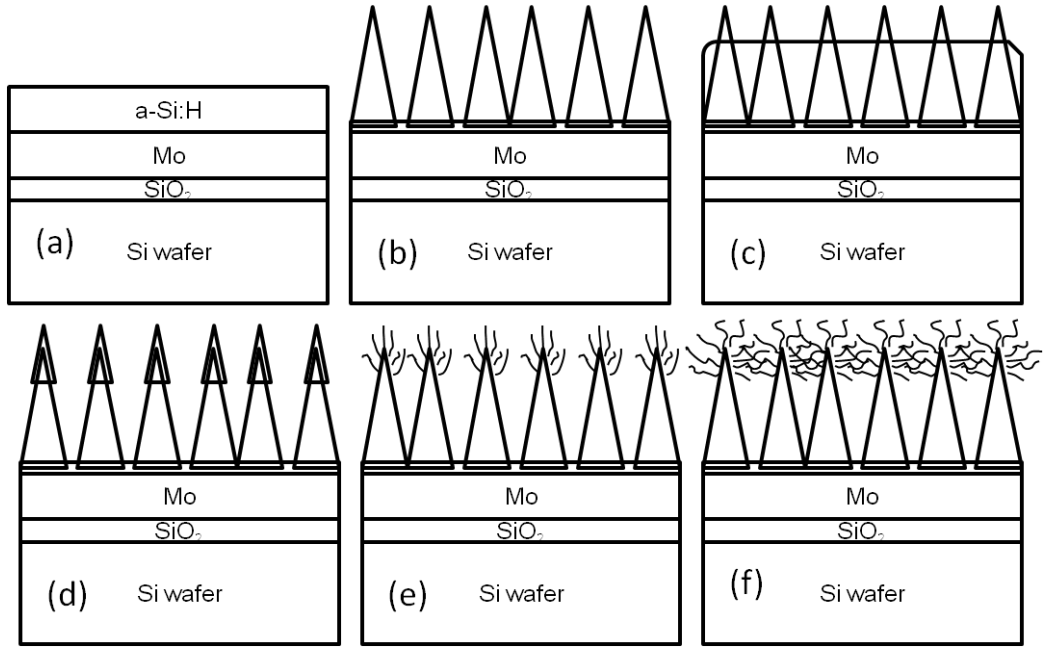

Figure 6.15 Scheme of the process for the growth of nanotubes on the tips of LPS (a) an oxidized piece of Si wafer with 120 nm Mo and 500 nm a-Si:H, (b) creation of LPS tips , (c) exposing process of tips by photolithography lift-off and plasma ion etching, (d) deposition of buffer layer of Ta 10 nm and catalyst Ni 5 nm on exposed part of tips, (e) growth process of CNTs on the tips like a forest (branches of a stem) and (f) formation of CNT network by increasing growth time of tubes.

For the growth of CNTs on the tips of the LPS, catalyst nanoparticles should be coated and confined only on the tips of these spikes. For this purpose the following steps were adopted. Firstly, positive photoresist S1813 was used to cover the whole surface of the laser microstructured a-Si:H film. Secondly, plasma ion etching was used to expose the tips. The etching gases were Ar, CF_4 and O_2 with flow rates 30:8:8 $scm^3min^{-1}cm$, respectively. Thirdly, after the removal of photoresist from the tips, thin layers of Ta and catalyst Ni (10nm and 5nm respectively) were deposited on the sample by d.c sputtering. Finally acetone was used to remove the photoresist and metals on the surface of the sample except the tips. The radio frequency (13.54 MHz) PECVD system was used to grow the CNTs. In the PECVD growth technique, creation of catalyst nanoparticles is essential so the sample was heated to alter the thin catalyst film into nanoparticles. NH_3 plasma was used to sharpen up the nanoparticles and reduce contact angle between nanoparticles and substrate. After the creation of nanoparticles, the sample was ready for the growth of CNTs. The growth of nanotubes was carried out for 5 minutes at the temperature of 525°C with feedstock gases C_2H_2 and NH_3 at flow rates 20 scm^3min^{-1} and 80 scm^3min^{-1}

respectively. The R.F. plasma power was 200 W and the pressure inside the chamber was kept at 5.5 Torr.

The surface morphology of the LPS microstructures and CNTs was observed on a Philips XL30 SEM with an accelerating voltage of 15 keV and working distance of 10 mm. Figure 6.16 (a) shows the morphology and microstructure of the Si spikes after excimer laser irradiation. It was observed that the average height of the LPS spikes was 1.5 µm and the diameter was 0.75 µm. The tips of LPS spikes were in the range of 50 to 120 nm. It has been observed from the experiments that the height and diameter of LPS spikes could be controlled by controlling the energy and shape of the excimer laser beam and the laser pulse frequency is responsible for the spacing between the spikes.

The SEM image of the as-grown CNTs on the spikes of LPS is presented in Figure 6.16 (b). Despite the deposition time of CNTs being only 5 minutes, the LPS spikes have been completely covered with CNTs.

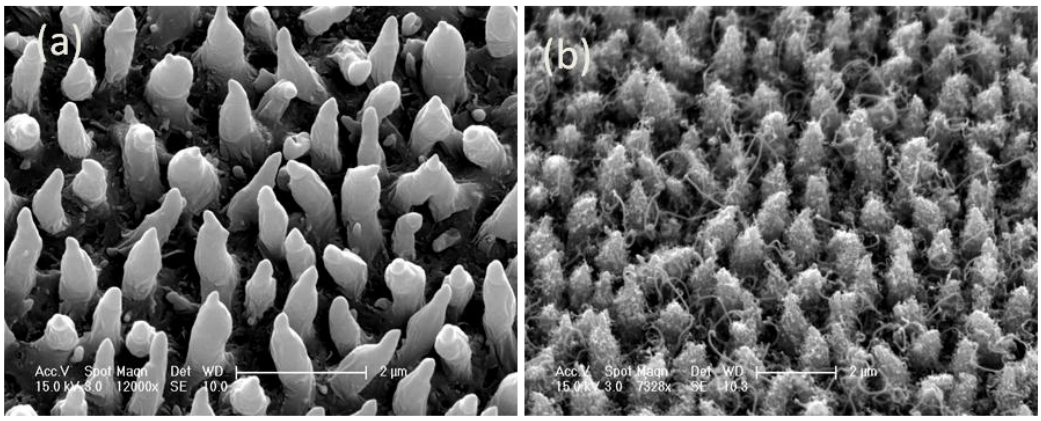

Figure 6.16 SEM images of LPS spikes and CNTs (a) LPS pikes after laser ablation, (b) as-grown CNTs on LPS spikes. In (b) On the tip of LPS there were 10 nm Ta buffer layer and 5 nm Ni catalyst

Higher resolution SEM images of as-grown CNTs on microstructured LPS tips are shown in Figure 6.17. Figure 6.17(a) shows the top view of CNTs on the LPS spikes. Figure 6.17(b) shows a more highly magnified image showing that the tip is densely covered with CNTs. It is clear from the images that CNTs are making a highly developed network on the silicon tips.

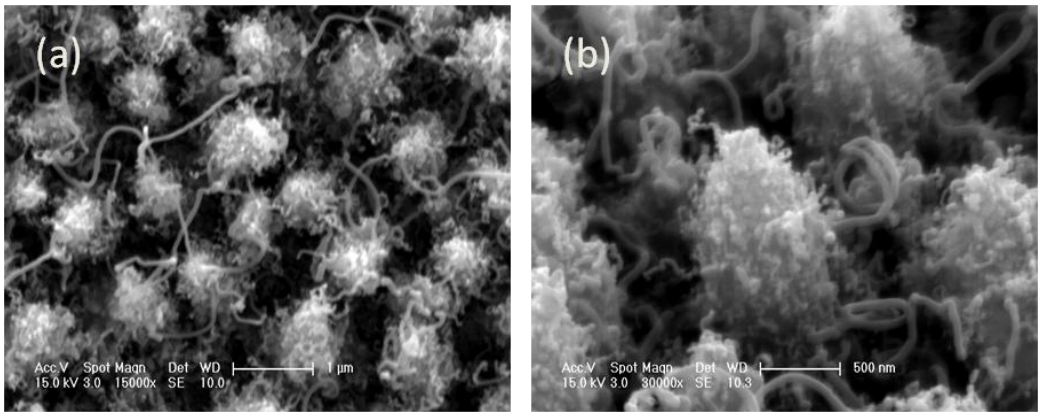

Figure 6.17 SEM images of CNTs on a-Si: H tips (a) overall top view of CNTs network (b) close up view of laser processed silicon microstructured towers with CNTs, the view was taken at 40°

It has been observed in this study that the growth of nanotubes can be controlled by changing the deposition parameters of PECVD system. It is predicted that the length of CNTs can be controlled by adjusting their growth time. If the growth time is too short, the tubes will be like branches of a stem on individual LPS spikes and if growth time is long, the tubes will reach their maximum length. They could make a network on all the spikes as shown in Figure 6.17. Both growth strategies have their own applications. Also the diameter of nanotubes could be controlled by controlling the size of nanoparticles on the tip of spikes.

As mentioned earlier, a buffer layer of Ta under the Ni catalyst was used to enhance the growth capability of the catalyst. Ta is a hard material with excellent properties usually used for high performance capacitors. This buffer layer of Ta prevents the interaction between amorphous silicon and carbon to form silicide during the growth of CNTs.

With the growth of CNTs on LPS spikes it may be possible to make an active matrix for large area field emission, charge storage devices and a number of biomedical applications. The application of CNTs on the tips of LPS in field emission is quite promising because a-Si is not a stable electron emitter and its threshold is higher. The growth of CNTs in these spike structures will enable to stabilize the process by providing a buffer layer. The field emission capability of a-Si and CNTs was tested

in the field emission chamber. A graph is plotted between applied voltage and anode current for a-Si, CNTs and a-Si-CNTs as shown in Figure 6.18. Initially, there was some increase in current and after that it was uniform because of an active ballistic layer of a-Si.

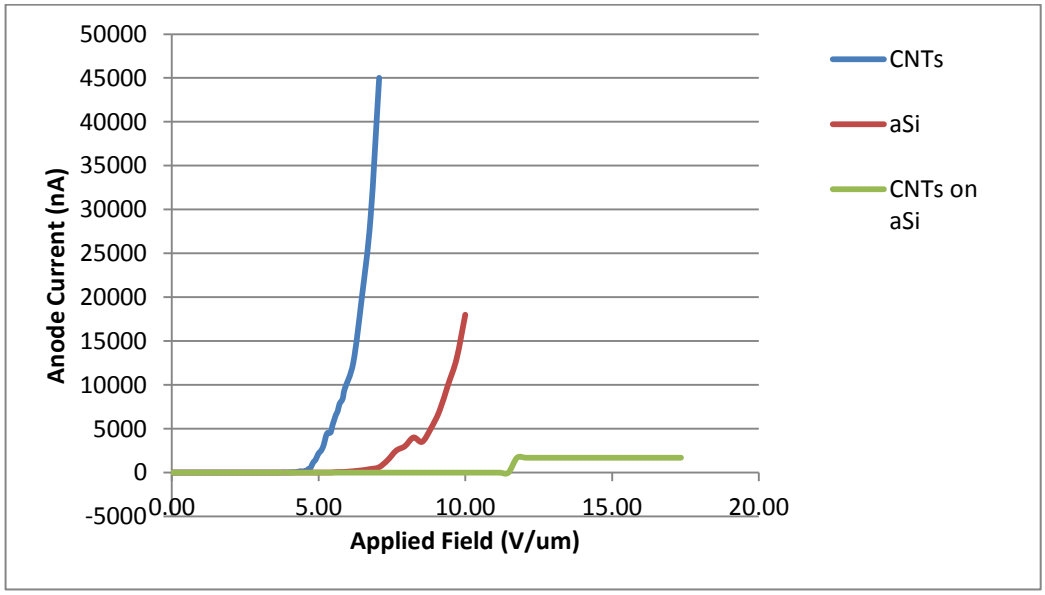

Figure 6.18 Plot between applied field vs anode current for a-Si, CNTs and a-Si-CNTs

It can be concluded that CNTs on the tips of LPS may play a role of an active ballistic layer to improve uniformity in electron emission.

In this study growth of CNTs on the tips of LPS was investigated with the help of radio frequency PECVD system using C_2H_2 and NH_3 gases. In this system growth has been done at low temperature. Photolithography and plasma etching were used to deposit catalyst nanoparticles on the tips.

6.5-Discussion

Excimer laser is a UV energy tool which could modify the thin layer of metal without damaging the substrate. It can only penetrate into a few nanometres and modify the top surface. So nanoparticles were created with the help of excimer laser. It has been demonstrated that a low energy beam is suitable to convert a thin film into nanoparticles. Thin films could be on Si substrates for the growth of CNTs or on PEN substrate for energy applications. A low energy beam of excimer laser can easily convert a very thin film into nanoparticles. The polymer materials Nafion and PEN were discussed here; their molecular formula, backbone structure and physical properties. It was discussed how a Nafion enable the motion of proton across the membrane.

Excimer laser beam of high energy was used to create spike-like amorphous Si structures. Growth of CNTs with a multi-step process was conducted on the tip of spikes. This research enabled us to produce a material which has large surface area and multi-branch structure. This material has great promise for future applications because it combines the properties of CNTs and LPS materials.

6.6-Summary

In this chapter the following outputs were observed:

- The excimer laser is an important tool for the surface modification of materials. The energy profile and beam shaping was studied.
- The two important polymer materials, PEN and Nafion were used as substrates here for the creation of nanoparticles by the excimer laser.
- The size of particle and laser beam energy was discussed. Excimer laser with energy from 81 mJ to 84mJ was appropriate for the creation of nanoparticles.
- A novel material was achieved for the first time in this research by the growth of CNTs on the tip of LPS spikes. A multi-step technique was used to grow CNTs on the tips.

References

1) D.G. Georgiev, L.W. Rosenberger, Y.V. Danylyuk, R.J. Baird, G. Newaz, G. Shreve and G. Auner, *Appl. Surf. Sci.* **249**, 45(2005)
2) Introduction of laser beam homogenizer, LINOS-A member of the Qioptiq
3) Teonex(PEN) Teijin Dupont Films
4) http://www.mecadi.com/en/literature_tools/encyclopedia/categorial/Ionomer/Nafion_copolymer_made_from_PTFE_and_perflourinate/
5) C.R. Wronski, J.M. Pearce, R.J. Koval, A.S. Ferlauto, R.W. Collins, *RIO 02 - World Climate & Energy Event*, 68(2002)
6) P. G**.** LeComber, *Phys. Scr.* **45**, 22(1992)

CHAPTER 7 PROTON EXCHANGE MEMBRANE FUEL CELL

The role of nanoparticles in energy devices is becoming more prevalent so after the study of nanoparticles created on PEN substrate with excimer laser irradiation it was decided to observe nanoparticles activities on this material for PEMFC. The focus of this chapter is to study the catalytic activity of nano-composites on laser processed PEN and Nafion. This chapter also describes the catalytic activity of laser processed metal dots on PEN and the performance of the PEN material in the PEMFC.

7.1-Proton Exchange Membrane Fuel Cell (PEMFC)

PEMFC is an energy device which takes fuel from one side and oxidant on the other, processes it and produces electricity. Two components of PEM fuel cell are very important; the proton exchange membrane and catalyst nanoparticles. The most usable membrane in PEMFC is Nafion which provides free ion sites for proton transport. This material is hydrophilic and transparent to UV light, so it is not possible to modify it by laser irradiation. The catalyst platinum is very important in the ionization of fuel (hydrogen) into protons and electrons at low temperature. Because of the use of platinum the cost of PEMFC is very high. It is possible to reduce the cost of PEMFC by replacing the carbon substrate with CNTs and platinum with Ni. CNTs have good storage capability of hydrogen fuel and by direct growth with catalyst Ni on the top could be suitable for the ionization fuel.

This work aims to provide a one step process for the formation of a fuel cell membrane. Currently there is difficulty in conventional PEN membranes with the

deposition of carbon materials and catalysts. This work shows that it is possible to form a conducting mesoporous carbon surface with dense arrays of catalytic nano-dots in a one step laser process that lends itself to large area and cheap processing. PEN was chosen as the test material. Although it is not an ideal membrane for transport, it has a surface barrier layer that can be modified by UV irradiation. The chemistry of the material allows transport of hydrogen through the modification and mediation of oxygen chains.

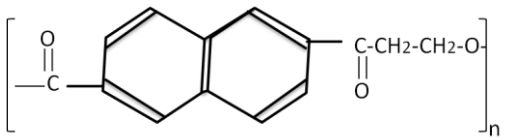

If the surface is successfully modified (carbonized) by laser irradiation, it may be possible to modify the internal chemistry to include more functional groups (SO_3 or SO_4) which are helpful in protonic transport. However, this is out of the scope of this work. Here the focus is on the surface modification of PEN with a single step process.

7.2-Prototype Design of PEMFC

As discussed in Chapter 3 a fuel cell consists of electrodes, an exchange membrane, gas flow channels and protecting side walls, as shown in Figure 3.1.

For the study of PEN as a proton membrane, a prototype model of fuel cell was designed. For this purpose two transparent Perspex sheets of 10x10 cm^2 were used as protecting side walls and mass flow channels. The Perspex sheets were threaded in such a way the reactants can easily flow through the channels. 5x5 cm^2 cross channels were milled to a depth of 0.2 cm in workshop. Within these channels the fuel can easily distribute and by-products go through the outlet as shown in Figures 7.1 & 7.2.

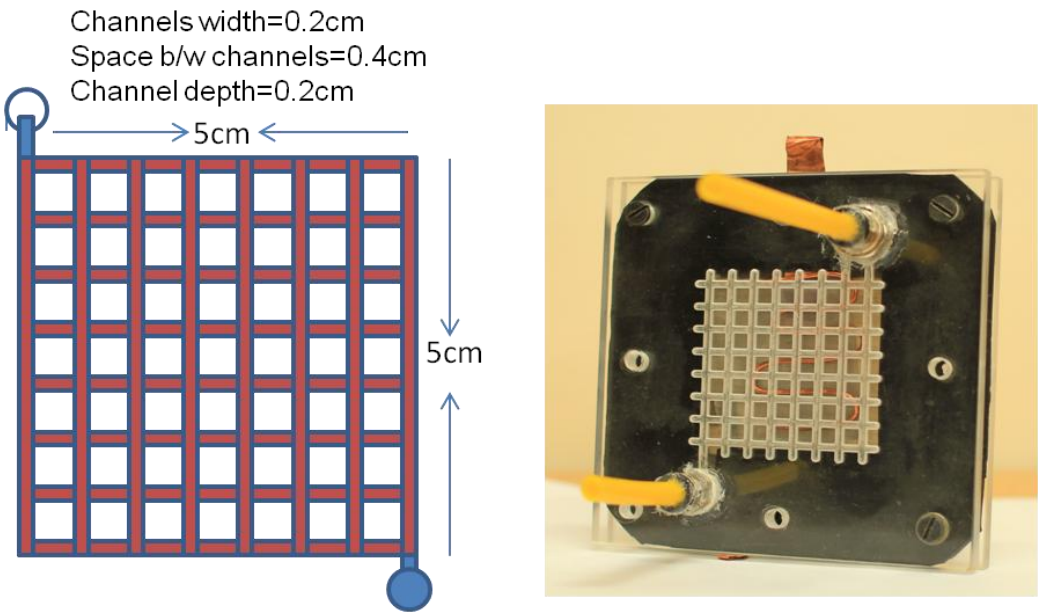

Figure 7.1 Drawing of mass flow channels and real image of the fuel cell

Rubber seals were prepared according to the size of the fuel cell to prevent leakage and both sheets were screwed to fix. The unit was easy to assemble.

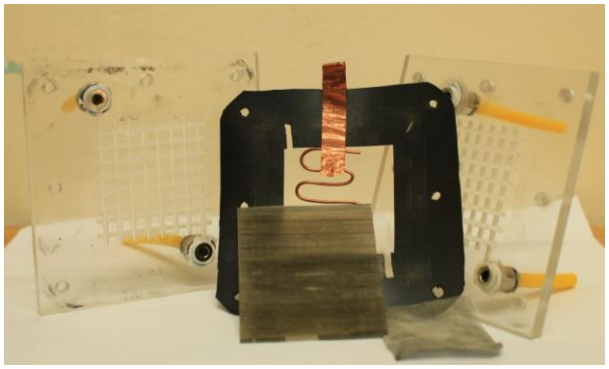

Figure 7.2 The image of all the accessories of fuel cell setup

For the conductivity, stainless steel mesh of 5x5cm^2 was used on both sides. PEN as a membrane was coated on both sides with Ni and ablated by laser which made nanoparticles. The fuel cell was assembled and tested by the Hydro-Genious Professional fuel cell apparatus. Hydrogen as fuel and oxygen as oxidant were produced from the electrolyser by the application of 1.6 V and less than 1 A current. The output was measured by a load provided by the Hydro-Genious Professional.

7.3-Catalytic Activity of Nanoparticles in Temperature Programmed Reaction (TPR)

Temperature programmed reactions were used to test the catalytic activity of Ni nanoparticles on flexible PEN substrate in the Fuel Cell Lab in St. Andrews University. The nanoparticles were created by excimer laser irradiation on PEN both at atmospheric pressure and in vacuum as described in Chapter 6. The first experiment was conducted on the nanoparticles created in atmospheric pressure. The substrate polymer with nanoparticles on the top was divided into small pieces and placed in a quartz funnel. The temperature was ramped at 5 °C/min up to 240 °C in a stoichiometric mixture of H_2 and O_2 diluted in argon. The idea was to see how effectively the Ni would catalyze the reaction between H_2 and O_2 to give H_2O. This would cause a trough in the mass spectrometer readings of the exit gas for the first two, and a peak in water. Unfortunately no changes were detected; this is perhaps not too surprising as these temperatures are rather low for such a reaction. The temperature range was also limited by the stability range of the polymer itself. Also, the amount of the Ni phase present may be small as shown in the plot of Temperature Programmed Reaction (TPRx) versus temperature in Figure 7.3. In this experiment, the metallic particles were processed in air, so were likely oxides. This was further explored by EDX as shown in Figure 7.6.

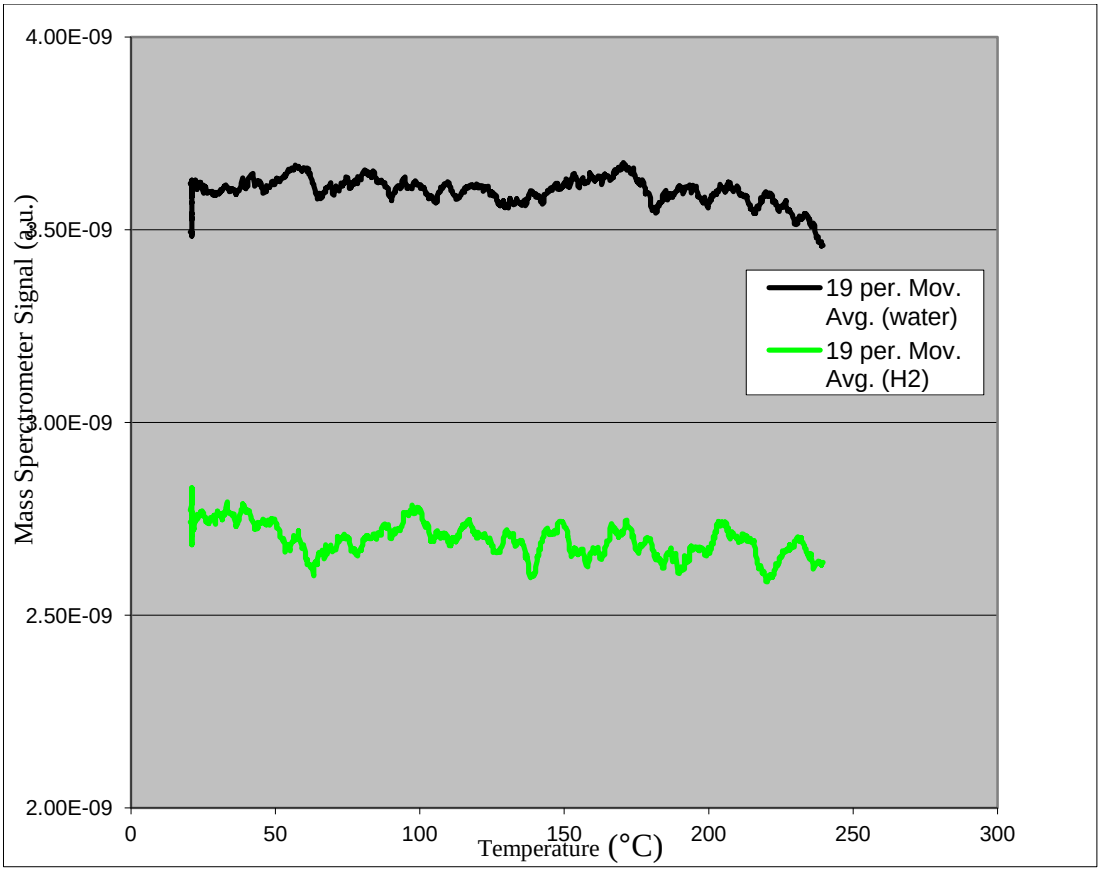

Figure 7.3 TPRx vs. temperature plot upto 240 °C. Nanoparticles were created in open air

The second run of TPRx was conducted on Ni nanoparticles created by laser ablation in vacuum on PEN. In this work, oxygen was excluded from the processing environment to ensure the particles were metallic. As before, H_2 and O_2 diluted in argon were passed over the sample and the temperature was ramped up at 10 °C/min, this time up to 800 °C.

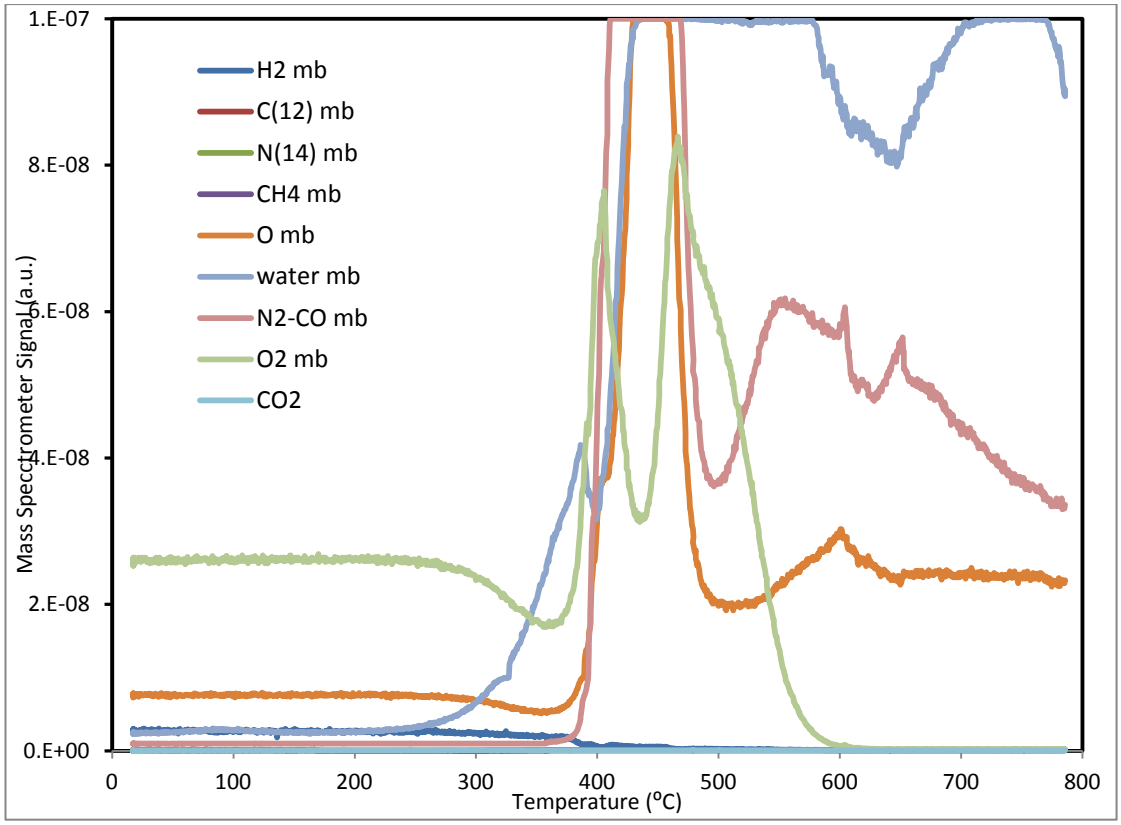

Figure 7.4 TPRx vs. temperature plot. Nanoparticler were created in vacuum

From the Temperature Programmed Reaction plot in Figure 7.4, H_2 and O_2 fell and water rose from just under 300 °C. This could possibly be a reaction of H_2 and O_2 to give water catalysed by the Ni on the sample (the sensitivity to H_2 is much lower than for O_2 or water). However, at a slightly higher temperature, very high values were seen for many species. These likely correspond to the decomposition of the sample to give CO and water. Other species give signals at the same mass to charge ratio as O_2 (32) and O (18) and these may be from products of decomposition. So, as to whether the Ni is catalysing the reaction between H_2 and O_2 it appears that might be but the huge peaks at slightly higher temperature which are caused by polymer decomposition must also be considered.

From TPRx experiments it is concluded that Ni nanoparticles may show some catalytic activity at higher temperature and the presence of O_2 in nanoparticles reduces its catalytic activity. This may be controlled by creating nanoparticles in vacuum.

7.4-Surface Modification and Working of PEMFC

As designed PEN fuel cell was tested with different laser energy processed PEN substrates. To observe the effect of laser in the surface modification of PEN and Ni nanoparticles four samples of PEN were prepared.

1- 15nm Ni on PEN with low laser energy (75 mJ)
2- Double laser irradiation first with 165 mJ on 50 nm Ti and second with 75 mJ laser energy on 15 nm Ni
3- High energy laser irradiation (165 mJ) on 50 nm Ni
4- High energy (180 mJ) laser irradiation on PEN without metal

The idea to prepare these samples was to check which laser energy is good for the conversion of the thin film into nanoparticles for the transport of protons in PEMFC.

SEM was used to observe the surface modification of PEN after laser irradiation.

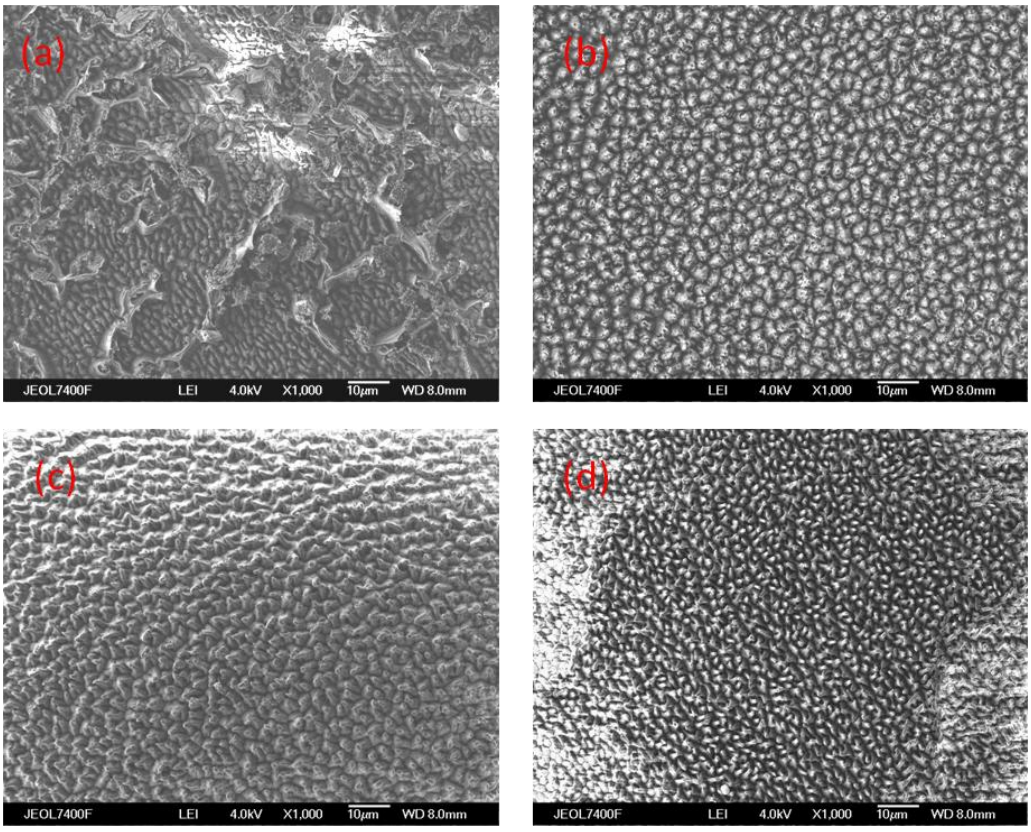

Figure 7.5 SEM images of laser processed PEN (a) 75 mJ laser energy on15 nm Ni, (b) double laser irradiation first 50 nm Ti substrate 165 mJ laser energy and second 15 nm Ni and 75 mJ laser energy, (c)165 mJ laser energy on PEN and (d) 180 mJ laser energy on 50 nm Ni

Sample one shows that low energy modified the surface and there were metal particles on the surface as shown in Figure 7.5 (a). The rest of the samples which were ablated with high energy excimer laser deformed the surface structure of PEN. There were bumps and tower like structures as shown in Figure 7.5 (b, c & d). Also quick re-solidification process smashed the surface structure of PEN.

Also some EDX tests were performed to confirm the presence of metal on the PEN. It was observed that by laser ablation the thin metal film was ablated and only some flakes identified the presence of metal as shown in Figure 7.6.

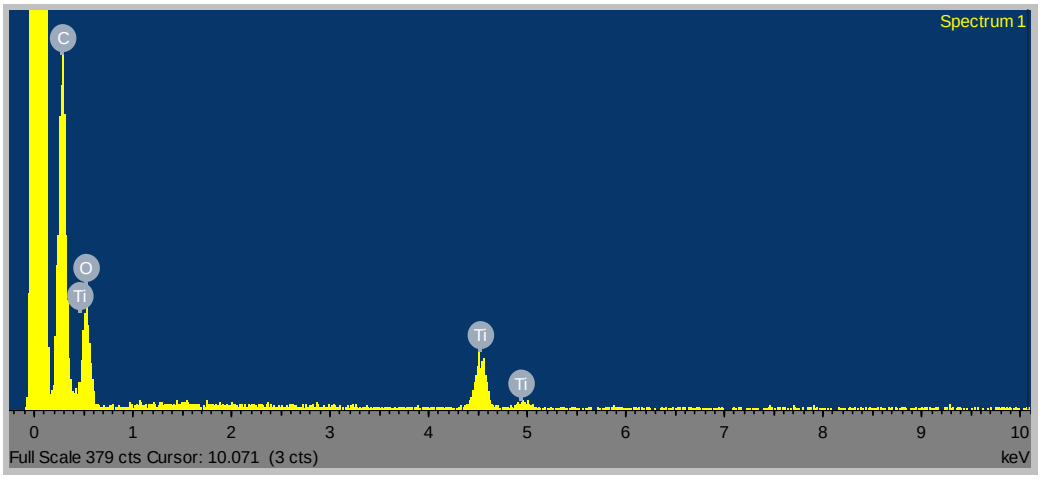

Figure 7.6 EDX spectrum of laser processed thin layer of Ti on PEN substrate

When transport and catalytic efficiency of these four samples were tested in the fuel cell apparatus, only the low laser energy processed PEN sample gave some indication of transport of protons. Although the signal was very weak some positive indication was shown. The rest of the three samples with high energy laser and double laser ablation process showed nothing. It is possible the PEM structure may be deformed completely by the high energy beam on these samples.

Initially Ni nanoparticles were tried as a catalyst in our fuel cell with PEN as the transport membrane. There were no significant results with Ni nanoparticles in the transport of protons. Only few millivolts signals were observed during experiments. Subsequently the catalytic activity of Ni nanoparticles was tested with Nafion. A paste of Ni nanoparticles and graphite powder was applied on Nafion. During the fuel cell test, it was observed that the catalytic activity of Ni was very poor, giving a signal of only a few tens of millivolts. A summary of the output results is shown in table 7.1.

Table 7.1: Summary of the PEMFC results

Membrane	Catalyst	Open Circuit Voltage
Laser processed PEN	Ni	4 mV
Laser processed PEN	Pt	4 mV
Nafion	Ni nanoparticles in carbon paste	80 mV
Nafion	Pt nanoparticles in carbon paste	0.5 V

7.5-The Use of Carbon Based Materials

The plan of this research was to study carbon based materials for the enhancement in conductivity and performance of the energy devices. For this vision a detailed study on the growth of CNTs and graphene was conducted. Expertise was gained in how to grow CNTs on the tip of amorphous materials. Also it was learned to prepare single layer graphene on a variety of substrates by chemical exfoliation technique in the Manchester University.

It was hoped that laser irradiation convert PEN into a mesoporous conducting membrane. Although laser irradiation carbonized PEN, it was not fully conducting. It was decided to use carbon based materials to enhance its conductivity. Initially for this purpose a paste of platinum nanoparticles and graphite powder was prepared. The paste was applied on some laser processed PEN samples and a sample of Nafion. The samples were dried on hot plate at 80°C about half an hour. It was observed that the membranes were conducting. The samples were loaded in the PEMFC apparatus one by one and tested for the catalytic activity. It has been observed that the PEN membrane had very low signal whilst the Nafion membrane showed excellent output. The experiments were repeated many times but the result was same.

7.6-Discussion

Two materials Ni and Pt were tried in the fuel cell setup for the proton transport and conductivity. Although there were limitations of the catalytic activity with fast degradation, the conclusions regarding PEN are as:

PEN is not specifically designed for fuel cell applications, and the transport mechanism is limited as has been observed. However, the aim of this work was to look at surface modification to prepare anode and cathode electrodes in a single step, using the modification of the existing barrier layer. It recognised that the chemistry of the polymer could be modified to enhance proton exchange. PEN is a material which could be processed for the preparation of fuel cell membrane because PEN

has high temperature and mechanical stability. The good thing regarding the use of PEN is its absorption of UV light which made it possible to prepare nanoparticles by laser irradiation as discussed in Chapter 6.

The other factor is its surface conductivity which could be improved by laser interaction and transformation to conducting carbonised surface. In this research surface conductivity was also improved by the preparation of a paste of carbon powder and catalyst nanoparticles in water.

Comparing PEN with Nafion, Nafion is a soft polymer with more than 22% content of water and is transparent to UV light. It was not possible to create nanoparticles by laser ablation.. The role of the membrane in PEMFC is very important. It provides temporary centres (fixed charge sites) where the moving ions can be accepted or released and the presence of free volume for the proton transport across the polymer. In PEMFC the proton transport follows a mechanism, known as the vehicle mechanism. In this mechanism protons are transported through free volume by "hitching a ride" on certain free species (water molecules). The well known membrane polymer for PEMFC is Nafion in which conductivity of ions based on the vehicle mechanism is the transport mechanism. The hydrophilic property of Nafion made it possible to provide vehicle (water molecules) for protonic transport. On the other hand PEN is a hydrophobic material; it does not absorb water to provide transport to protons. Nafion has a backbone of Teflon for mechanical strength and sulfonic acid groups ($SO_3^-H^+$) for proton transport as discussed in Chapter 6. In our experiments we tried to utilize PEN as a membrane for PEMFC by laser processing but this material does not have the sulfonic or sulfuric acid groups which provide free sites for the proton transport.

The backbone structure of PEN is very much similar to PEEK (polyaryletherketone) which is another membrane material for PEMFC. In this material aromatic hydrocarbon polymers can be employed as the polymer backbone. Sulfonated PEEK is a good material as a membrane in fuel cells; the only disadvantage is that operation must be at high temperature. For PEN, it may be possible to use it as fuel

cell membrane by modifying its structure with the addition of sulfonic acid functional groups.

The other thing which may have contributed to the failure of our experiments was the catalyst. The catalysts used in this research do not have catalytic activity at low temperature. The fuel cell experiments were conducted with Ni nanoparticles on a standard Nafion and it was observed that Ni is not a good catalyst for proton transport in PEMFC. When Pt nanoparticles were tested on Nafion membranes at room temperature, the output was encouraging. However, careful engineering of the size and quality of nano-dots could be helpful to show some catalytic activity.

In summary, PEN may be a material for energy and other flexible devices with some structural changes because this material has the capability to be modified by excimer laser irradiation. Additionally its transition temperature is better than other polymer materials. It is an attractive proposition to use reel to reel processing of plastic with expanded excimer beams to produce a single process could make it conducting and form nanoparticles on it at the same time. This would be a significant step in manufacturability of low cost green energy materials. So, with this technology material processing time and cost will decrease.

7.7-Summary

In this section of the thesis we briefly researched the following:

- A PEM fuel cell was designed and crafted in the workshop.
- Laser processed PEM and Nafion were tested as proton transport membranes.
- The Ni nanoparticles which were created by the excimer laser irradiation as discussed in Chapter 6 were tested for catalytic activity in a TPRx experiment. Both metallic and oxide particles were tested.
- The performance of the laser processed PEN and traditional Nafion as a proton exchange membrane was tested in the fuel cell unit. It has been observed that as a polymer PEN has some active sites but not enough for a stable proton exchange.
- Pastes of Ni with graphite powder and Pt with graphite powder were prepared. Their catalytic activity on laser processed PEN and Nafion were observed in the fuel cell. It has been analysed that Pt is good for ionization of H_2 and Ni has some activity on Nafion.

CHAPTER 8 CONCLUSIONS AND CONSIDERATION FOR FUTURE WORK

A general summary of the targets of this PhD research is presented in this chapter. Conclusions and suggestions for the future work on CNTs and laser processed materials are also discussed for energy applications.

8.1-Summary of the Targets Achieved

As highlighted in the Introduction, the main targets to be achieved within this research were:

1. To design and build a system for the growth of CNTs
2. Control of the growth process parameters
3. Creation of nanoparticles for CNTs
4. Growth of CNTs
5. Growth of graphene
6. Laser processing of polymer substrates and nano-dots
7. Production of Nano-composites for energy applications

The design and fabrication of a new PECVD system used for the growth of CNTs, graphene and the integration of laser processed silicon materials was a major part of this research work. For this purpose the first stage was to build a system for the growth of CNTs and graphene. Design, fabrication and optimisation of a novel PECVD system was carried out to make effective nanotube structures. This was the first unit for CNT deposition to be developed at Dundee.

Because there was no CNTs growth history in the University of Dundee, all system controlling parameters such as temperature, pressure inside the chamber, R.F plasma power, ratio of the feed stock gases were analysed for effective growth of CNTs. Under optimum conditions growth of CNTs was achieved by the PECVD system. Different types of substrates were used in the growth of CNTs such as silicon wafer, silicon dioxide and polymer.

In the PECVD system, the growth of CNTs effectively depends upon the catalyst. Meta-stable transition metals were tested as a catalyst and it was observed that Ni was best for our system conditions. The nanoparticles used in the growth of CNTs were created by thermal evaporation, excimer laser irradiation and liquid based catalysts by spin coating. It was observed that thermal annealing and plasma treatment technique for the creation of nanoparticles was favourable for CNTs optimum results.

The role of the buffer layer in the low temperature growth of CNTs was examined to improve the quality of CNTs in PECVD. A detailed study was conducted on the role of the catalyst material and the buffer layer underneath the catalyst thin film. The surface adhesion and interaction energy for the catalytic activity were discussed. With selection of the buffer layer material it was observed that growth is possible at low temperature (140°C).

Experiments were conducted to grow graphene by PECVD and chemical exfoliation. For the chemical exfoliation section some time was spent with the A.K. Geim research group (Condensed Matter Research Group) at Manchester University.

The excimer laser irradiation for the modification of surfaces is a novel technique. A brief study of excimer laser irradiation was conducted in this research. Nanoparticles were created on polymer (PEN) through excimer laser processing. This work for the first time realises a potential new one step process to fabricating large surface area electrodes for energy devices. In that process the excimer laser was used to create porous carbon material for the surface of a proton exchange membrane. A study has been conducted to observe the behaviour of PEN and Nafion polymer materials during processing by UV laser irradiation.

A novel material was achieved for the first time in this research by the growth of CNTs on the tip of spike-like structured a-Si prepared by laser irradiation. A multi-

step technique was used to grow CNTs on the tip. This CNT network increased the surface area of the material which may be attractive for the charge storage capacity of lithium ion batteries, hydrogen storage, and a field emission buffer layer.

A PEMFC was designed and built to test the protonic transport in polymer materials, especially PEN and Nafion. Both Nafion and laser processed PEN was tested as possible membrane materials in the fuel cell. The catalytic activities of metallic and oxidized Ni nano-materials were tested using TPRx. It was concluded that metallic Ni nanoparticles may have some catalytic activity at higher temperature.

8.2-Suggestions for Future Work

Although the preparation of CNTs by PECVD was optimized, there are still several possibilities to improve the quality of CNTs in this system. Stability of the system temperature was always an issue. It may be possible to replace the whole temperature control unit by a new one which would be more stable and have the capability to go to higher temperature. A number of attempts to grow CNTs on the tip of AFM cantilevers were tried but there was not a suitable holder for it and tips were broken during growth process. It may be possible to make a tip holder to grow CNTs for imaging and other applications. During experiments it was observed that the alignment of CNTs mostly depends upon the biasing. It may be possible to grow aligned CNTs on particular sites by the addition of a biasing unit in the PECVD chamber. Raman studies are very promising for the characterization of CNTs and graphene and should be tested.

Because the primary focus of the research was to develop a system for the growth of CNTs and graphene and to deploy them for the improvement of energy devices, more than half of research time has been spent on the optimization of the growth of carbon based materials.

Laser irradiation was mostly conducted on the surface barrier layers of PEN to make it a mesoporous carbonized material. PEN has an insulating barrier layer and it was tried to modify this barrier layer in a single step process. It should now be possible to apply this single step process to other polymers to make them porous material. Also,

some work is required to change PEN's internal chemistry to make it a more suitable material for proton exchange.

As discussed in Chapter 2 CNTs have the capacity for hydrogen storage, so it was planned to grow CNTs directly on the electrodes of a PEMFC and to increase its performance. The poor protonic transport results of the PEN prevented this. It could be possible in future to grow CNTs on laser processed PEN after the modification in the internal structure of this material.

Finally, the silicon processing that produced spike like or nano-wire like structures could be exploited in the field of Li ion battery electrode technology. As mentioned in Chapter 3, some semiconducting nano-composites have the capability to split water molecules. Further research may be possible on the water splitting activity of a-Si:H spike structures with CNTs.